Advances in Organic Photoconductor Technology

David S. Weiss*

Department of Chemical Engineering, University of Rochester, Rochester, New York 14627

Martin Abkowitz

Enabling Technologies, 1198 Gatestone Circle, Webster, New York 14580, and Department of Chemistry, University of Rochester, Rochester, New York 14627

Received May 1, 2009

Contents

* Corresponding author. E-mail: dweiss2@rochester.rr.com. Tel.: 585-544-3561.

1. Introduction

An "organic photoconductor" (OPC) or "organic photoreceptor" is the photoelectric element that is at the heart of the electrophotographic (EP) printing process. The terms organic photoconductor, OPC, and organic photoreceptor are used interchangeably in the literature, although the former refers to the materials and the latter refers to the device. OPCs are organic photoelectronic devices that have reached a high level of sophistication. Optimization of OPC design drove, and was at the same time facilitated by, scientific exploration of photogeneration, electronic transport, and interfacial processes in disordered molecular materials and heterogeneous media. The OPC systems designed and characterized to support electrophotography in fact provided a platform for fundamental studies of key photophysical processes in novel materials, many of which have come to currently find an even broader range of application.

In this article, we will review recent advances in organic photoconductor (OPC) development, focusing on the key materials and their influence on device performance in the electrophotographic process. In practice, the materials are fabricated into a large-area thin-film photoreceptor on either a metal tube or a flexible plastic substrate. This topic was reviewed in this journal in 1993 by Law,[1] and there are many excellent "older" reviews of OPCs[2−6] in addition to those of a more recent vintage.[7−13] The title of Law's review, "Organic Photoconductive Materials: Recent Trends and Developments", reflects the focus of the review in terms of the synthesis and characterization of light-absorbing materials with possible application as the charge-generating component of an organic photoreceptor for an electrophotographic process. Some attention was also given to literature describing photogeneration mechanistic studies. In this review, we

10.1021/cr900173r
Published on Web 10/22/2009

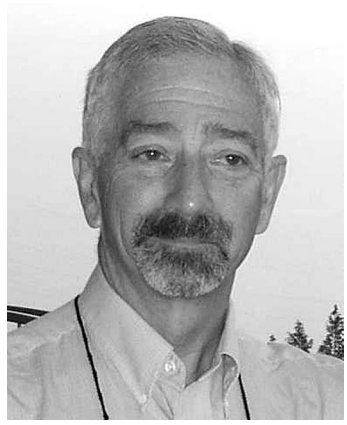

David S. Weiss can be reached at dweiss2@rochester.rr.com or dsweiss@che.rochester.edu. He received his Ph.D. in chemistry from Columbia University in 1969. In 1978, following a postdoctoral fellowship at Iowa State University and Assistant Professorship at the University of Michigan, he joined the Eastman Kodak Company. He retired as a Scientist Fellow in 2009. Currently, he is a Senior Scientist in the Department of Chemical Engineering at the University of Rochester. His research focuses on organic electronic materials and devices with emphasis on organic photoreceptors for electrophotographic technologies. He holds 19 U.S. patents and is author on more than 90 publications. He is coauthor of Organic Photoreceptors for Imaging Systems (Marcel Dekker, Inc., 1993) and Organic Photoreceptors for Xerography (Marcel Dekker, Inc., 1998), and he is coeditor of the Handbook of Imaging Materials, second edition (Marcel Dekker, Inc., 2002). He has been an Associate Editor of the Journal of Imaging Science and Technology and has served as general chair of international conferences. In 1999 he received the Chester F. Carlson Award from the Society for Imaging Science and Technology, in 2004 he was named an IS&T Senior Member, and in 2008 he was awarded IS&T Fellowship. He has served on the IS&T board as a vice-president and is currently Treasurer of the Society. He is a long-time member of the American Chemical Society.

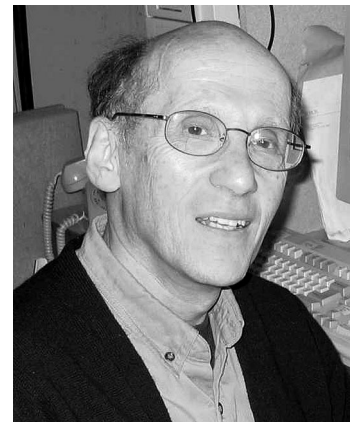

Martin Arnold Abkowitz can be reached at mabkowitz@mailaps.org or abkowitz@chem.chem.rochester.edu. Abkowitz received his Ph.D. in physics from Syracuse University in 1964. In 1965, he was Andrew Mellon postdoctoral fellow at the University of Pittsburgh. In 1965, he joined the Webster Research Center of Xerox Corporation where he was a Principal Scientist until retirement in 1999. Currently he is a Visiting Scientist at the University of Rochester. Abkowitz has chaired Gordon and international research conferences and serves on several international research advisory panels. He is a fellow of the American Physical Society and has served on the New Materials Prize Committee and the Committee on Applications of Physics of that society. Abkowitz has also served as chair of the New York State Section of the APS. He has served as Adjunct Professor of Physics at the University of Rochester and has been an Industrial Coprincipal Investigator at the NSF Science Center on Photoinduced Electron Transfer at the University of Rochester. Abkowitz's current research interests include injection and interfacial phenomena, electronic transport and the dielectric properties of amorphous semiconductors, and disordered molecular and composite materials. In addition, Abkowitz has participated in the design of polymer-based electronic and transducer devices including imaging receptors. He has 174 cited publications including major reviews and encyclopedia and book chapters and 35 U.S. patents issued or pending. Abkowitz has made over 250 contributed and invited presentations at international conferences.

will focus on the OPC as a photoelectric device integrated into the electrophotographic process with emphasis on literature published since Law's extensive review in 1993. To provide the reader with a link to the past we will begin with a brief synopsis of the major topics in the 1993 review. Then, since the history and development of organic photoreceptors is intimately intertwined with the development of electrophotographic copiers and printers, we include a brief history and description of the electrophotographic process as it is practiced today including the technological change from copiers to printers. Next, we will describe the basics of the OPC "design of choice" and how the materials are formulated into a multilayer OPC with optimized photoelectrical functionality. Included will be descriptions of how OPCs are characterized and evaluated for performance with respect to the critical device characteristics in the electrophotographic process. Because OPCs are devices that are optimized for the specific electrophotographic process chosen by a manufacturer, and the interactions of the OPC with various process elements will influence its device characteristics, the optimized OPC device characteristics from different manufacturers will differ. That is to say, the OPC formulation, architecture, and device characteristics are optimized for the particular electrophotographic process for which it is intended, and indeed, it is sometimes the marketing arm of a company (analysis and consideration of image-quality requirements and consideration of OPC "life" versus replacement cost are but two examples) that will dictate which OPC characteristics are most important. Following this, we will discuss the current understanding of the mechanistic details pertaining to two of the most important device functions: charge generation and charge transport. Modern OPCs often have several other functional layers in addition to those in which charge is generated and transported, and we will describe some of the chemistry behind the design of undercoat and overcoat layers. Alternative OPC architectures will be discussed, and finally, we will discuss some of the more important OPC interactions in the EP process and describe how these interactions influence the device characteristics.

With all of the above considerations, one realizes that reviewing OPCs encompasses a broad range of topics and, of necessity, some will be inadequately covered. In addition, because OPC progress has been largely driven by the industrial development of electrophotographic copiers and printers, the publication record is sometimes incomplete. OPC details are the intellectual property of a company and, as such, are of considerable value. Thus, the actual OPC formulations used by a particular manufacturer in a machine are typically not divulged in the open literature. Published accounts are more often than not descriptions of the effects of formulation, etc., on the functional characteristics of OPCs that have not, and perhaps never will, be commercialized. Thus, the development of organic photoconductor technology is a fascinating blend of science, engineering, and the desire of a manufacturer to maximize profits. Our goal is to provide the reader with a comprehensive overview of this technology and describe how the various aspects have worked together such that, today, OPCs are the key technology in a multibillion dollar industry.

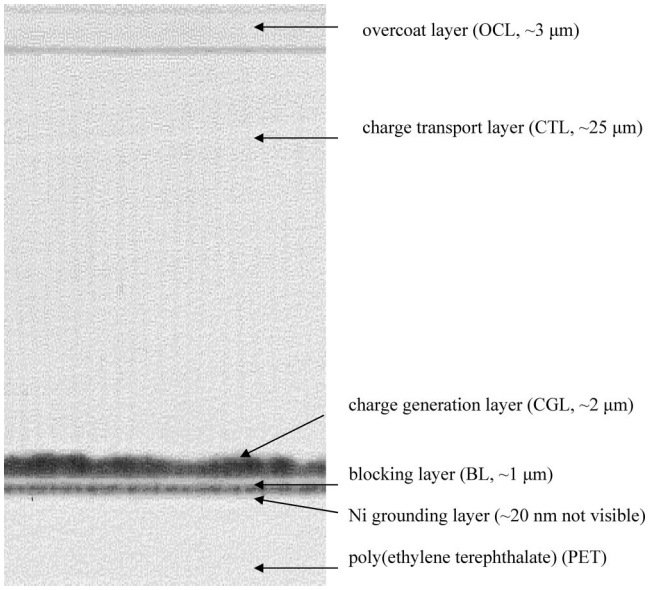

Figure 1. Cross-sectional photomicrograph of a multilayer OPC. From free surface to substrate, the functional layers are as follows: protective overcoat layer (OCL), charge-transport layer (CTL), charge-generation layer (CGL), charge-blocking layer (BL), grounding electrode (Ni), and substrate (PET).

As with any established technology, many acronyms have been coined for commonly used terms. Since we will make liberal use of such terms, a brief listing follows:

- BL = blocking layer
- CGL = charge-generation layer
- CGM = charge-generation material
- CTL = charge-transport layer
- CTM = charge-transport material
- h-CTM (HTM) = hole-transport material
- e-CTM (ETM) = electron-transport material
- EP = electrophotographic
- OCL = overcoat layer
- OPC = organic photoconductor
- MDP = molecularly doped polymer
- UCL = undercoat layer

Acronyms have also been coined for many of the chemicals used in OPC formulations. These can be obscure as they are very often based on common nomenclature. We will define these terms as they occur.

1.1. OPC Device Description

Simply speaking, an OPC is a large-area thin-film device that converts light into charge. Figure 1 is a photomicrograph cross section of a multilayer OPC. The insulating OPC materials are sequentially deposited on a conductive substrate, which is usually an aluminum tube or a metalized polymer. In Figure 1, the substrate is nickelized poly(ethylene terephthalate), PET. The Ni layer is too thin to visualize. From the free surface to the substrate, the functional layers in this OPC are as follows: protective overcoat layer, charge-transport layer, charge-generation layer, charge-injection blocking layer, nickel, and substrate. The chemistry of each of the functional layers will be discussed later. OPCs in which the charge-generation and charge-transport functions are in separate layers are called "dual-layer" OPCs, and when these are combined, "single-layer" terminology is used. Both single- and dual-layer OPCs have been commercialized. In general, single-layer OPCs are found in low-end consumer printers and dual-layer OPCs are used in more demanding print applications. As might be expected, single-layer OPCs are less expensive to manufacture, but they do not have the photoelectrical characteristics necessary for high-speed, high-quality printing (section 3.1).

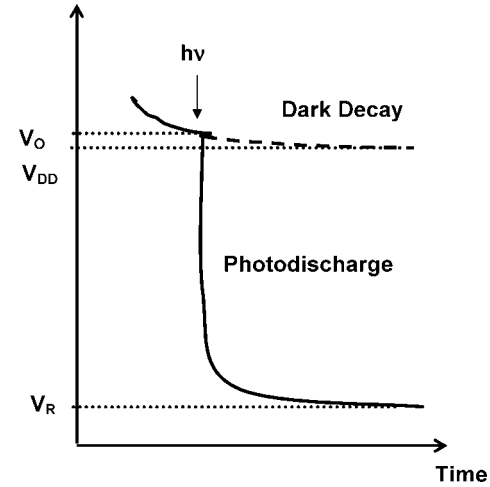

Figure 2. Photodischarge characteristic of an OPC. At the time between exposure and development, the difference between the OPC surface potential for areas that are unexposed (dashed line) and exposed (solid line) is the image potential. The residual potential, V_R, is the lowest surface potential achievable by photodischarge.

In use, the OPC surface receives a charge that is subsequently discharged in areas exposed to light. Thus, the basic OPC functional requirement is that, in the dark, it is a good insulator but it becomes conductive when exposed to light. To carry out this function, two key materials are utilized: a light-absorbing charge-generating material (CGM) and a charge-transporting material (CTM). The physics of an OPC can be closely approximated by a parallel place capacitor where the surface charge density, Q, prior to exposure is related to the surface potential, V, through the capacitance of the material, C, as $Q = CV$. Thus, on acquisition of a surface charge, a field, E, is created across the device of magnitude V/L where L is the device thickness. A "typical" surface potential is −500 V, and a typical field is 2×10^5 V/cm. Light is absorbed by the CGM and charge is created, which subsequently drifts under the influence of the applied field to discharge the device. The OPC surface now has an electrostatic latent image, and the electrophotographic process utilizes the difference in surface potential between exposed and nonexposed areas to create a printed document. The electrostatic latent image has been visualized using scanning electron microscopy.[14] The photodischarge characteristic of an OPC is illustrated in Figure 2. On exiting the charging device, the surface potential decays (dark decay), but the charging process is adjusted such that, at the time of exposure, the surface potential is at the desired potential, V_0. In OPC areas that are not exposed, the dark decay continues as shown. V_{DD} is a characteristic that is determined at some designated time after charging (such as the time for the OPC surface to reach the development station). In exposed areas, the surface potential undergoes rapid photodischarge. A plot of surface potential as a function of time after exposure is commonly called the "photoinduced discharge curve" (PIDC). The settle-down surface potential after exposure is determined by the photosensitivity of the CGL, the intensity of the exposure, and the OPC charge-transport characteristics. The OPC residual potential, V_R, is the lowest photodischarged surface potential achievable for

a particular OPC. In all commercial photoreceptors, single or dual layer, most of the photodischarge occurs by the drift of positive charge (holes) under the influence of the applied field from their site of generation. Thus, if the exposure is through the OPC "free" surface, the surface potential usually has a positive charge for single-layer and a negative charge for dual-layer OPCs.

2. Background

The story of the development of electrophotography is an object lesson in the connections between technology development, product development, and scientific understanding. Here we describe Carson's invention, how the technology evolved with the development of OPCs, and the changes in OPCs that were driven by the shift from copiers to digital printers.

2.1. Chester Carlson and the Electrophotographic Process

The story of Chester Carlson (1906−1968) and electrophotography has been told many times.[15−21] Carlson's younger years were difficult. At age 17 he lost his mother, and his father, a barber, was crippled with arthritis and was often unable to work. Nevertheless, Carlson went to a community college in California and was subsequently admitted to Caltech. Graduating in 1930 with a degree in physics, he had great difficulty in finding employment. Finally, he joined the P. R. Mallory Company patent department, where he eventually became department head. During this time he went to night school at New York University and obtained a law degree. Intellectually curious and always looking to improve his position, Carlson searched for a new technology that might have future promise. At the same time, Carlson's work experience in a patent department had familiarized him with the difficulty of making permanent multiple copies of legal documents. His scientific reading prompted him to the realization that photoconductivity might provide the key to a new copying technology. After his wife protested odoriferous kitchen experimentation with photoconductive materials such as amorphous sulfur, he rented a room in the Astoria section of Queens, New York, where he set up a laboratory and hired an assistant (Otto Koreni). The concept was deceptively simple:

(1) Prepare a thin film of a photoconductive material on a conductive substrate.

(2) Ground the conductive substrate and rub the surface of the film with an appropriate material to cause it to become electrostatically charged.

(3) Contact-expose the charged surface through an image mask such that, in the exposed areas, the electrostatic charge is dissipated due to the materials photoconductivity. The surface now has an imagewise electrostatic charge pattern.

(4) Cascade the charged surface with oppositely charged particles (he used lycopodium powder) so that the powder is attracted to and adheres to the charged areas of the surface. The electrostatic "latent" image has now been converted into a visible image of particles on the photoconductor surface.

(5) Transfer the powder from the photoconductor to wax paper by contact.

(6) Fix the transferred powder to the paper by gentle heating. This completes the process and the photoconductor film could be cleaned in preparation for the next cycle.

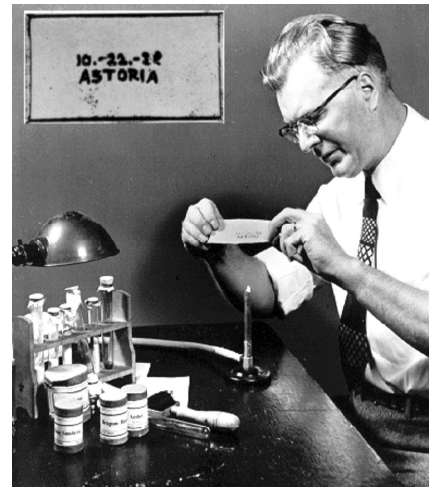

Figure 3. Photograph of Chester Carlson reenacting the fixing process in the creation of the first electrophotographic print (shown in the upper left insert).

The fundamental steps—charge, expose, develop, transfer, fuse, and prepare the photoreceptor for reuse—are all found in today's electrophotographic printers. The term "xerography" from the Greek (dry writing) was later coined to describe his process. The first electrophotographic copy along with a picture of Carlson reenacting the fixing process is shown in Figure 3. In April of 1938, Carlson filed his seminal U.S. Patent. Figure 4 shows the cover page of U.S. patent 2,297,691, which was issued in 1942. Over the next few years, Carlson was unsuccessful in interesting over 20 of the major companies of the day in his invention. The inability of established companies to recognize and support disruptive technologies is an interesting and well-known phenomenon, and the eventual success of electrophotography has been showcased in many books.[22,23] However, in 1944 the Battelle Development Corporation (a subsidiary of the Battelle Memorial Institute) agreed to fund a small project to further the invention, and in 1947 the Haloid Coporation, a small photographic company in Rochester, New York, acquired a license for the process. Carlson subsequently moved to Rochester to be near his creation, but he was never actually employed by the Haloid Corporation, Haloid-Xerox, or Xerox. In all, Carlson obtained 38 U.S. patents related to electrophotography. Six were assigned to Battelle, 20 to Haloid-Xerox and Xerox, and 12 were Carlson's alone. Carlson is the sole inventor on most of the patents. In 1949 the XeroX Copier Model A was introduced. This machine required 14 manual operations and had minimal success in the marketplace. In 1959 Haloid-Xerox introduced the Xerox 914, the world's first fully automatic copier, and this product proved to be truly revolutionary. The electrophotographic process of the Xerox 914 is essentially unchanged today but there have been substantial advances in all of the process elements.

2.2. Key Advances in Electrophotographic Process Elements

Electrophotographic copying and printing became a commercial success because of technical improvements in all of the key process steps.[8,16,17,24] Charging the photoconductor surface by rubbing with a handkerchief (Carlson's technique) was impractical for a commercial product, and one of the major technology developments was that of "corona charging" by means of a scorotron device.[25] In this device, corona

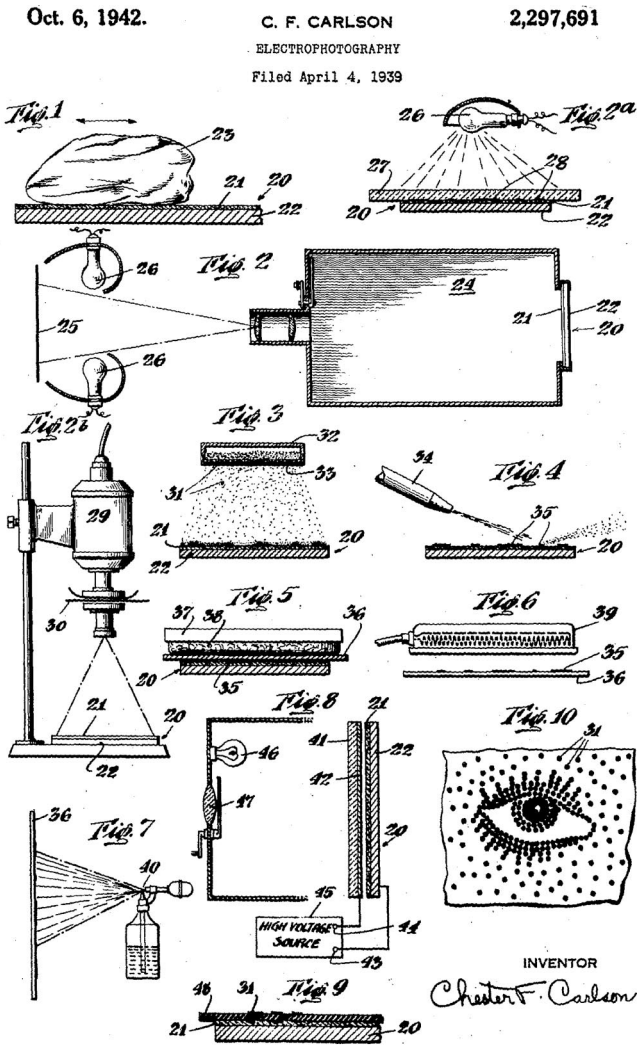

Figure 4. Cover page from Carlson's 1942 U.S. Patent.

wires are biased at a high potential (6−8 kV) to generate corona ions that are attracted to the ground plane of the photoreceptor. A wire grid is interposed between the corona wire and the photoreceptor surface and is biased at the desired "shut off" photoreceptor surface potential. Development subsystems have been engineered for the precise delivery of charged particles to the electrostatic image on the photoreceptor surface,[26] and lycopodium powder has been replaced with polymer-based "toner". Until very recently, all toner was a blend of mainly polymer and carbon or pigment that was ground and classified for the desired size range. Toner charge is induced by triboelectrification produced by contact with an appropriate material (these are often "carrier" particles comprising a magnetic material with a polymer coating), and included in a toner formulation are additives to control and stabilize the level of toner charging. Recently, "chemical" emulsion polymerization methods have been commercialized for toner production.[27] The chemical method allows for precise control over the size and morphology of the toner particles. The Carlson exposure method (long incandescent light exposures through a mask) was replaced in copiers with an optical system. In this exposure system, either a xenon flash or a scanned "white" light is reflected from the surface of a document to the surface of the charged photoconductor. With the development of electrophotographic printers, the exposure is accomplished with either laser or light-emitting diode (LED) array optical systems that are driven by computer files to create halftone exposures on the charged photoreceptor surface. Likewise, there have been significant developments in image transfer and fusing, etc. And finally, the evolution of the composition of the thin film of photoconductive material on a conductive substrate, which came to be called the photoreceptor, has been the focus of many previous review articles.[1,7,11,12] Two key factors led to the evolution of photoreceptors from inorganic materials such as Se to organic materials (section 2.3). One was that, with organic materials, it was possible to tailor the photoreceptor absorption and photosensitivity to the new exposure systems, and the second was that it became possible to separate photogeneration and transport of charge into independently optimized layers.

2.3. Photoreceptors for Copiers Versus Printers

In the beginning, all electrophotographic machines were "copiers". That is, the electrostatic latent image was formed on the photoreceptor by reflection of the exposing light (xenon flash or slowly scanning "white" light) from a document (typically a printed page with black ink) onto the surface of the electrostatically charged photoreceptor. With a flash exposure, the entire image is reflected onto a flat film-based photoreceptor. With a scanning-exposure system, the photoreceptor could be either film or drum-based. There is a subtle difference in the physics of photodischarge when a charged photoreceptor is exposed with a pulse of light that is short with respect to the time it takes charge to transit the film versus a longer exposure with less-intense light (as in a scanning system). In the former case, all of the photogenerated charge (CV) is produced essentially instantaneously and transits the film en masse. In this case, called space-charge-limited discharge, the internal field goes to zero in areas where the charge has traversed. Alternatively, emission-limited-discharge occurs when the exposure occurs over a long time and the internal field decreases incrementally and uniformly. The physics behind these two extremes of photodischarge have been analyzed by Chen.[28] Another factor is that short, high-intensity exposures may give rise to Langevan (diffusion-limited bimolecular) recombination resulting in decreased sensitivity (reciprocity failure) relative to low-intensity exposures.[29−31]

Since black printed areas of the document do not reflect the exposing light, the corresponding areas on the photoreceptor remain charged. The development process then entails contacting the photoreceptor with toner particles that have a charge opposite that of the photoreceptor. This embodiment is called "charged area development". In all copiers, the development process was "binary" in the sense that the photoreceptor surface either was charged or not, and these areas were either developed with toner or not. The difference in surface potential between the charged and photodischarged areas of the photoreceptor is called the image potential. In practice, a few hundred volts of image potential is required for the development subsystem. The transfer of toner from the photoreceptor to the final receiver (typically paper but sometimes a clear plastic sheet for overhead transparencies) was (and still is) accomplished by a combination of surface contact and electrostatics. Typically, toner transfer to the receiver is accomplished by contacting the receiver with the image and applying an electrostatic charge to the receiver back surface with sign opposite that of the toner.

The major fundamental requirement of the photoreceptor in an electrophotographic copier is that it must have low

dark conductivity and high photoconductivity (to visible light reflected from an original document) such that there is enough of a difference in surface potential between exposed and nonexposed areas that development occurs in the latter and not the former.

Although a film of sulfur was used in Carlson's original experiments, the first commercial Xerox copiers utilized thin films of amorphous selenium and later alloys of selenium and arsenic and tellurium. These inorganic semiconductor materials had relatively high dark conductivity, (which could be reduced by break-in procedures), and high photosensitivity. When charged positively (holes are mobile), these were photosensitive to exposure with a "white light". However, they had little or no photosensitivity to exposure with red light. This led to the characteristic of early copiers to be "blind" to a document containing information colored red. Other considerations were that these materials had high dielectric constant (high surface charge density for a given surface potential), had high dark decay unless properly broken in after deposition, and required preparation by vacuum evaporation. Selenium based photoreceptors were brittle and therefore difficult to prepare as flexible belts. In addition, there were environmental costs.

As mentioned above, today virtually all electrophotographic machines are printers and true copying machines are becoming scarce. There is a fundamental difference between an electrophotographic copier and printer, and it has to do with how the electrostatic latent image is created on the charged photoreceptor surface. In a printer, the photoreceptor is exposed according to a computer-resident image file and the exposing light is pulsed on and off using a laser-diode and rotating hologon scanner or an array of LEDs. The term "laser printer" is generic for electrophotographic printers even if the writing system uses LEDs instead of lasers! Nowadays, a copy of a document is made with a "scanner" which reflects light from the document onto a detector and stores the data in an image file that is subsequently rendered and printed. The data-rendering process converts the image into a halftone that is used to address the exposure system. Thus, in a printer, the charged photoreceptor is exposed serially in a pattern of small dots. An array of 600 dots-per-inch has dot diameters of approximately 40 μm and 1200 dot-per-inch, and higher resolution printers are becoming available. Also, since the imaging exposure is scanned, the photoreceptor area no longer has to match that of the original document; however, there is still a 1:1 relationship between the toned image on the photoreceptor and the final print.

The change from copiers to printers, particularly small printers, was facilitated by the development of organic photoreceptors and compact light sources. In a printer, the photoreceptor no longer had to be photosensitive to the wavelengths associated with the reflection of white light but rather to wavelengths associated with laser diodes in the near-infrared or LEDs (typically red). The "traditional" selenium-based inorganic photoreceptors are insensitive to light at these wavelengths but were, in a drum configuration, very successfully utilized in larger digital production engines using blue light from relatively bulky gas lasers.

Another change in the process was that the writing system could expose either the background areas (which are toner-free in the final print) or the printed areas (areas where toner is deposited in the final print). Most text-based documents are predominantly "background" and some printers utilize a development system in which the photodischarged areas receive toner. This is called "discharged area development". Exposing the "text" rather than the "background" places fewer demands on the writing system. However, if the image to be reproduced is pictorial, this distinction loses its meaning.

Finally, for a full-color image, an image file is created for each subtractive color: cyan, yellow, magenta, and black (C, M, Y, K). There are several methods for creating a multicolor print. Each color can be successively developed on a single photoreceptor, or a separate photoreceptor can be used for each color. In either case, the developed image can be transferred either directly to the receiver or to an intermediate. All of these methods have been commercialized.

Digital imaging has placed new demands on the OPC: photosensitivity to near-infrared laser and LED exposures, the ability to support the imaging of a halftone pattern of small dots, the need for reduced charge injection from the electrode (blocking layer), and improved lifetime (overcoat layer) are some key features that have been mentioned in review articles.[32−37] In many respects, the shift from black-and-white copying to color printing has been enabled by the simultaneous development of organic photoreceptors with the required physical and photoelectrical characteristics. In the subsequent sections, we will discuss the materials comprising an organic photoreceptor, their functions, and device performance characteristics in the electrophotographic process.

2.4. Organic Photoconductive Materials pre-1993

In this section, we give a brief review of the major topics covered by Law in his 1993 review "Organic Photoconductive Materials: Recent Trends and Developments".[1] This review, with 335 references, is a comprehensive introduction to organic photoconductor materials as utilized in electrophotographic photoreceptors. The review had two major topics: materials and mechanisms.

The largest section, "Classes of Organic Photoconductive Materials", focused on several classes of CGM materials. One group of CGMs is sensitive to exposure with near-infrared light (laser or LED) and the other to visible light (LED). Chemical structures of these materials are given in Figures 5 and 6, respectively. The near-infrared light-sensitive materials include phthalocyanines, squaraines, and trisazo pigments. The visible light-sensitive materials include perylenes, bisazo pigments, the charge transfer complex between poly(*N*-vinyl carbazole) (PVK) and 2,4,7-trinitrofluorenone (TNF), and the dye−polymer "aggregate" between certain thiapyrylium salts such as 4-(4-dimethylaminophenyl)-2,6-diphenylthiapyrylium perchlorate and bisphenol A polycarbonate. Each of these CGMs was discussed in terms of its synthesis, electronic absorption characteristics, solid-state polymorphism, and key electrophotographic characteristics. The latter included spectral range, dark decay of the surface potential and sensitivity to light (erg/cm^2 to photodischarge to one-half the initial potential and/or the rate of photodischarge V/erg/cm^2). A key mechanistic observation is that efficient charge generation occurs when the CGM is in pigment form and the molecules are relatively planar and are stacked face-to-face. Such stacking arrangements give rise to polymorphism. With phthalocyanines, for example, the stacking energetics is relatively weak and many polymorphs have been identified. As a pigment, the long wavelength absorption is red-shifted relative to the absorption in solution, and this has been ascribed to intermolecular

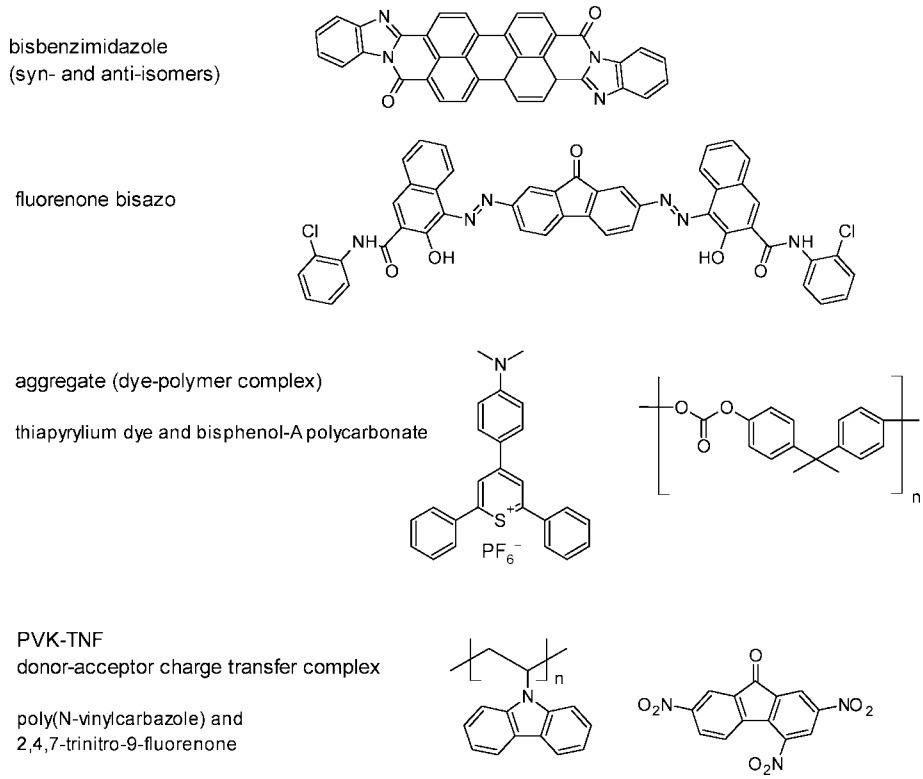

Figure 5. Chemical structures of visible light-sensitive charge-generation materials.

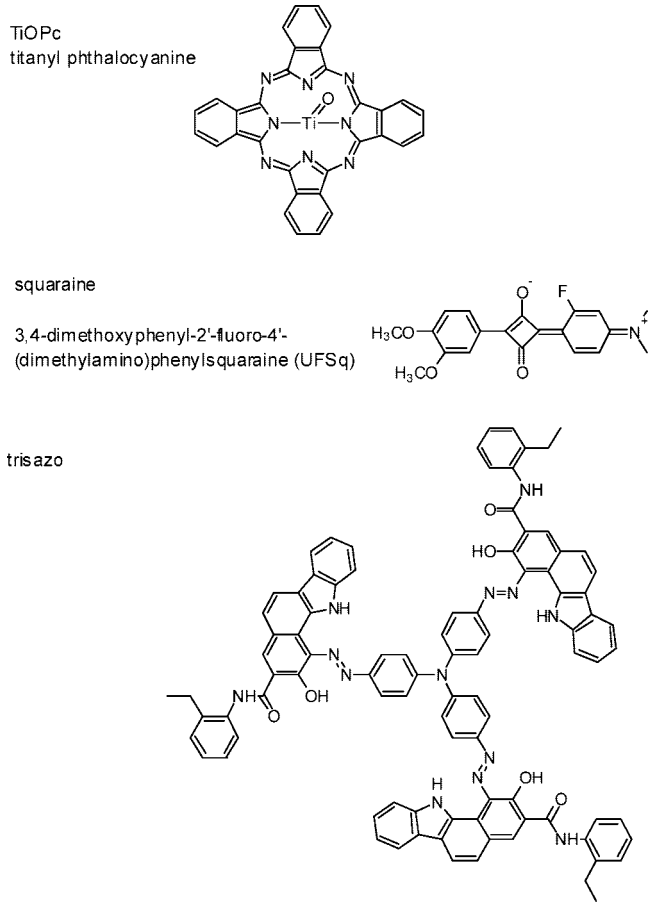

Figure 6. Chemical structures of near-infrared light-sensitive charge-generation materials.

charge-transfer interactions between adjacent molecules in the stack. Polymorphs are usually characterized by their X-ray powder diffraction pattern, but visible, near-infrared,

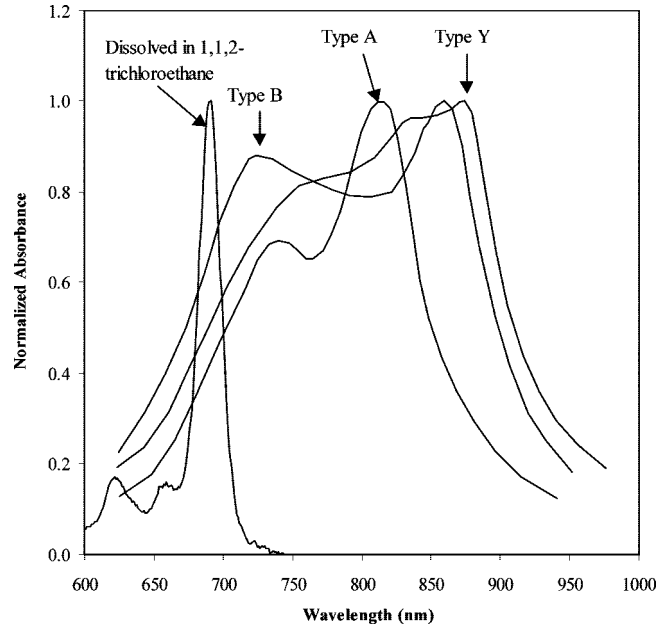

Figure 7. Absorption spectra of TiOPc pigment polymorphs (data from ref 39) and in solution.

and infrared absorption, as well as ^{13}C NMR spectroscopy,[38] have also been used. Figure 7 shows the absorption spectra of the Y, A, and B polymorphs of titanyl phthalocyanine (TiOPc) as reported by Fujimaki et al.[39] compared with TiOPc dissolved in 1,1,2-trichloroethane. Photoreceptors prepared from the three polymorphs (Y, A, and B) had different dark decay (13, 32, and 85 V/s, respectively) and photosensitivity at 800 nm (0.75, 2.50, 1.60 erg/cm^2 for a photodischarge from −600 to −300 V). In other publications, several other polymorphs of TiOPc have been identified. As commented by Law,[1] "some of the compositions reported between different laboratories are similar". Because com-

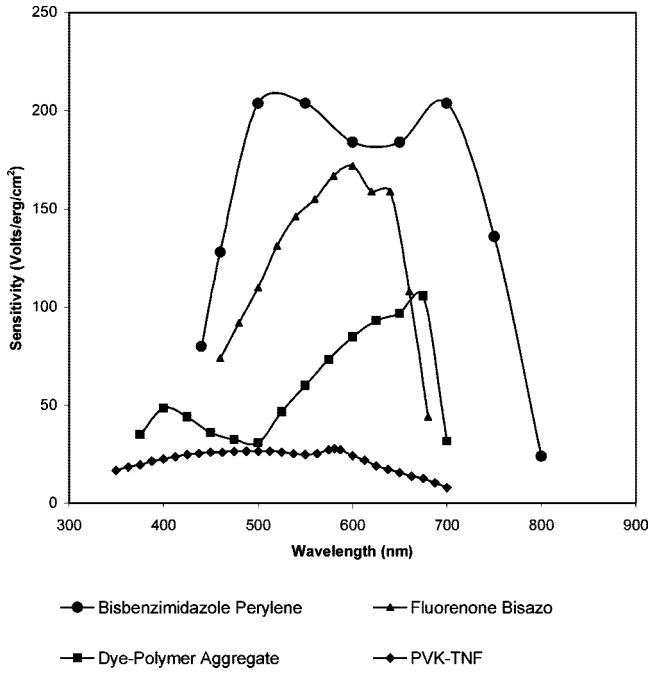

Figure 8. Photosensitivity action spectra of typical visible light-sensitive charge-generation materials: bisbenzimidazole perylene (data from ref 40); dye−polymer aggregate (data from ref 42); fluorenone bisazo (data from ref 41); PVK−TNF (data from ref 43).

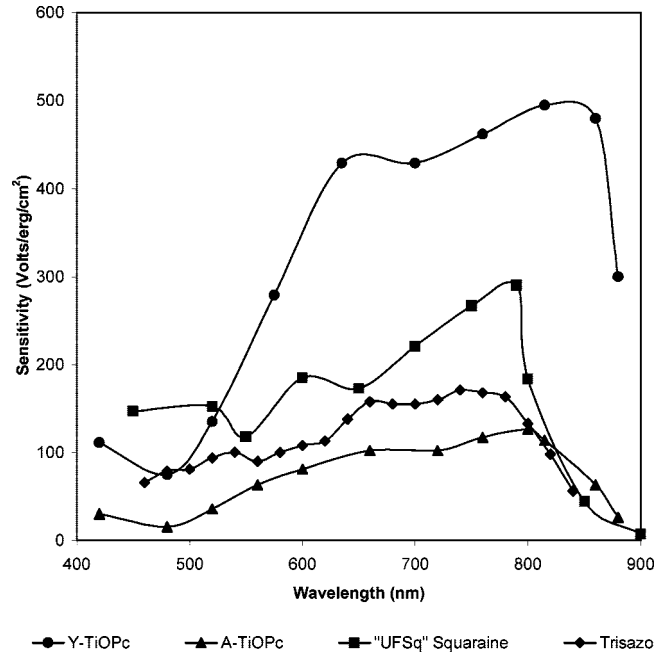

Figure 9. Photosensitivity action spectra of near-infrared light-sensitive charge-generation materials: Y-TiOPc (data from ref 39); A-TiOPc (data from ref 39); "UFSq"; squaraine (data from ref 44); trisazo (data from ref 45).

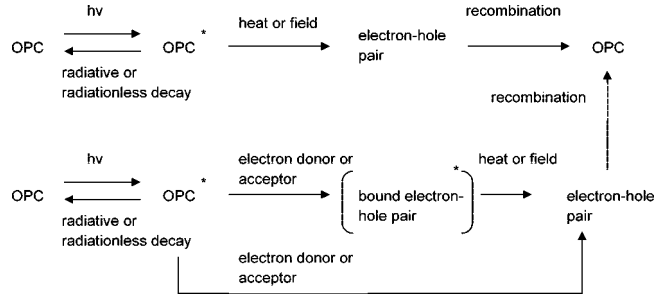

Figure 10. Conceptual scheme for intrinsic and extrinsic (via electron transfer with an electron donor or acceptor as shown) photogeneration adapted from Law.[1]

panies wish to obtain patent rights to unique polymorphs, each will emphasize whatever characterization method shows differences (sometimes small) between their proprietary forms and polymorphs reported by others. The types of generation material pigments used in OPCs have not changed. Copier machines required CGMs sensitive to visible light because the OPC was exposed by reflection from a (sometimes colored) document. OPCs in printers require CGMs that are sensitive to the wavelength of the exposing light, and at the time of Law's review, it appeared that near-infrared laser-exposure systems would dominate. However, the predicted switch to near-infrared exposure systems has not occurred. Electrophotographic printer manufacturers today have the option of choosing either visible or near-infrared laser or LED array exposure systems. Thus, pigments sensitive to visible light and pigments sensitive to near-infrared exposure are all found in commercial OPCs. Figures 8 and 9 show the photosensitivity action spectra for OPCs with CGMs sensitive to visible and near-infrared light, respectively. Comparing OPC sensitivities from different laboratories is problematic because the measured sensitivity depends on many factors besides the CGM: OPC architecture and formulation, OPC capacitance (thickness), the applied field (surface potential), and the method chosen to determine sensitivity. In these figures, the data in publications from various laboratories was recast into the units of V/erg/cm^2: bisbenzimidazole perylene,[40] fluorenone bisazo,[41] dye−polymer aggregate,[42] poly(*N*-vinylcarbazole) and 2,4,7-trinitrofluorenone (PVK−TNF) charge-transfer complex,[43] A-TiOPc and Y-TiOPc[39] "UFSq" squaraine,[44] and trisazo.[45] Thus, the values of the sensitivities are not absolute. Nevertheless, the relative response as a function of wavelength is useful information, and it is found that this generally follows the OPC absorption spectrum.

The section "Mechanistic Studies" discussed photogeneration models and experiments using OPCs based on phthalocyanines, perylenes, and azo pigments and the effect of the hole-transport material on the OPC photosensitivity. Charge generation is either intrinsic or extrinsic as shown in Figure 10. In intrinsic photogeneration, light is absorbed by the charge-generation material (usually dispersed pigment particles) to create an excited state, exciton, which subsequently ionizes to form an electron−hole pair. In extrinsic photogeneration, the excited state reacts with an electron donor or acceptor and the subsequent electron transfer reaction generates the charge pair. This process may or may not proceed via an excited-state complex (exciplex) or charge-transfer complex. In either case, the separation of the initially formed charge pair occurs thermally and/or under the influence of the applied field.

Several experimental techniques have been used to study photogeneration mechanisms in OPCs. Quenching of the CGM fluorescecence by the application of an electric field is a method that has been applied to many materials. Photogeneration in the X-form of TiOPc pigment in the presence of an electron acceptor (2,4,7-trinitrofluorenone) was found to occur via singlet exciton diffusion to the pigment surface and formation of an exciplex with the acceptor.[46] In the absence of an electron acceptor, there is some evidence that O_2 is involved in charge generation of

phthalocyanines. Studies of bisbenzimidazole perylene with electron donors (hole-transport materials) indicate an extrinsic mechanism for charge generation.[47] Studies on charge generation in bisazo and trisazo[45] pigments were reviewed. In all cases, the data were consistent with charge generation involving electron transfer between the pigment exciton and the electron donor hole-transport materials.

In this review, we will focus on research published after 1993. During this time there has been a great deal of research on finding new CGMs and CTMs. However, with increasing sophistication of the printers for which the OPCs were destined, another focus was the optimization of OPC device performance with new materials and/or extra layers. In the next section, we will discuss OPC architecture and layer formulation details. In subsequent sections, we will discuss critical device parameters for OPC performance.

2.5. OPC Development History

In 1970 IBM introduced the Copier I. This was the first machine to use an "organic" photoreceptor. "Organic" is used here in the generic sense to mean polymers, dyes, pigments, additives, etc. that are, in principle, laboratory creations from carbon-based starting materials. The IBM organic photoreceptor was a single layer of photoconductive material coated on a metallized polymer web. The material comprised a 1:1 charge-transfer complex between poly(*N*-vinylcarbazole) (PVK) and 2,4,7-trinitro-9-fluorenone (TNF), and it had low photosensitivity at wavelengths <600 nm (see Figure 8).[43,48] Because of toxicity concerns around TNF, the commercial lifetime of this photoreceptor was relatively short. Nevertheless, it demonstrated the feasibility of an "organic" photoreceptor in the electrophotographic process and it stimulated extensive research on the mechanistic details around charge generation and charge transport in organic materials. In 1978, the Eastman Kodak Company introduced a single-layer OPC based on a complex between a pyryllium dye and bisphenol A polycarbonate.[49−51] This photoreceptor had high photosensitivity to approximately 700 nm (see Figure 8). In the late 1970s, charge-generation materials were developed with sensitivity to near-IR laser exposure.[52] Today, EP machines utilize exposure systems of either visible-light LED arrays or near-IR lasers and essentially all electrophotographic photoreceptors are OPCs. The major exceptions are machines that utilize amorphous silicon based photoreceptors. Amorphous silicon photoreceptors are durable but expensive to manufacture, and the market penetration is low. In subsequent sections, we will describe how OPCs have continued to evolve with the aim of improved device performance in the electrophotographic system.

3. OPC Architecture and Fabrication for Digital Printers

The OPC is a large-area thin-film device formulated to optimize photogeneration and transport of charge to create an electrostatic latent image on the OPC surface. If one examines reviews of OPC technology, one sees that, shortly after the introduction of OPCs, comparisons were made between OPCs and other photoreceptor materials such as a-Si, Se, and As_2Se_3, and this later evolved into discussions over specific OPC materials for charge generation using laser and LED exposures, improved charge transport, and improved wear resistance.[6,33,37,53]

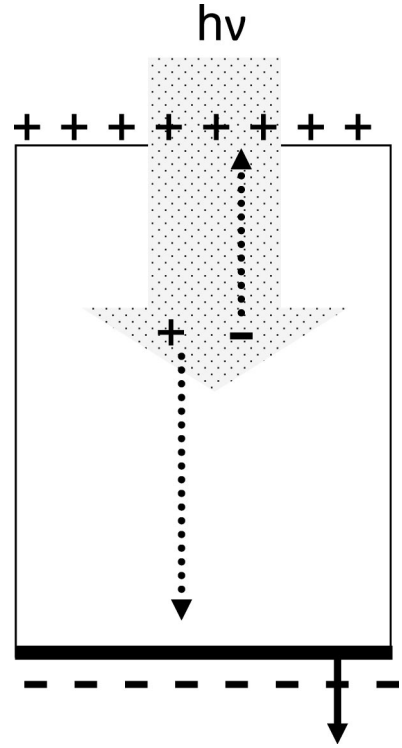

Figure 11. Schematic of photodischarge of a positively charged single-layer organic photoreceptor. The ground electrode is represented by a solid black line. Light is absorbed throughout the device and photogenerated charge drifts in the applied field as shown, resulting in photodischarge.

Current products utilize OPCs with surface areas from 200 to 10 000 cm^2. Small-area OPCs were developed for low-volume home and small office machines where a small machine footprint is important, while the large-area OPCs are found in high-volume commercial printers. Several OPC architectures have been commercialized. The simplest is the so-called single-layer OPC. In this architecture, the materials for both charge generation and charge transport are formulated into a single layer. Thus, light absorption occurs throughout the layer and both holes and electrons are transported to effect photodischarge. This is shown schematically in Figure 11. In principle, the single-layer architecture can be photodischarged by exposure through the free surface with either a positive or negative surface charge, but in practice the former is preferred because hole transport is much more effective than electron transport. This will be discussed in more detail later (section 6). The most common architecture, particularly in high-volume printers, is the dual-layer OPC. In this architecture, the charge-generation and charge-transport functions are formulated in separate layers with a relatively thin charge-generation layer (CGL) near the electrode, which is overcoated with a thick (hole-transporting) charge-transport layer (CTL). Dual-layer OPCs with this architecture must be negatively charged. Alternative OPC architectures will be discussed later (section 3.5).

3.1. Single-Layer Versus Dual-Layer OPCs

In the simplest embodiment of an OPC, the photoconductor is a single layer with several components: insulating polymer binder, CGM (usually phase separated from the polymer binder as a dispersed pigment or a molecular complex formed in situ), hole-transporting CTM (h-CTM), and electron-transporting CTM (e-CTM). The CTMs are

dissolved in the binder polymer. Since both positive charge (holes) and negative charge (electrons) must be transported to completely discharge the surface voltage (Figure 11), both types of CTMs are generally present.[54] Although charge generation occurs in the CGM, this material is present at low concentration and dispersed in the binder polymer. Therefore, charge transport must occur by first "injecting" the charge from the CGM into the appropriate charge-transport material dissolved in the binder polymer. Because charge transport is a strong function of CTM concentration and the presence of >50 wt % of monomeric CTM will degrade the OPC physical characteristics, it is necessary to optimize the relative amounts of hole and electron CTM.[55] Because electron transport is much less efficient than hole transport, single-layer OPCs are usually formulated such that hole transport is dominant. This requires that they receive a positive surface charge for front surface exposure or a negative surface charge for rear exposure. One way to avoid degrading the physical characteristics due to the addition of monomeric CTM is to incorporate the CTM moiety into a polymer.

Because of the reliance on both hole and electron transport in single-layer OPCs, their performance is generally inferior to the dual-layer OPC architectures. However, for low-volume applications, the performance characteristics are adequate, and because of their lower manufacturing cost (fewer functional layers), single-layer OPCs are often used in home and small-office EP printers.

In the dual-layer OPC, each layer is optimized for its specific photoelectric function such that optimum performance is obtained with this architecture. In the electrophotographic process, a dual-layer OPC receives a negative surface charge. Light is absorbed in the CGL and the photogenerated positive charge is transported through the CTL as shown in Figure 12. At the same time, to completely erase the field lines in the exposed area, negative charge must move to neutralize the positive countercharge residing on the ground plane. The latter must occur to also avoid degredative buildup of negative space charge in the CGL.

Typically, the OPC thickness is 20−25 μm and the surface potential is 400−800 V. This is the result of a balance between several competing requirements. One factor is the maximum toner density required for image quality. Thus, for monolayer toner coverage, one needs to match the OPC and toner surface charge densities. Assuming a parallel plate capacitor model, an OPC of 20 μm at −500 V has a surface charge density of 4×10^{11} charges/cm^2. A typical charge-to-mass ratio of toner is around 15 μC/g, so for a 5 μm diameter particle, the charge density is 4×10^{11} charges/cm^2. A high OPC surface potential is desirable because charge transport is field-driven, and in addition, the high field between the OPC and the developer station is what drives the toner particles to the OPC surface. If the OPC is thicker the capacitance is lower so to maintain toner coverage, the surface potential has to be increased or the toner charge-to-mass has to be decreased. However, too high a field across the OPC can cause an unacceptable increase in dark decay, and a low toner charge-to-mass increases toner "dusting". If the OPC is made thinner, the surface potential must be lowered and/or the toner charge-to-mass ratio raised to maintain toner coverage, and these changes can have an adverse effects. In a study of the dark and photoelectrical characteristics of a single-layer OPC, it was determined that the optimum thickness was 15−20 μm.[56] Single-layer OPCs

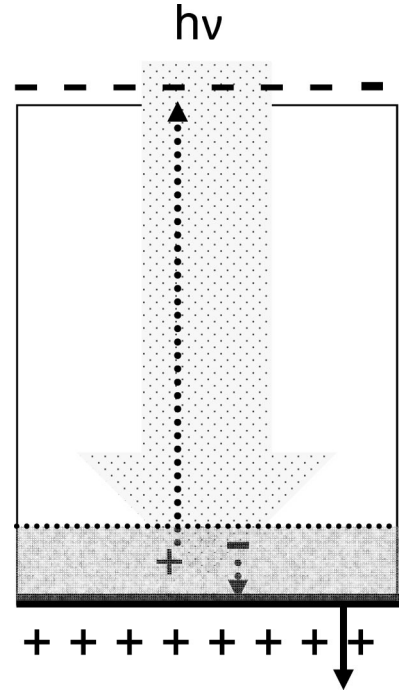

Figure 12. Dual-layer OPC architecture. In this diagram, the relatively thin charge-generation layer (CGL) is textured and the relatively thick charge-transport layer (CTL) is clear. The ground electrode is represented by a solid black line. Light absorption and photogeneration occur in the CGL, and charge is subsequently transported as shown to effect photodischarge. In this OPC architecture, photodischarge occurs mainly through the transport of positive charge (holes).

of 5−30 μm were prepared. The CGM titanyl phthalocyanine (TiOPc); the hole-transporting CTM, a dimeric hydrazone hole-transport CTM prepared from *p*-diphenylaminobenzaldehyde; the electron-transport CTM, 1,1-dioxo-2-(4-isopropylphenyl)-6-phenyl-4-(dicyanomethylidene)thiopyran; and polyvinylbutyral binder polymer were used in the ratio 1:16:4:4.5. This study included the following OPC characteristics: positive and negative corona charging, photosensitivity, and residual potential. With the thick OPC, the photosensitivity at 840 nm (strongly absorbed by the CGM) with positive charging was almost an order of magnitude higher than for the negatively charged OPC. This was interpreted as indicating that there is minimal contribution of electron transport in the photodischarge because the mobility of electrons with this CTM is $<10^{-8}$ cm^2/(V s), which is 2−3 orders of magnitude less than that of the hole CTM.

There are several other considerations with regard to thickness for OPCs in a digital process. In the standard dual-layer configuration, positive charge is transported from the CGL through the bulk of the device to the OPC surface. During this transit, the charges will experience Coulombic repulsion, which causes the width of the latent image on the OPC surface to be larger than that of the exposed area in the CGL.[36] This causes a decrease in resolution, and at some point, the halftone dot structure will be compromised. Such an effect has been reported.[57] Chen has calculated that the optimum OPC thickness is about one-fourth the pixel size.[35] Thus, for 1200 dpi imaging, the ideal OPC thickness would be 5 μm. If charge generation occurs at the OPC surface, this effect will not be observed. Chen has also calculated that, in the formation of a single-pixel line latent image, there is little difference between a single-layer and dual-layer OPC.[58] However, Mizuta and co-workers report that, in an

experiment with 12 μm OPCs using liquid toner (<1 μm particle size), an image of lines with 10 μm separation could be achieved with a single-layer but not a dual-layer OPC.[59] Aizawa and co-workers have developed a technique to measure the width of a latent image and have found that, with a dual-layer OPC, the latent image width increases as the OPC thickness increases and also increases with increasing hole mobility.[60] It is suggested that the latter effect is due to increased lateral spread of holes as they transit the OPC.

3.2. OPC Formulation Basics and Fabrication

As we have shown, OPCs are multilayered. In this section, we discuss some of the basics for formulating and coating the photoconductive layers. The key formulations are those of the CGL and CTL. CGLs are generally pigment dispersions prepared by milling of pigment and binder in an appropriate solvent. Pigment polymorphism is often an important factor, and this will be discussed in a subsequent section. The key functional characteristic of the CGL is that the pigment absorbs the imaging light and generates charge. The CGL formulation may or may not have hole and/or electron charge-transport materials.

The CTL is formulated as a solution containing the binder polymer and charge-transport materials (CTMs). The CTM concentration is usually 40−50% by weight of the CTL. When the CTL is the top surface and contacts the various EP process elements, its abrasive wear characteristics are important. It has been found that abrasive wear is related to the polymer entanglement density with bisphenol A polycarbonate.[61] As the binder polymer molecular weight increases or the CTM content decreases, the entanglement density increases and the wear characteristics are improved.

It is highly desirable that the coated OPC have a very smooth surface. Coatings out of organic solvents can have a variety of surface artifacts related to drying conditions. To prevent this, virtually all OPC formulations contain trace quantities of a surface-active component (surfactant). The specific surfactant is chosen such that it has no effect on OPC performance, but it is worth mentioning because it is almost always present in the top layer of the OPC.

A final component, often added to OPCs, is an antioxidant at around a few wt % to retard oxidation due to exposure to the oxidizing chemicals produced during corona charging.

In all architectures of OPCs, after light absorption by the CGM and charge generation, to accomplish complete photodischarge, both positive and negative charges must drift under the influence of the applied field to the oppositely charged surface. If the transport of either sign of charge is inefficient, photodischarge will be incomplete. A key electronic characteristic of CTMs is that hole transport is much more effective than electron transport. As a consequence, all commercialized OPCs rely on hole transport as the dominant process in OPC photodischarge. Thus, to be effective, single-layer OPCs must include an electron-transport material in the formulation, and in dual-layer OPCs, the CGL is typically very thin (submicrometer) and may also include electron-transport materials. In subsequent sections, we will discuss the mechanistic details around the materials and mechanisms of charge generation and transport and how charge-transport characteristics impact image formation in the EP process.

An important consideration in coating multilayer films is control of interlayer mixing. If there is no mixing, the layers will not adhere to each other, and if there is complete mixing, the unique functionality of the layers will be lost. So penetration of the coating fluid into a previously coated layer must be just right. Formulation and coating expertise is obtained through experience, and developing a manufacturable OPC requires empirical optimization. Changing the degree of layer mixing can dramatically affect OPC performance, even though the overall composition is the same. It is important to keep this in mind because it is not only the materials in the layers but also how the multilayer structure has been prepared that determines OPC performance.

OPCs are mainly configured as drums or belts. In both cases, essentially identical photoconductive formulations are on a conductive layer that is grounded in the EP process. Drums are generally aluminum with diameters of 1 in. to about 10 in. In this case, the aluminum serves as the substrate as well as the electrode. Belts are often poly(ethylene terephthalate) or a similar polymer film on which is deposited a thin layer of metal to serve as the electrode. Common metals are Ni, Al, Ti, etc.

Fabrication of a belt OPC begins with a large roll (web) of metalized substrate. Typically all of the other OPC layers are coated on the web by pumping the solution or dispersion through a hopper onto the moving substrate. A typical coating order might be thin adhesive layer, charge-injection blocking layer, CGL, CTL, grounding stripe. Web-coating speeds can be fast (>10 m/s), and long footage (tens of thousands of feet) can be prepared at low cost. In addition to the photoconductive layers, it is necessary to coat an edge stripe of conductive lacquer that contacts the electrode. It is through the edge stripe that ground contact is made to the OPC belt in the electrophotographic printer. It is often possible to coat the layers sequentially in one pass as long as the initially coated layer is dried sufficiently such that it is not damaged during the overcoat process. After each layer is coated, the web passes through a drying section. Residual solvent levels must be kept very low to avoid deleterious effects on the OPC photoelectrical characteristics. CGL formulations are generally dispersions and CTL formulations solutions and they are in-line filtered in the coating process. Solution and/or dispersion stability is not a major issue because formulations can be prepared just prior to coating. The dried OPC web is then slit to width and chopped to length. Often there is a physical inspection for coating defects prior to chopping. The cut-to-size OPC may receive perforations or markings at this stage of fabrication so its position can be monitored in the machine. Finally, the belt is formed by ultrasonic sealing. Commercial OPC belts may be anywhere from 1 to 4 ft in diameter, and the width is determined by the size of the receiver to be used in the printing machine. Key advantages of the OPC belt configuration are low substrate cost, low fabrication cost, and large size (gives flexibility to the positioning of the various EP process elements and allows for several image frames in a single belt revolution). Disadvantages include possible mechanical failure of the substrate (particularly the seam), web "kinking" during handling, plastic deformation, loss of ground contact due to wear of the conductive stripe, the need to keep track of the seam that cannot be imaged, and the need to monitor and control the belt position to accommodate belt flutter.

Drum OPCs are fabricated by dip- or ring-coating of the various layers. In both processes, the drum is dipped into a tank of solution or dispersion and slowly withdrawn to create the desired layer. In dip-coating, the layer thickness is

determined by the withdrawal speed and the physical characteristics of the formulation. In ring-coating, the drum is withdrawn through an annulus which determines the thickness of the liquid on the drum. For multilayer coatings, the drum with a dried layer is dipped into another tank containing the formulation for the subsequent layer. Since the previously coated layer is in contact with the second-layer formulation for a considerable time, the choice of solvent is critical to obtain the appropriate layer interface. As formulation is removed from the coating tank, it is replenished from a reservoir. To fabricate the OPC, each layer is coated separately in a batch process. Dip-coating formulations must be optimized for long life in the dip-coating tank and for coating quality.[62] For example, in a dip-coating, gravity will cause the coated layer to sag such that, at the bottom of the tube, the layer will be thicker. A typical dip coating order might be as follows: a single layer for smoothing (see below) and charge-injection blocking, CGL, and CTL. Thus, even though a web and a drum OPC may have identical final-layer compositions, the formulations used to prepare these layers may be very different.

Prior to coating, the aluminum receives specific finishing treatments depending on the application. The surface on which the layers are coated must be smooth, and this might be accomplished with diamond turning or a similar finishing operation. If a laser exposure is to be used in the EP process, any light not absorbed in the CGL will be reflected and cause an interference pattern in the image. This can be prevented by specific surface patterning to scatter any nonabsorbed light. To prevent dark charge injection, the Al might be anodized. Another way to accomplish these objectives is to coat one or more layers on the "raw" aluminum tube to carry out the functions of smoothing, charge-injection blocking, and light scattering. The drum metal serves as the ground electrode in the EP process. Advantages of drum OPCs include lack of a seam and a fixed position in the EP process. Disadvantages include substrate cost (for large, high-quality tubes), lack of space for EP process elements, and high fabrication cost due to a sequential batch manufacturing process. For home and small-office applications, the high manufacturing cost structure of drum OPCs has been negated with the use of inexpensive, thin-walled tubes, by coating many tubes in a single dip, and by ultrahigh manufacturing volumes. For high-quality, high-volume machines, one finds both belt and drum OPCs in use.

The electrode is often overlooked but is a critical OPC component since it serves as the ground plane for all the electrophotographic processes occurring at the OPC. Chen has calculated that the upper limit for the sheet resistance of the conductive layer is $\sim 10^4$ Ω per square.[63] Nonuniform corona charging is the consequence of too high a resistivity. For drums, the Al serves as the electrode, and in most commercial belts, the electrode is a vacuum-deposited metal (Al, Ti, Ni, etc.). If "rear" exposure is part of the EP process, it is necessary that the electrode be transparent to the exposing light.[64] Other conductive materials have been developed such as nanodispersed semiconductor coatings, but most commercial belt OPCs use the metalized polymer.

In commercial OPCs, there are usually additional layers that perform specific functions. Two commonly added layers are an undercoat layer (UCL) and an overcoat layer (OCL). The UCL layer is placed between the electrode and the CGL. It might serve several purposes:

(1) A charge-injection blocking layer (BL) to prevent unwanted dark-charge injection from the electrode into the OPC. At the high fields produced by charging the OPC (25−35 V/μm), the possibility exists that there might be significant charge injection from the electrode into the OPC. If the OPC has a negative surface charge, the injected holes would be efficiently transported through the bulk of the OPC. This might result in a high rate of overall dark discharge or the dark decay might be localized at the site of a small coating defect. In an EP process where the discharged areas are developed with toner, localized dark injection produces what are called "charge-deficient spots" that are visible as small toned areas in an area of the print where there should be no toner. If numerous, this is an objectionable print defect. Either condition is undesirable, so a hole-injection blocking layer is quite common. Since this layer is an insulator with respect to hole injection and transport, its use in an OPC will result in a residual potential after photodischarge. Thus, with such materials, the BL is made as thin as possible ($\sim$1 μm). Recent research has revealed that polymers having bound electron-transporting CTMs, which allow accumulated negative charge in the CGL to pass to ground, are especially effective hole BLs.

(2) The undercoat layer may serve a smoothing function. In particular when the substrate is aluminum, the initially prepared surface is usually rough and a relatively thick smoothing layer (several micrometers) is added between the substrate and the CGL. This layer may also serve as a charge-injection BL and, if appropriately formulated, as a light-scattering layer to prevent interference patterns due to reflected light from a laser exposure. As with the BL, if this layer is insulating, an undesirable residual potential will be observed when the OPC is photodischarged. Thus, it must simultaneously block charge injection from the electrode and allow transport of charge of the opposite sign from the CGL to ground.

(3) Finally, the undercoat layer may serve as an adhesive tie-layer to ensure that the adjacent layer adheres to the electrode surface. For use as an adhesive, the undercoat layer is very thin (<1 μm).

In the electrophotographic process, the photoreceptor surface is contacted by several process elements (cleaning, development, toner transfer) and is exposed to the corrosive chemicals from the corona chargers. An overcoat layer may protect the OPC from physical wear and damage as well as chemical attack.

3.3. Production Release Criteria

Because OPC performance is incredibly sensitive to trace impurities, great care is taken to ensure that all formulation materials meet strict purity specifications. Nevertheless, the only way to be sure that the materials are acceptable is to actually fabricate the OPC and submit it to rigorous EP testing. This will typically occur when there is a new "batch" of a formulation material. Fabrication "events" are also monitored with rigorous EP testing of the OPC before product release.

Since the OPC is a large-area device, the device characteristics (physical, dark electrical, photoelectrical) must be uniform. Defects of pixel size (40 μm for 600 dpi) or greater are unacceptable. This places a premium on cleanliness and coating quality (uniform and defect-free). The uniformity requirement may not be obvious. Since the OPC can be treated as a parallel place capacitor, the surface potential is

directly related to the capacitance, which is inversely related to the film thickness. For a 25 μm OPC with a surface potential of 500 V, a 5 μm deviation in thickness will change the surface potential by 100 V. This may be insignificant in a low-quality binary desktop printer but will be unacceptable in a high-quality office or production printer utilizing a multilevel exposure where surface potential deviations of ~10 V will produce noticeable print artifacts.

As a large-area device, it is obvious that any coating defects will produce image artifacts. The level of screening depends on the requirements of the printer for which the OPC is intended. For high-quality EP printers where the OPC is an expensive replaceable part, visual inspection is required. This may be of a small subset or up to 100% inspection. Since digital EP images consist of a halftone array where the pixels are on the order of a few tens of micrometers in diameter, coating defects of this size, if present in sufficient numbers, will cause observable print defects. Because such small coating defects are not visible to the naked eye, full EP process testing is a necessary component of the release-for-sale process. Such testing may be carried out on a sample from every production "event".

Finally, before release, a subset of a production run is subjected to electrical-only electrophotographic testing. Electrical-only testing typically involves multiple cycles of corona charging, exposure, and erase (10 000 or more cycles would not be unusual) under nominal and other designated environments of temperature and humidity. The OPC characteristics of interest are chargeability (initial surface potential and dark decay with standard corona charging set points), photosensitivity (photodischarge with a known exposure), and residual potential (after erase). These characteristics must remain constant or changes must be slow enough for compensation by the process control in the printer for which the OPC is intended.

3.4. Dual-Layer OPC Examples

A few recent examples of OPCs will illustrate how the architecture is structured for maximum performance in the EP process.

In recent publications, the OPCs used in some Ricoh printers have been described in detail. One OPC was for use in a monochrome multifunctional printer (Ricoh Imagio MP1350) with a printing speed of 135 pages per minute.[66] An OPC life of 2 million prints was achieved. The baseline OPC architecture had an aluminum drum, an undercoat smoothing layer (SL) with inorganic pigment filler, CGL, and CTL. The first step in improving OPC life in the machine was to identify the major cause of OPC removal. It was found that this was due to what they called "background fouling". Their EP process utilized a development system in which photodischarged areas of the OPC were developed with toner. OPCs were found to have increasing dark decay with use, and eventually the dark decay lowered the surface potential such that toner was developed in areas that should be "white". Eventually this became noticeable, and the OPC had to be removed. It was determined that the mechanism was high-field hole injection from the aluminum drum substrate, and three measures were taken. First, an undercoat hole-blocking layer (BL) was coated between the substrate and the undercoat-smoothing layer (SL). Second, the CTL thickness was increased to reduce the field across the OPC. Third, the OPC cleaning system was redesigned to reduce abrasive wear and scratching of the OPC. In their conventional OPC cleaning system, the cleaning brush rotated in a direction opposite that of the OPC. In the redesigned system, the brush and the OPC rotate in the same direction at slightly different speeds. With the new architecture and cleaning system, the OPC charging stability was degraded and it was necessary to improve the electrical conductivity of the UL by optimizing the amount of inorganic pigment filler.

A photoreceptor with different architecture was developed for the Ricoh Aficio AP3800C color printer.[67] In this paper, an OPC was described with a 5 μm metal oxide reinforced protective overcoat layer (OCL). The OPC architecture is aluminum drum, undercoat layer of inorganic pigment in a binder, CGL, CTL, and OCL. The addition of alumina had a dramatic effect on the OPC wear rate depending on the specifics of the EP process. However, it was necessary to add several components to achieve the objective. First, hole-transport material was added to prevent an undesirable residual potential. The OCL is essentially a second, more wear-resistant, CTL. Second was the addition of an unsaturated polycarboxylic acid to act as a particle stabilizer for the alumina in the binder polymer. Third, an antioxidant was added to prevent image smearing due to corona gases. It was found that the reduction in wear rate correlated with in increase in image defects due to increased OPC surface conductivity. So, the amount of filler was adjusted to obtain the optimum wear rate in the EP process.

3.5. Alternative Dual-Layer Architectures

There are two alternative dual-layer OPC architectures that have received attention. Both relate to having an OPC that functions with a positive surface potential. Positive charging has the advantage that corona charging is more uniform and less corona byproducts are produced.

3.5.1. Inverted Dual-Layer

One method is to invert the standard dual-layer architecture with the CGL being the free, corona-charged surface.

The main disadvantage of the inverse dual-layer architecture is that the CGL is very sensitive to corona gases (see Corona Fatigue, section 9.1) and wear in the EP process. However, with a protective overcoat, this architecture has excellent performance. A positive charging OPC for a liquid toner EP process has been developed by a group from Samsung Electronics Co.[68] The architecture for this OPC is inverse dual-layer with the CGL as the "top" layer. Liquid toner uses a hydrocarbon liquid carrier (Norpar 12, Exxon), so it was necessary to put a protective overcoat on the CGL to prevent leaching. In addition, the toner particles in a liquid toner are very small (submicrometer) and have a high charge-to-mass ratio. Therefore, it was necessary to increase the OPC surface charge density at a given surface potential by increasing the OPC capacitance (thin OPC). The substrate was a polished aluminum drum. The primary CTL binder was polycarbonate-Z and the CTM was a carbazole hydrazone dimer in a 1:1 ratio. The CTL was ring-coated out of THF. The CGL was TiOPc in polyvinylbutyral (PVB). Considerable experimentation was required to identify a CGL solvent that would give the optimum CTL−CGL interface. Mixtures of butyl and ethyl acetate were used. The CTL totally dissolved when the CGL solvent was 100% butyl acetate. When 100% ethyl acetate was used, the CGL−CTL interface looked good but the resulting photoreceptor gave a high residual potential when photodischarged. Because the

CGL formulation contained no hole-transport material, it was speculated that the high residual potential might be because the CTM in the CTL had low solubility in this solvent and, therefore, did not diffuse sufficiently into the CGL during the coating operation. The CTM was more soluble in butyl acetate, but coatings using a butyl-to-ethyl acetate ratio of 7:3 had poor surface uniformity. This dilemma was solved by modifying the CTL by the addition of a second CTM with greater solubility in ethyl acetate. Thus, to achieve optimum OPC performance, the CTL formulation was modified to contain two CTMs in a 1:1 ratio and the CGL solvent was a 3:7 ratio of butyl to ethyl acetate. The overcoat was prepared from an aqueous polyurethane dispersion. Because the overcoat is relatively insulating, the residual potential increased with charge/expose/erase electrical cycling, but the increase was within the limits of acceptability.

3.5.2. Dual-Layer with Electron-Transporting CTL

Another method uses the standard dual-layer geometry but formulates the CTL such that electrons are transported rather than holes. Considerable research has been carried out to develop polymer films that transport electrons, and in some cases, these have been used as CTLs in positive charging dual-layer OPCs. Unfortunately, because of electron-transport limitations in the CTL, this type of OPC has to our knowledge not been commercialized. See section 6.3 for discussion of dual-layer OPCs based on electron-transporting CTLs.

4. OPC Characterization and Critical-to-Function Performance Characteristics

There are many excellent reviews on the physics of xerography and the critical-to-function performance factors required of the photoreceptor.[69−71] As mentioned above, OPC characterization is a standard part of an OPC production release protocol. In addition, characterizations are carried out to determine the effects of changes in formulation and/or architecture. Measurements to determine fundamental characteristics (dark decay, photosensitivity, quantum efficiency, charge mobility, etc.) are often carried out on photoreceptors, which differ from what might be eventually used in a printer. The layer of interest (CGL or CTL) may be isolated or the OPC may be modified with the application of a vacuum-deposited electrode (Au is common) on the free surface.

For an OPC in an electrophotographic process, it is the critical machine parameters that drive the device and, therefore, the materials requirements. Cyclic operation establishes associated dwell times within which each of the underlying photoelectronic processes must be carried to completion in the OPC. Following the charging step, surface charge must be retained until the photoreceptor reaches the exposure station, clearly imposing a limit on the acceptable rate of dark decay. Exposure must result in complete discharge of relevant areas by the time the OPC has reached the development zone. In addition to a photosensitivity requirement for the CGL with a given light source, the photodischarge rate specifies the transit time required for photoinjected carriers, which in turn specifies a drift mobility (mean velocity of carriers per unit applied field). The requirement that each cycle result in uniform print quality implies that the OPC must be uniformly discharged and clean at initiation. "Cyclic stability" imposes two requirements, namely, that there be minimal trapping at the interfaces between functional layers and that there be virtually no bulk trapping of space charge in the bulk of the OPC.

4.1. Dark Decay

A key step in the electrophotographic (EP) process is the creation of a surface charge on the insulating OPC. An OPC resistivity of 10^{14} Ω cm will produce a dark decay of ∼20 V/s at a field of 2×10^5 V/cm. For a standard dual-layer OPC, the surface charge is always negative. For a single-layer OPC, the surface charge can have either polarity. In all of today's EP printers, charge is applied by creating an air corona of appropriate polarity near the OPC surface such that the ions are attracted to the OPC ground plane and accumulate on the surface of the intervening insulating OPC. The charging device may employ a thin wire (as in a coratron or scoratron) or a conductive roller held at high potential. OPCs are usually treated as perfect insulators, so a parallel plate capacitor is an appropriate model. Thus, the surface charge density (Q) and surface potential (V) are related through the capacitance (C) as $Q = CV$. The capacitance per unit area (A) is determined by the materials dielectric constant (ε) and thickness (l) as $(C/A) = (\varepsilon\ \varepsilon_0)/l$, where ε_0 is permittivity of free space. A relative dielectric constant of 3, verified by bridge measurements, is typical for the nonpolar compositions used. For an OPC of 25 μm with a surface potential of 500 V, C/A is 3.2×10^{-10} Farads/cm^2, corresponding to a surface charge density of 10^{12} charges/cm^2. Assuming the surface is composed of molecules with an area of 100 Å^2 (10^{-14} cm^2/molecule), only ∼1% of the surface molecules are associated with the surface charge. From these relationships, it is clear that, for a fixed surface potential as the OPC thickness increases, the surface charge density decreases. However, the field ($E = V/l$) across the thicker OPC is lower, so field-dependent processes such as charge generation and transport will be less effective. As discussed previously, to obtain the desired print density there is a complex interplay between the OPC initial and exposed surface potentials, the surface charge density, and the toner charge per mass and development station bias.

Dark decay (V/s) is an important characteristic of an OPC because, although process control will attempt to maintain V_0 and V_{DD}, an electrophotographic printing system will in general not tolerate a significant drop in V_0. Such a drop will lower the available image potential for toner development. Also, in a discharged development process, if the dark decay becomes too great (or to put it more accurately, the surface potential in nonexposed areas becomes too low), a low density of toner particles (background development) may occur. At some level, this becomes an unacceptable image artifact. If the dark decay becomes nonuniform, it may produce nonuniform photodischarge and development.

A quantity of interest is the rate of dark discharge (V/s) as a function of time, field, and environment, relative to the time between corona charging, exposure, and development.

Dark decay in an OPC is mainly due to the transport of holes, and where and how these charges originate has been the subject of many investigations. Holes in the OPC can originate via charge injection from the ground electrode or the OPC free surface, or from the bulk from the CGM and/or CTM or a combination of sources. In general, the surface potential of an OPC will increase with corona charging and eventually level off as the internal field approaches ∼10^6 V/cm. On exiting the corona charger, the surface potential dark decays at a rate that is typically initially rapid and

decreases with time (Figure 2). The details of the dark decay are complex and depend on the nature of the corona-charging device, environmental conditions, and prior charge/expose history of the OPC. This is an important point: the charging and dark-decay characteristics of an OPC are not solely a characteristic of the materials but are influenced by the EP process in which it is being used.

Since OPCs are formulated for hole transport, the following discussion will neglect any contribution of electron transport to dark decay. Of course, electron transport must be considered in OPCs so formulated.

In electrophotographic processes, the OPC surface potential may range from about −400 to −800 V. Electrode materials with high work functions (Ni, Ti, Cu, Al) are generally chosen as the ground layer to minimize hole injection. Since charge injection from the electrode is undesirable, a thin charge-injection blocking layer is usually coated on the electrode to prevent direct contact with the materials of the OPC (CGM and CTM). It has been shown that a CTL can make ohmic contact with an electrode such as Au or carbon-filled polymer, and in fact, the current characteristics from such contacts have been used to extract useful data relating to hole mobility.[72,73] Thus, at high fields or with certain electrodes, hole injection into the OPC can occur. Details about the blocking layer will be discussed in section 7.

Charge injection from the free, corona-charged surface is unlikely when the surface is negatively charged, because OPCs are devices in which the primary carriers are holes. Nevertheless, if CGM is at or near the surface (as in a single-layer or an inverse dual-layer OPC), negative charge injection is possible. It is possible for positive charge to be injected into the OPC surface because the oxidizing species in the air corona have the potential to oxidize the CTM to its radical cation.[74] This chemistry is discussed in more detail in section 9.1.

Finally, if charge is trapped in the bulk of the OPC, it can be released and transported through the OPC as the applied field increases during corona charging. Charge depletion during charging is a characteristic of many OPCs, and Mishra and Pai have calculated the expected dependence of surface potential on surface charge density.[75] The expected capacitive charging, $Q = CV$, is not observed because charges released during charging reduce the surface potential. When all available charge has been removed, the charging will continue capacitively. Results were presented for a dual-layer OPC with a 25 μm CTL and 1 μm CGL, and it was found that there was a "continuum" of carrier release times, indicating that, during corona charging, depletion will occur both under the charger and after the OPC exits the charger. The latter is what is typically characterized as "dark decay".

Scott and Lo have examined the dark-decay characteristics of films of *p*-diethylaminobenzaldehyde-1,1-diphenyl hydrazone (DEH) in bisphenol A polycarbonate and concluded that the data was consistent with charge injection from the Al electrode and depletion charging.[76] An activation energy of 0.54 eV was obtained from the dark-decay rate as a function of temperature.

Several groups have investigated the charging characteristics of OPCs to investigate the sources and characteristics of the trapped charge. Lin and co-workers used an electrical-only system to determine the dark decay upon exiting a corona charger before and after irradiation with a halogen lamp (8 mW/cm^2).[77] The dark-decay characteristics (V vs time) were differentiated to obtain the current (dV/dt) and the difference between the before and after exposure charging current ascribed to the detrapped charge. The amount of trapped charge was found to increase with increasing exposure, indicating that charge generation and trapping are CGM related.[78] In subsequent work, they found that the amount of trapped charge increased with CGL thickness.[79]

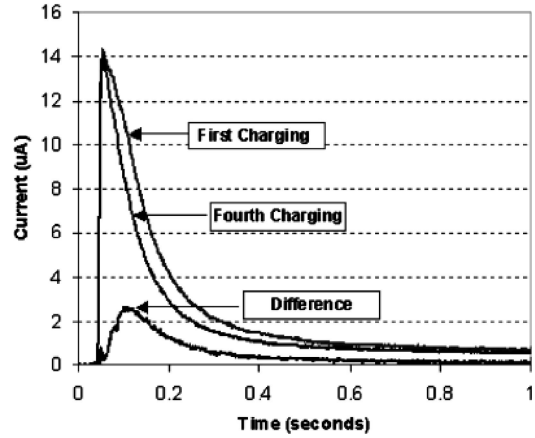

Figure 13. Charging current vs time for a dual-layer OPC with phthalocyanine based CGL. Excess charge is observed only on the first charging, and subsequent chargings (after an 8 min dark rest or positive charging to reduce the surface potential to zero) were identical. The difference current gives the time-dependent depletion current. Reprinted from ref 81 with permission of IS&T: The Society for Imaging Science and Technology, sole copyright owners of *Journal of Imaging Science and Technology.*)

Montrimas and co-workers investigated the charging characteristics of a wide variety of OPCs (including single-layer, double-layer, and inverse double-layer) using a technique in which the OPC was charged in small increments on a rotating device.[80] The amount of charge drawn from ground and the surface potential were determined on each cycle. By examining the effects of sequences of both positive and negative corona charging, several important conclusions were obtained. Charge originating in the CGL pigment is extracted during corona charging. In the case of an OPC with CGL (0.5 μm) of X-H_2Pc, the amount of charge was as high as $\sim 10^{12}$ charges/cm^2. Once depleted of charge, the OPC charged capacitively but the trapped charge was restored by exposure to light or a dark rest. Charging the OPC with a polarity that causes electron trapping at the CGL/CTL interface produces a high field region such that, on subsequent charging with the opposite polarity, the charge acceptance is reduced. Similarly, holes can accumulate at the interface of a barrier layer or the free surface such that, on subsequent charging with opposite polarity, they are released and the charge acceptance is reduced.

Weiss and co-workers characterized OPC charging by measuring the time-dependent current flowing from ground during corona charging.[81] Integration of the current transient gives the amount of charge delivered. Figure 13 shows a typical result for a dual-layer OPC with phthalocyanine CGM. Films of bisphenol A polycarbonate charged capacitively, but the OPC had excess charge on the first charging cycle ($\sim 10^{11}$ charges/cm^2) after light exposure or dark rest. Once depleted of charge by a first charging cycle, the OPC charged capacitively. That is, the current flowing from ground (Q) in subsequent charging (an 8 min dark rest or positive corona charging was used to reduce the surface potential to zero) was essentially identical to CV. For this OPC, ~27% excess charging current is needed relative to

an insulating film of the same thickness. The time for the depletion charge to reach a maximum was determined by the charger−OPC time constant. The activation energy for thermal generation of depletable charge was 1.0 eV. The low-level, steady-state current observed during charging (Figure 13) is due to exposure of the OPC with light (mainly from excited nitrogen[82]) from the corona charger during charging. Some time ago, Gallo and co-workers estimated that, for a Se photoreceptor, as much as 25% of the charging current is "wasted" due to light exposure during charging.[83] For the OPC and charger used in this study, about 5% of the charging current is due to light exposure during charging. A commercially available visible light-sensitive OPC (dye−polymer aggregate based CGL) exhibited only ~3% depletable charge, and thermal generation did not occur at 70 °F.

Prolonged exposure of an OPC to light absorbed by the CGM or CTM can cause an increase in dark decay. These effects are discussed in section 9.2.

4.2. Photodischarge

Characterization of the photosensitivity of an OPC is necessary for quality control of a commercial OPC and for studying the effects of formulation, architecture, exposure wavelength and intensity, environment, etc. For quality control or comparing similar OPCs, a relative sensitivity might be adequate, but for mechanistic studies, a quantum yield would be more useful. In the days of copiers that used "white" light to expose the OPC, it was appropriate to use a similar exposure (xenon flash filtered to remove the UV, for example) for purposes of characterization. However, today's printers have monochromatic exposure systems using red or near-IR light, so white light sensitivity is no longer meaningful. Unfortunately, there is no standard method and comparing literature values for OPC photosensitivity is problematic.

Measurements to determine fundamental characteristics (quantum efficiency of generation materials, mobility, etc.) are often carried out on photoreceptors that differ from what might be eventually used in a printer. The layer of interest (CGL or CTL) may be isolated or the device may be modified with the application of a vacuum-deposited electrode (Au is common) on the free surface. Common fundamental characterizations include quantum efficiency as a function of field and wavelength, and mobility. Mobility will be discussed in the following section. The quantum efficiency of carrier generation has several definitions as applied to OPCs. On the one hand, it can refer to the number of ion pairs generated per photon incident or absorbed. This fundamental characteristic might be determined experimentally by fluorescence quenching, or calculated based on a model such as the Onsager model (section 5). On the other hand, photodischarge efficiency can be determined based on the decrease in surface potential per photon absorbed or incident. The photoinduced discharge (PIDC) method is commonly used to characterize OPCs as a function of field, wavelength, temperature, humidity, exposure intensity, etc. The photoreceptor is corona charged to apply the desired field and is photodischarged. Using the parallel plate capacitor model, $Q = CV$ (terms as defined previously), the change in surface charge density can be calculated from the decrease in surface potential. The change in surface charge density per unit area per photon incident or absorbed is a measure of photosensitivity. This measure includes the efficiency of charge generation, injection into the CTM, and transport through the device. Because of carrier bimolecular recombination and range limitations, the quantum efficiency determined using this method may depend on the light intensity and the extent of photodischarge. The photodischarge method is carried out with either continuous or flash exposures. With continuous exposures ($J/cm^2/s$), the surface potential is monitored as a function of time. One measure of OPC photosensitivity that relates to the electrophotographic process is the exposure required to discharge the photoreceptor a fixed amount, often 50%, from an initial potential. This is typically carried out using exposures (wavelength and duration) relevant to a particular electrophotographic process. The photoreceptor sensitivity is usually reported in terms of J/cm^2, although the inverse is often used to report spectral sensitivity because it is convenient to have numbers that increase with increasing photosensitivity. A related method is to determine the initial photodischarge rate (dV/dt). This can be related to the decrease in surface charge density through the capacitance, $dQ/dt = C(dV/dt)$. The light intensity is kept low and the discharge time is kept short to avoid space charge perturbations during charge transport and to keep the field essentially constant. The ratio of the decrease in surface charge density to the exposure ($photons/cm^2$) is a measure of photodischarge efficiency. In fact, the photodischarge per exposure ($V/J/cm^2$) is another commonly used metric for OPC photosensitivity. When determined as a function of field, data obtained in this manner can be analyzed in terms of the Onsager models (section 5). Because photosensitivity depends on field (surface potential per unit OPC thickness) and the exposure produced decreases in surface charge density (related to the change in surface potential through $\Delta Q = C\Delta V$), meaningful comparisons can only be made between OPCs of similar thickness, charged to similar initial potentials, and exposed to similar discharged potentials. The photosensitivity action spectra shown in Figures 8 and 9 were calculated from published data from various sources by taking into account the change in surface potential.

For a process using a flash exposure, the photoreceptor discharge is determined at several exposure levels (with the surface potential determined at a fixed time after the exposure) and the data is plotted as surface potential (V) vs log(exposure, J/cm^2). An arbitrary photodischarge point (typically 50%) can be determined from this plot for comparison purposes. The utility of this characterization is that the exposure characteristics and the timing for reading the discharged surface potential directly relate to the printing process. As discussed above, short high intensity exposures may give rise to Langevan recombination, resulting in decreased sensitivity (reciprocity failure) relative to low intensity exposures.[29−31]

An often overlooked sensitivity factor is that there are more photons per energy unit (J) as the wavelength increases. For example, to deliver the same energy will require about 30% more photons/J at 820 nm than at 630 nm. Thus, for a photoreceptor with a given quantum efficiency for carrier generation, the sensitivity will increase with increasing wavelength of the exposure source.

4.3. Charge Transport: Drift Mobility and Carrier Range Considerations

In an OPC, photodischarge occurs via transport of charge through the device under the influence of the applied field. The charge velocity, and the time it takes for the charge to

transit the film, are critical because these characteristics determine the time necessary to create the OPC latent image. In addition, the carrier range, or the distance the charge moves before experiencing shallow or deep trapping, is of key importance. If the carrier range is less than the thickness of the OPC that it must transit, a residual potential will result, which might give rise to image defects, especially if the residual increases with electrophotographic cycling.[84,85]

Drift mobility of holes in CTL films is most conveniently measured by the canonical small-signal time-of-flight (TOF) technique.[86,87] However, for a given composition of the CTL, and all other conditions analogous, the same drift motilities can be inferred by analyzing transport-limited xerographic discharge in bilayer photoreceptors.[28,88] In TOF, the MDP film is prepared with semitransparent blocking contacts and maintained at a bias that is high enough to ensure that the transit time of any excess injected carrier is shorter than the bulk dielectric relaxation time. The sample is exposed to a very short and weak pulse of strongly absorbed light. For a CTL-only sample, the exposure might be 337 nm from a nitrogen laser incident on the positive semitransparent electrode. Under these circumstances photoexcited transport molecules are oxidized at the positive electrode to the radical cation (the "hole" in transport terminology). In a sample with a CGL, the exposing wavelength would match the absorption spectrum of the CGM. Following excitation and charge generation, a chain of redox steps occurs where electrons are progressively transferred from neutral molecules to their neighboring radical cation under the influence of the applied field. The concentration of the advancing pulse of holes is kept low such that the applied field remains uniform during their transit. In the ideal case, the current from the advancing pulse of holes is constant until the leading edge reaches the counterelectrode, after which it rapidly decreases. The transit time is generally taken as the time at which the current begins to drop. The usual procedure is to draw tangent lines to the current plateau and the current decrease and where they intersect is taken to be the transit time. From the transit time, the drift mobility is calculated as the velocity per unit field, (cm/s)/(V/cm), with the units $cm^2/(V\ s)$. Often the current transient does not have a flat but a sloping plateau due to a dispersion of carrier velocity during transit, and in the extreme, it may not be possible to identify a transit time. In this case, the transit time is determined using a log−log plot of the current−time data. For a given MDP film of known thickness, the drift mobility is usually studied as a function of concentration and composition as a function of applied field and temperature.

The importance of the drift mobility of a CTM with respect to photodischarge of an OPC will be discussed below. It should also be kept in mind that the time-of-flight experiment is carried out with the film sample biased at a constant field while, during the photodischarge of an OPC, the field decreases behind the advancing charge front. Thus, lagging charge experiences a decreased field and, therefore, has decreased velocity such that the charge spreads out during the film transit. The time-of-flight experiment determines the velocity of the fastest charge, but it is the slower charge that will determine how well the CTL functions during EP cycling.

The photoreceptor must retain charge in the dark and also be photosensitive enough to discharge exposed areas to at least one-half their initial charge potential when irradiated with (nominally for a midvolume laser printer engine) 4−10 $ergs/cm^2$. The xerographic gain or quantum efficiency of supply describes the fractional number of surface charges neutralized per absorbed photon. For a dual-layer OPC, it is a complicated convolution of the quantum efficiency of generation in the charge-generation layer, CGL, the efficiency of carrier injection from the CGL to the CTL, and the transport parameters of the CTL. For this discussion, we will for the moment ignore issues of charge generation and focus on transport. In dual-layer OPCs, the majority of photodischarge occurs via charge transport through the CTL, with the CGL playing a minor role. In the transport lexicon there, are essentially two parameters that constitute the figures of merit characterizing charge motion through the polymeric CTL.[89,90] These are (i) the drift mobility μ, which is the measure of "how fast" the carrier moves per unit applied field, and (ii) the normalized carrier range, $\mu\tau$, (τ is the free carrier lifetime against deep trapping), which is "how far" the injected carrier moves per unit field before becoming immobilized in a deep trap. The time for a photoinjected carrier to traverse the CTL is called the transit time. The transit time t_{tr}, and mobility μ are related to specimen thickness, L, according to $t_{tr} = L/\mu E$. The importance of mobility as a critical parameter in the electrophotographic process can be understood as follows: For an increase in the exposure intensity d(F), the final decrease in surface potential d(V) is proportional to the number of injected carriers and the distance they travel within the CTL. During xerographic discharge, a charge of CV_0 (C is the CTL capacitance and V_0 is the initial voltage) traverses the bulk and induces time-dependent variation in the electric field behind the leading edge of the injected carrier front. Thus, as the fastest carriers transit the CTL, the electric field behind them is reduced, and the carriers behind the leading edge transit at a lower field, which in turn makes their velocities lower. Thus, during xerographic discharge, the transit times of individual photoinjected carriers become dispersed over a wide range, typically about an order of magnitude. For discharge to proceed to completion, even in the complete absence of deep trapping, enough time is required for the slowest carriers in the packet to exit the layer before the photoreceptor reaches the development zone—nominally 0.3−1.0 s after exposure in midvolume printers. The latter must be allowed for in practice. Thus, carrier mobility in this particular illustration should exceed 10^{-6} $cm^2/(V\ s)$. For example, consider that a dual-layer photoreceptor with a 25 μm CTL, in which there are no deep traps, is subjected to a light flash intense enough to ultimately induce complete discharge (CV_0 of absorbed photons). Consider further that, in this CTL, the mobility $\mu = 10^{-6}$ $cm^2/(V\ s)$ at $E = 10^4$ V/cm and that the device is initially charged to 1000 V. It can be calculated that, under these conditions, the device will have a residual voltage of 20 V after 0.3 s or 7 V after 1 s. Incomplete discharge, unless compensated for, might result in an inadequate toning potential and a toned density less than desired. Note further that if the mobility is even lower, the results can become totally unacceptable. For example, when the mobility is 10^{-7} $cm^2/(V\ s)$ under the conditions just described, the residual voltage a full second after exposure is 60 V, even in a completely trap-free CTL! In light of the foregoing illustration for the trap-free case, which sets the mobility benchmark, the effect of traps in the polymeric CTL must be of paramount concern. More precisely, we are concerned with traps whose release time at ambient temperature discernibly exceeds the period of a complete electrophotographic cycle.

In the present context, we take the latter as the operational definition of a deep trap. With such traps present, it is clearly the case that, after repeated charge−expose cycling, some quantity of image-degrading charge would remain immobilized in the bulk for times now exceeding the period of a complete xerographic cycle. If ρ is the density of uniformly trapped space charge in a CTL of thickness L and relative dielectric constant ε, then there is an associated residual potential V_R, where $V_R = \rho e L^2/(2\varepsilon\,\varepsilon_0)$, where e is the electronic charge and ε_0 is the free space permittivity.[91] In a nonpolar dielectric medium ($\varepsilon = 3$) with a layer thickness of 25 μm, as few as 10^{13} electronic charges trapped per cm^3 already give rise to a residual of 19 V! Unless process control utilizing electronic feedback correction can be employed, bulk trapping induced space charge buildup during cycling can result in severe image degradation. Residual potential arising from bulk trapped space charge is a critical electrophotographic process parameter. A residual potential can be related to normalized carrier range ($\mu\tau$) in the weak trapping limit from the physically plausible *ansatz* that the residual potential corresponds to that applied voltage for which the carrier range is about one-half the specimen thickness L. Thus, $\mu\tau$ is approximately $L^2/2V_R$. On this basis, the tolerable trap density is defined by the requirement that the $\mu\tau$ product in practical devices should typically exceed 10^{-6} cm^2/V. Even highly purified polymer will typically contain many chemical impurities in the 1−10 ppm range, which the foregoing calculations show is vastly higher than permissible trap levels. However, chemical impurities even when present at relatively high concentration can be rendered trap-inactive by employing molecular design principles to guide the overall choice of active materials. Concepts derived from scientific understanding of photogeneration, injection across interfaces, and electronic transport in disordered organic materials, in combination with the unique compositional flexibility characteristic of the organic solid state, were together responsible for making multilayer OPCs the dominant practical receptor technology for electrophotography.

4.4. Electrical-Only Cycling

Electrophotographic performance characterizations are necessarily carried out on the photoreceptor in an apparatus that has the key elements of the electrophotographic process. The most "relevant" apparatus would, of course, be the fully configured printer. However, the use of such a complex device is often undesirable, or unnecessary, for screening purposes. In the laboratory, it is common to use "electrical-only" test fixtures in which the process always includes charge and expose, and may include erase (or unique process elements), with the surface potential being determined after the application of each. With an apparatus such as this, it is possible to determine process-relevant characteristics such as chargeability, dark decay, photosensitivity, and residual potential, all as a function of cycling. Of course, large changes in any of these characteristics are generally undesirable and long cycling (10 000−100 000 cycles) is often necessary to adequately determine the "electrical" stability of the photoreceptor to the electrophotographic process. Such stability is a necessary, but not sufficient, condition for eventual commercialization, and extensive testing in the machine for which the photoreceptor was designed is always the final step in the development process. Other factors, often connected to the device physical characteristics (wear rate, corona chemical sensitivity, layer adhesion, seam strength, etc.), may in fact determine the eventual success or failure of a particular OPC in a printer.

An interesting use of electrical-only cycling has been described by Tse and co-workers to determine the characteristics of recycled OPC drums.[92] They obtained 70 used Canon EX OPC drums from a toner cartridge remanufacturer and examined them for thickness, charge acceptance, dark decay, and photodischarged voltage. In addition, two used drums were subjected to extended full process testing (12k prints) in a Hewlett-Packard Laserjet 4 printer. In the full process testing, the wear rate was constant at 0.5 μm/1000 prints, the mean charge acceptance decreased 6 V/1000 prints, and the dark-decay ratio (the initial surface potential divided by the surface potential after 1 s in the dark) went from 0.99 to 0.96 at 12k prints. On the basis of a combination of acceptance/rejection criteria and follow-up printing with end users, it was determined that almost 50% of the used OPCs were reusable. This result is interesting because the critical dark and photoelectrical performance characteristics of an OPC must not change to the point where the EP process can no longer maintain the required print quality, and in practice, an OPC is removed when image quality becomes unacceptable. This might be due to mechanical damage, such as wear, scratches, belt seam failure, or OPC delamination, etc., or a change in the photoelectrical characteristics, such as high dark decay or residual potential. However, an OPC might also be removed for preventive maintainence, because it is a component that is relatively easy to replace, or because of print job procedures. For example, a large commercial printing company may schedule an OPC change before the start of a long print run to avoid having the OPC fail while the job is being printed. On the other hand, low-volume consumer printers often have a cartridge containing an OPC drum such as those described above and when the toner runs out the cartridge is replaced even though the OPC may have considerable remaining life. Tse's study demonstrates that, indeed, many of the used OPCs in returned cartridges can be recycled.

5. Charge-Generation Layer: Materials and Mechanisms

In this section, we will review research related to the development and functions of the charge-generation layer (CGL). As discussed previously, charge-generation materials (generally pigments) in the charge-generation layer (CGL) absorb the imaging light and generate charge. In terms of OPC function, the pigments are typically divided into visible and near-infrared absorbing classes. For purposes of this discussion, we will discuss them according to their chemical family: phthalocyanines, molecular complexes, azo compounds, perylene compounds, and mixed pigment OPCs. As much as possible, the discussion will focus on post-1993 research, as the latter was covered in the review by Law.[1] Appendix 2 of ref 9 will provide the reader with a list of charge-generation materials, their chemical structures, and commonly used acronyms.

A photogeneration model that has been successfully used in the study of inorganic semiconductor-based photoreceptors (such as amorphous Se and alloys with As)[93] is based on a 1938 theory from Onsager describing the recombination of ions as influenced by their Coulombic attraction and an applied field.[94] In this model (Figure 14), an upper excited state partitions between a geminate ion pair with efficiency η_0 and radiationless decay to the first singlet state, S_1. The

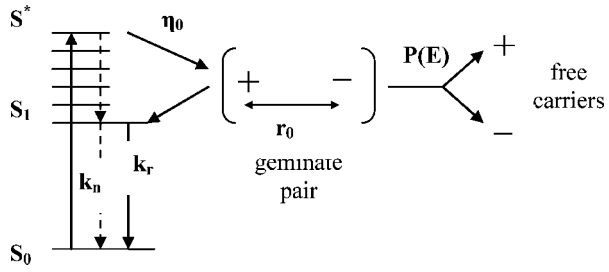

Figure 14. Onsager model for charge generation. Following excitation to an upper excited state, charge separation occurs to form a geminate charge pair with efficiency η_0 separated by r_0. The geminate pair recombines or separates into free carriers under the influence of the applied field.

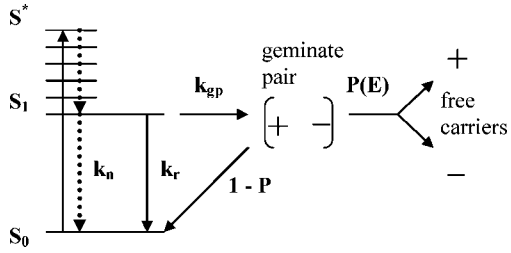

Figure 15. Internal conversion model for charge generation. Following excitation to an upper excited state, and radiationless decay to the first excited singlet state, there is a competition between nonradiative decay (k_n), radiative decay (k_r), and geminate pair formation (k_{gp}). The geminate pair partitions between recombination and field-assisted dissociation into free carriers, $P(E)$.[113]

geminate pair, initially separated by a distance r_0, can then either recombine to form S1 or produce free charges under the influence of an applied field with probability $P(E)$. The field dependence of charge generation is fit to the model using η_0 and r_0 as adjustable parameters. The latter incorporates the field dependence of carrier generation. Over the years, the model has been modified with respect to the functionality of the ion-pair distribution.[95,96] Key predictions of the Onsager model are that the photoconductivity is wavelength-dependent with a threshold at energies greater than the S1 absorption threshold and the fluorescence from S_1will be unaffected with the application of a field. As will be seen in later discussion, these features are rarely observed in organic photoconductors. In most organic photoconductors, the quantum yield for carrier generation is independent of wavelength, the threshold occurs at the onset of absorption into the S_1 state, and application of a field has an effect on fluorescence from S_1. These features have led to the "internal conversion" model for charge generation in OPCs (Figure 15). In this model, rapid internal conversion leads to S_1 and geminate pair formation occurs in competition with radiative and radiationless conversion to S_0.[97] The mechanistic details of charge generation in OPCs depend on the specific CGM and the CGL formulation (polymer binder and additives such as electron donors and/or acceptor molecules), and as will be seen, the internal conversion model just described has been modified to account for specific observations. Nevertheless, the Onsager model is still applied to the analysis of photogeneration in OPCs.

The pigments utilized as the light-absorbing and charge-generating materials in the OPC have been extensively investigated. In the following, we describe each class of material and discuss our current understandings with respect to preparation, fabrication, and charge-generation mechanism. In practice, the materials used in commercial OPCs have near unity quantum efficiency for charge generation at the high fields used in the electrophotographic process. Thus, the development of new materials has focused on charge-generation material synthesis, pigment preparation, device fabrication, and electrophotographic performance.

5.1. Phthalocyanine Pigments

Many commercial OPCs utilize phthalocyanines as the pigment in the CGL, as these are photosensitive to the near-infrared light used in hologon laser-exposure systems. We will use the shorthand XMPc in describing these molecules where XM is the ligand and central metal of the phthalocyanine (Pc) molecule. Typical phthalocyanines used as charge-generation materials (CGM) are H_2Pc, TiOPc, and HOGaPc. Much of the research related to these materials has been to produce unique polymorphs with high OPC photosensitivity and to develop procedures for their production. The absorption and photosensitivity characteristics of polymorphs of TiOPc are illustrated in Figures 7 and 8.

5.1.1. Polymorphism

Phthalocyanines are relatively planar molecules that, when crystallized, tend to produce polymorphs that have unique spectral characteristics. Typically they are differentiated by X-ray powder diffraction, absorption spectroscopy, and infrared spectroscopy. As mentioned previously, because different polymorphs have different photogeneration characteristics, companies have patented specific polymorphs and the methods of production using combinations of solvent and heat treatments. Different research groups have applied their own nomenclature to polymorphs produced in their laboratories. However, examination of the published X-ray powder patterns indicates that some polymorphs identified as unique are in fact the same, or mixtures, or differ in the degree of crystallinity. For TiOPc, over two dozen unique polymorphs have been claimed.

Phthalocyanines are difficult to purify because they are insoluble in all the common solvents. However, they will dissolve in concentrated acid, and a purification process called acid pasting entails dissolving the pigment in a strong acid followed by precipitation into water. This procedure produces amorphous TiOPc. Mayo has reported on a detailed study of acid pasting of TiOPc using sulfuric acid.[98] However, this technique leads to degradation of the phthalocyanine and the formation of phthalimide, as well as ring sulfonation. An alternative treatment has been developed using mixtures of trifluoroacetic acid and dichloromethane to dissolve TiOPc followed by precipitation into various solvents to produce seven different TiOPc polymorphs (Type I, II, III, IV, X, Z-1, Z-2).[99] Watanabe and co-workers produced TiOPc A-, B-, C-, F-, and Y-polymorphs by treating acid-pasted TiOPc with various solvents.[100] The polymorphism of HOGaPc has been investigated, and a highly photosensitive form, type V, has been identified.[101] HOGaPc is much more stable to acid pasting than TiOPc.[102]

As shown in Figure 7, in solution TiOPc has a strong absorption at 690 nm. When crystallized, the highly photosensitive Y-polymorph absorption is red-shifted and split into absorption bands at 755 and 875 nm. The details behind the red shift and band splitting have been the subject of several studies. Mizuguchi and co-workers have proposed that the absorption changes are due to molecular distortion, which reduces the molecular symmetry, and interplanar $\pi-\pi$

interactions.[103] Hinch and Haggquist have calculated that rotation of the molecule about the TiO axis and variation in the crystallite size produces changes in the X-ray powder diffraction similar to what is experimentally observed with various polymorphs.[104] Fujimaki reported that the photoconductivity of Y-TiOPc decreases with increasing temperature due to the desorption of water;[105] Okada and Klein have observed that water (about one water molecule per 45 TiOPc molecules) is reversibly released on heating the Y-form above 70 °C, and at 250 °C, it converts to the A-form.[106] Mizuguchi and co-workers have found that TiOPc crystals grown from water are phase I with a surface of Y-type.[107] These studies suggest that the popular Y-TiOPc polymorph contains weakly adsorbed water, which causes molecular distortions and produces the observed spectral changes.

Metal-free phthalocyanine, H_2Pc, has an X-form polymorph with near-infrared photosensitivity. However, by examination of X-ray powder diffraction and infrared spectra, Kubiak and co-workers have suggested that the X-form is actually a crystalline tetramer of 1,2-dicyanobenzene.[108] In addition, they found that the conversion of the β-form of MgPc to the α-form occurs reversibly in the presence of air. On the basis of this observation, they suggest that, in general, the α-forms of M(II)Pc are actually complexes with N_2 and O_2.

These studies strongly suggest that many of the so-called polymorphs of the phthalocyanines used as charge-generating materials in OPCs may in fact be complexes involving water (ClAlPc,[109] X-MgPc[110]), oxygen, nitrogen, or even the solvent molecules used in their production.[100] Or, in some cases, they may not even be phthalocyanines. Thus, the situation regarding phthalocyanine polymorphism remains unsettled. Using specific procedures, researchers have produced pigments called phthalocyanine polymorphs, which are excellent for use in OPC formulation and which can be characterized by any number of means and can be patented, but whose chemical structure is unclear.

5.1.2. Intrinsic Charge Generation

Photogeneration in an OPC can occur with or without the presence of a sensitizer. Figure 10 shows a general mechanistic scheme for charge generation. The basic features of the photophysics are light absorption and exciton migration to the pigment surface where charge generation occurs either intrinsically or via electron transfer to surface states with an electron donor or acceptor molecule. Actually, there is experimental evidence that intrinsic charge generation may occur via adsorbed molecules, such as oxygen and/or water, on the pigment surface. Charge generation is assumed to be independent of the applied field to produce a geminate electron−hole pair, which can subsequently recombine or be separated due to the applied field. This model is sometimes referred to as the "internal conversion" model because the initially produced singlet undergoes rapid internal conversion to the first excited singlet state (Figure 15). This model is different from the "Onsager" model in which charge generation occurs directly from the initially produced singlet state (Figure 14).[9] Subsequent to separation, the charges are transported and the field across the OPC is discharged.

It is instructive to begin the discussion with single-layer OPCs containing only pigment. Phthalocyanine fluorescence has been used as a probe for understanding the photophysics of charge generation. The fluorescence spectra of α-, β-H_2Pc evaporated films are shown in Figure 16.[111] The band

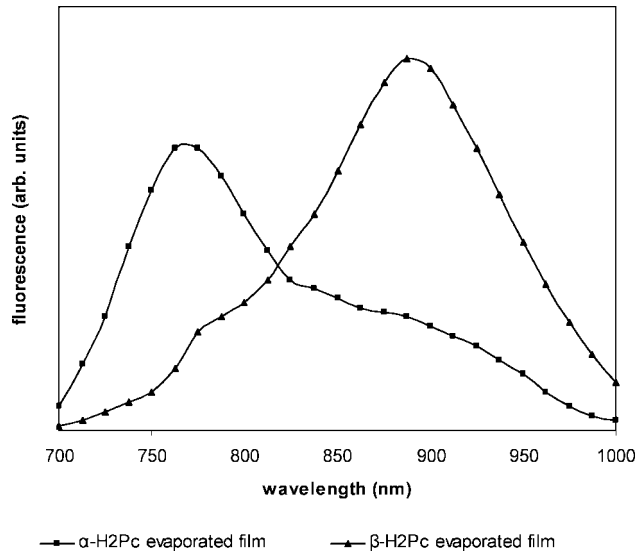

Figure 16. Fluorescence spectra of evaporated films of α-, β-H_2Pc (data from ref 111).

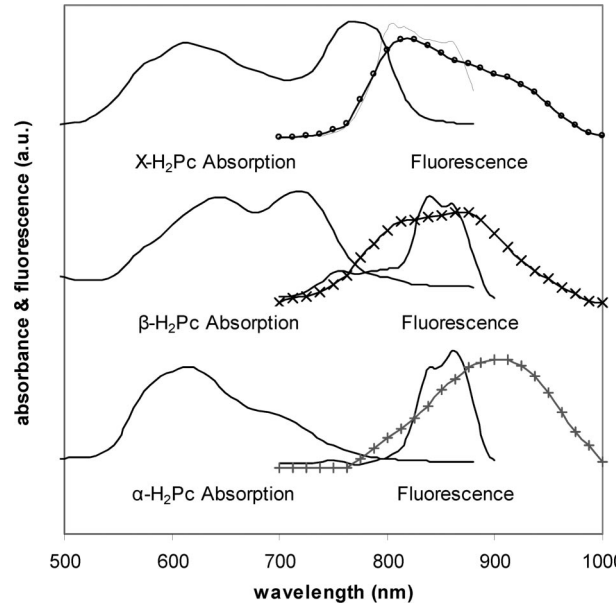

Figure 17. Absorption and fluorescence spectra of α-, β-, and X-H_2Pc dispersions (1:1) in polyvinylbutyral films (data from ref 112) and fluorescence data of powders (symbols) (data from ref 111).

positions were observed to depend on the sample type (films, powders, compressed pellets), and the maxima were found to shift due to heating (from light exposure during the measurement) and pressure (in compressed pellets). The fluorescence lifetimes of the samples as compressed pellets were reported as 0.35, 0.21, and <0.1 ns for α-, β-, and X-H_2Pc, respectively, and the fluorescence quantum yields were estimated to be on the order of 10^{-4}. The absorption and fluorescence spectra of thin coatings of α-, β-, and X-H_2Pc dispersed (1:1) in polyvinylbutyral (PVB)[112] and the fluorescence spectra of the powders[111] are shown in Figure 17. In this study, the lifetime of the X-polymorph fluorescence was reported as 1.7 μs. The fluorescence spectra are sensitive to both the pigment morphology and physical form. This comparison serves as a caution that weakly emitting species are difficult to study and the emitting species may depend on the chemical as well as the physical characteristics of the sample.

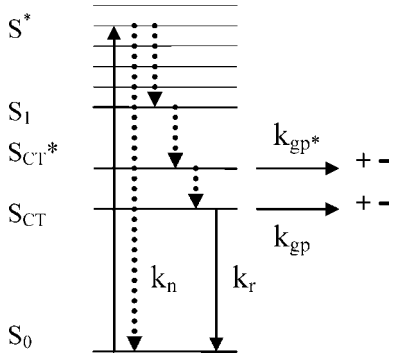

Figure 18. Schematic diagram of the internal conversion model for charge generation in Y-TiOPc. The symbols are defined as in Figure 15. In this model, excitation leads via internal conversion to two charge transfer states (S_{CT}), both of which give rise to charge generation.[117]

Extensive studies have been carried out by Popovic and co-workers, using field-dependent fluorescence quenching as a probe of the photogeneration of charge.[113] Photogeneration in films of β-H_2Pc dispersed in bisphenol A polycarbonate were investigated using electric field-induced fluorescence quenching and delayed fluorescence.[114] Delayed application of the collecting field showed that the geminate electron−hole pair has a lifetime of tens of milliseconds. The particles in this study were about one micrometer in size. This is much larger than the particles that might be found in a typical dual-layer OPC where a pigment-based CGL would have a total thickness of only a fraction of a micrometer. Similar studies were carried out with X-H_2Pc (5% pigment in bisphenol A polycarbonate), where the limiting quantum efficiency for charge generation was found to be ~0.8.[115] Popovic and co-workers have more recently extended these studies to other phthalocyanines. The photogeneration mechanisms of TiOPc(I), TiOPc(IV) (also called Y-TiOPc), HOGaPc, and x-H_2Pc have been compared by looking at field-dependent quenching of both the fluorescence amplitude and the lifetime.[116] These studies were used to distinguish between two pathways for charge generation. Quenching of the fluorescence amplitude (but not the lifetime) would occur when the field quenches a state that is a precursor to both the fluorescent singlet state and the carrier generation. Quenching of the fluorescence lifetime would occur if both fluorescence and carrier generation originated from the first excited singlet state. Films were prepared at 60 wt % pigment in polymer. The field dependence of fluorescence quenching at low field was quadratic, which was interpreted as indicating that the charge-generating excited state was neutral as opposed to having charge-transfer character. For all of the phthalocyanines, the fluorescence exhibited a fast and a slightly red-shifted slow component and both amplitude and lifetime quenching occurred. The data for HOGaPc, TiOPc(I), and TiOPc(IV) indicate the presence of a precursor state as well as exciton charge generation. The importance of charge generation from the trapped state in x-H_2Pc is unique. A more detailed investigation of charge generation in Y-TiOPc has been reported by Popovic and co-workers.[117] The mechanistic scheme is shown in Figure 18. In this model, there are two low-energy states with charge transfer character with lifetimes of 45 and 234 ps, and charge generation occurs from both. Interestingly with increasing high humidity, the efficiency of charge generation increases and the fluorescence is quenched. Water apparently interacts mainly with the short-lived state. The authors propose that the charge-generation efficiency depends on the relative positions of the neutral and charge transfer states with high efficiencies occurring when the charge-transfer state is isoenergetic with or slightly below the neutral state.

Saito and co-workers used electroabsorption to study films of phthalocyanine pigment in a silicone polymer.[118] With Y-TiOPc absorptions attributable to charge transfer, excitons were observed and it was suggested that the strength of the charge-transfer interaction would determine the free carrier generation efficiency. Using exciton−exciton annihilation, Gulbinas and co-workers found that formation of the geminate charge pair in a sample of Y-TiOPc dispersed in PVB (30 wt %) occurs about 1 ps after excitation, while the fluorescence from the relaxed singlet state has a lifetime of 0.12 ns.[119] This data is consistent with the internal conversion model if charge generation occurs from a nonrelaxed lowest excited state. More recently Yamaguchi and Sasaki used electric-field-modulated picosecond time-resolved fluorescence spectroscopy and have identified two singlet excitons in the fluorescence decays of Y-TiOPc dispersed in PVB with lifetimes of 72 and 175 ps.[120] The primary precursor to charge generation was identified as the shorter-lifetime exciton with intramolecular charge-transfer character. Upon application of a field (30 V/μm), the lifetime of the longer-lived exciton was decreased (166 ps) while the other was essentially unchanged (69 ps). This was interpreted as a field deceleration of internal conversion from the charge-transfer (CT) exciton to the Frenkel exciton.

The picture that emerges regarding intrinsic charge generation in phthalocyanine pigments is very complex. The charge-generation efficiency depends on the phthalocyanine chemical structure, the synthesis method, the presence of trace impurities, the polymorph, the binder polymer, and the presence of other molecular species such as water, nitrogen, and oxygen. Tsuchiya and Omote have shown that polymer binder and milling time have an effect on photosensitivity,[121] and it seems likely that film-preparation details (residual solvent, drying time, etc.) will also be of importance.

5.1.3. Extrinsic Charge Generation

In 1971 Hackett reported that OPCs with X-H_2Pc dispersed in poly(*N*-vinyl carbazole) had charge-generation efficiencies approaching 70%.[122] Charge generation in 60 wt % X-H_2Pc dispersed in poly(vinyl acetate) is enhanced in the presence of either electron donors (*N*,*N*′-diphenyl-*N*,*N*′-di(*m*-tolyl)-*p*-benzidine) (TPD) or acceptors (2,4,7-trinitrofluorenone) (TNF).[46] The observation of concomitant fluorescence quenching led to the proposal that the mechanism involved singlet exciton migration with exciplex (excited state charge-transfer complex) formation at a site on the pigment surface associated with adsorbed donor/acceptor. The exciplex subsequently dissociates to free carriers in competition with nonradiative decay to the ground state. The excitation migration range is estimated to be 0.1 nm. Takeshita and co-workers used time-resolved absorption spectroscopy to investigate charge generation in phase I and IV TiOPc in the presence of hole-transport material.[123] The final coatings comprised binder/pigment/CTM (1:1:1). For example, irradiation at 800 nm in a film using tetraphenyl-*p*-benzidine as the CTM gave rise to a broad absorption centered at ~1600 nm, which was interpreted as the aggregated cation radical of the CTM. From the field dependence of the transient absorption, it was concluded that charge generation occurs through a field-dependent and a field-independent

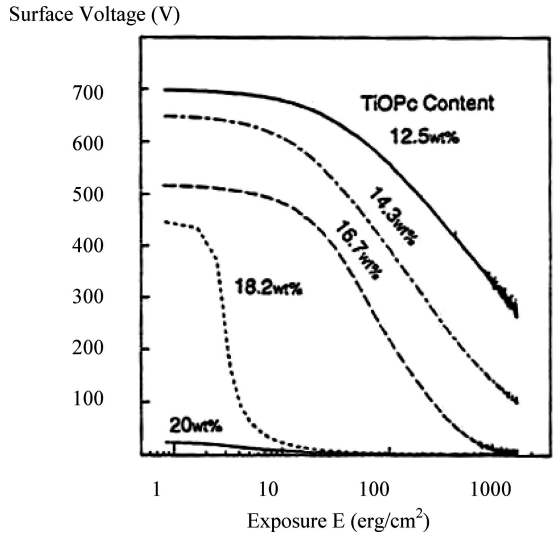

Figure 19. Photoinduced discharge curves (780 nm) for a single-layer photoreceptor of α-TiOPc in polycarbonate as a function of the pigment content. (Reprinted from ref 125 with permission of IS&T, The Society for Imaging Science and Technology, sole copyright owners of IS&T's NIP9: International Conference on Digital Printing Technologies Proceeding.)

route. On the other hand, Schreiber and co-workers examined the photoconductivity action spectra and found that there was no difference in the hole-generation efficiency for a sample of TiOPc (polymorph was not mentioned) with and without added hole-transport material.[124]

All commercial OPCs rely mainly on hole transport for photodischarge and therefore contain significant amounts of hole-transporting materials. These materials have a dual role: to sensitize photogeneration and to transport charge.

5.1.4. Photodischarge Characteristics

Films of pigment in a binder polymer are the simplest possible single-layer OPC formulation. Recall, however, that, subsequent to charge generation, both charge polarities must be transported under the influence of the applied field to have complete OPC photodischarge. The presence of an insulating binder polymer separating the pigment particles makes efficient charge transport problematic. However, depending on the binder polymer, the pigment particles will tend to form chains in the coated film and charge transport can occur from particle to particle within a chain. Kitamura and co-workers found that the dark and photodischarge characteristics of α-H_2Pc in polycarbonate depended on the pigment content (Figure 19).[125,126] The photoinduced discharge curves were obtained by positively charging the OPC followed by continuous exposure at 780 nm. Photodischarge in this case is dominated by the transport of holes through the OPC. Several features are noted. First, in none of the photodischarge curves does the discharge begin when the exposure is initiated. Instead there is an "induction period", leading to what is commonly called an "S-shaped" photoinduced discharge curve, which becomes less pronounced as the pigment concentration is increased. Second, above 18 wt % pigment, the dark conductivity was such that the OPC did not retain the surface charge. The hole drift mobility was determined as a function of field and pigment content. However, little current from transported charge was observed with the first exposure, and several exposures were necessary before a "typical" transient current was observed and the mobility could be determined. It was found that the hole drift mobility increased from 10^{-6} at 20 wt % pigment to over 10^{-5} at 30 wt % pigment and approached 10^{-4} cm^2/(V s) at higher concentrations. These observations illustrate a fundamental issue with pigment-only single-layer OPCs. The pigment particles contain hole traps and charge carriers experience severe transport limitations at low pigment concentrations because the particles are surrounded by insulating polymer. When the particle concentration is increased to improve the mobility, the dark conductivity increases to unacceptable levels due to pigment particle chain formation. There are several explanations for the characteristic S-shaped photodischarge curve. The earliest, and simplest, is based on the idea that, in a heterogeneous system such as this, charge transport probably occurs at the contact points between pigment particles since the polymer binder is insulating. Thus, at high fields, a charge might be trapped at a "structural" trap (or dead-end site) and further transport is impossible until the field drops sufficiently that the available thermal energy enables the charge to "back up" and find an alternative transport route.

Kubo and co-workers have investigated the induction effect in the photodischarge of a positively charged single-layer OPC with 23 wt % X-H_2Pc in a mixture of polyester and melamine polymer.[127] It was found that the exposure to reach the photodischarge threshold was essentially equal to CV. The threshold exposure decreased linearly with temperature and increased linearly with surface potential. The threshold exposure activation energy decreased with increasing surface potential from 0.067 (2.4×10^5 V/cm) to 0.049 eV (4.5×10^5 V/cm). This is essentially the same as the activation energy for photogeneration of charge in x-H_2Pc.[115] The activation energy was also determined for the maximum photodischarge rate, which occurs after the threshold exposure. Here it was observed that the photodischarge rate increased with increasing temperature with activation energy of ~0.16 eV independent of field. The authors proposed that the observed characteristics suggest that the prevailing theories were inadequate. However, Hoshino successfully modeled the photodischarge of a positively charged single-layer OPC film of 15 wt % X-H_2Pc in a polyester binder using the structural trap model with a trap length estimated at 70−130 nm.[128] Omote and co-workers have also studied hole transport in films of X-H_2Pc in polystyrene and polyvinylbutyral (PVB).[129] An induction period was found for both binder polymers, but the effect was reduced for PVB. The high field mobility approached 10^{-6} cm^2/(V s), and the activation energy for hole transport was ~0.1 eV at 6×10^5 V/cm.

Enokida has reported the hole mobility characteristics of single-layer OPCs with various TiOPc polymorphs in various polymer binders.[130] Electrons were immobile in these films. At 30 wt % pigment in bisphenol A polycarbonate, the γ-form (also known as the Y-form) had a hole mobility ~10^{-4} cm^2/(V s) at a field of 1.3×10^5 V/cm, while the α-form hole mobility was lower by 1 order of magnitude. In polystyrene, the γ-form mobility was reduced by almost 2 orders of magnitude. Thermally stimulated current was used to study hole detrapping. Mobility for the β-form could not be determined because the carrier generation efficiency was too low. Detrapping activation energies for the α- and β-forms were 0.15 and 0.42 eV, respectively.

To fabricate a functional single-layer OPC, it is desirable that the formulation include a charge-transport material. For example, Kobayashi and co-workers fabricated a single-layer

OPC from 30 wt % X-H_2Pc in a binder of polyester and melamine resin (4:1). The energy to photodischarge from +600 to +300 V decreased from 0.9 to 0.6 μJ/cm^2 with the addition of 4 wt % tetracyanoethylene (TCNE).[131] Interestingly, the addition of TCNE increased the hole mobility by a factor of 2. Another approach was described by Nishino and co-workers in which TiOPc and a perylene pigment were blended by covacuum deposition and then dispersed by ball milling.[132] A small amount of copigment (~2 wt %) was added to a solution containing 30 wt % each of a hole- and an electron-transporting CTM and bisphenol A polycarbonate binder polymer. The perylene pigment has visible absorption and the phthalocyanine has near-infrared absorption, so the resulting OPC has photosensitivity from 400 to 900 nm with either a positive or negative surface charge. When positively charged, this OPC had enhanced photosensitivity by a factor of ~4.7 at 500 nm and ~1.5 at 750 nm relative to an OPC containing ~1% TiOPc as the CGM. On the basis of quenching of the perylene fluorescence by TiOPc in the copigment and analysis of the electroabsorption spectra, it was proposed that energy transfer from the perylene to the phthalocyanine is the mechanism of sensitization.

Yokota has carried out detailed investigations on a single-layered OPC with the CGM X-H_2Pc and a mixture of hole and electron CTMs in bisphenol-Z polycarbonate.[133] The weight ratios were as follows: CGM/h-CTM/e-CTM/binder (3/40/10/50). The spectral sensitivity action spectrum of the OPC mirrors the OPC absorption spectrum when the OPC is positively charged but has a minimum at the CGM absorption maximum when negatively charged. This observation was explained by proposing that, when the OPC has a positive surface charge, photogeneration occurs near the surface but, when negatively charged, photogeneration occurs near the Al substrate where a Schottky barrier may enhance the photogeneration efficiency.[134] Phonon-assisted exciton diffusion is proposed, and the data fit to a model having a 5 μm exciton diffusion length. To expand this model, it was proposed that the achievable resolution at the edge of an exposed area of a charged OPC is limited by the phonon diffusion length.[135] A resolution limit of 2400 dpi is calculated based on this model, and this is increased with increasing CGM concentration.

Most of the investigations of OPCs with phthalocyanine pigment based CGLs are with the dual-layer architecture. For example, the Y- and A-TiOPc data shown in Figure 9 were with a dual-layer architecture with a CGL of pigment in polyvinyl butyral (1:1 by weight) and a CTL of 4-(4-methylstyryl)-4′,4″-dimethoxy triphenyl amine in polycarbonate (3:4 weight ratio).[39] Kanemitsu and co-workers have reported the field dependence of the photosensitivities of single- and dual-layer OPCs with H_2Pc CGM using the initial photodischarge rate to calculate the photogeneration efficiency.[136] The CTL was a 1:1 solution of DEH in polycarbonate. The approximate efficiencies are as follows: 0.004 and 0.01 (α-form single- and dual-layer), 0.03 (β-form single-layer), 0.10 and 0.16 (X-form single- and dual-layer), and 0.30 (τ-form dual-layer). Daimon and co-workers have compared the sensitivities of OPCs prepared from several phthalocyanines in a dual-layer architecture with a 0.2 μm CGL of pigment in polyvinyl butyral (60:40 by volume) and 25 μm CTL of *N*,*N*′-diphenyl-*N*,*N*′-di(*m*-tolyl)-*p*-benzidine (TPD) 40 wt % in bisphenol-Z polycarbonate.[101] The photosensitivity was measured as the energy (mJ/m^2) to photodischarge the OPC from −800 to −400 V: 1.0 (Y-TiOPc), 1.3 (V-HOGaPc), 2.0 (II-ClGaPc), 2.1 (B-TiOPc), 5.3 (XI-HOGaPc). Enokida and co-workers found that the photosensitivity of a dual-layer OPC with a CGL based on τ-H_2Pc depended on the shape of the particles (needle vs granular) called type-I and -II, respectively.[137] The CGL was 0.2 μm pigment in poly(vinylbutyral) (1:1 by weight), and the CTL was 20 μm of 1,1-bis(*p*-diethylaminophenyl)-4,4-diphenyl-1,3-butadiene in bisphenol A polycarbonate (1:1 by weight). The energy to photodischarge the OPC from −600 to −300 V was 4.5 and 2.5 erg/cm^2 for type-I and -II, respectively. Kanemitsu and co-workers have carried out extensive studies to probe the efficiency of "charge injection" from a CGL of vacuum-deposited H_2Pc into a CTL of DEH in a polyester binder (1:2 by weight). The quantum efficiency of charge generation was determined with photoacoustic spectroscopy and xerographic discharge (calculated from the initial rate of photodischarge at 700 nm).[138] The latter process requires charge generation, injection into, and transport through the CTL. The ratio was used as a measure of charge injection efficiency. At a field of 5×10^5 V/cm, the values were 0.5 and 0.16, respectively, for an injection efficiency of 32%, which increased to 66% at 10^6 V/cm. At a lower field (10^5 V/cm), the generation efficiency was 0.18 and the injection efficiency was only 7.2%. This technique was used in a subsequent study where the concentration of DEH in the CTL was varied from 13 to 47 wt %.[139] The photogeneration efficiency increases with, but the xerographic efficiency is independent of, increasing DEH concentration. The explanation is that generation efficiency increases because, as the DEH concentration increases, the efficiency of hole transport away from the CGL increases but the xerographic efficiency is unaffected due to increased hole trapping at the CGL/CTL interface. Randolph and Neeley examined the charge-injection process using Marcus charge-injection theory.[140] A series of dual-layer OPCs were prepared with a TiOPc CGL and a CTL of 40 wt % CTM in bisphenol A polycarbonate.[141] Six CTMs were chosen to span a range of oxidation potentials from 0.45 to 0.89 V versus Ag/AgCl. The rate of electron transfer from photooxidized TiOPc to the CTM was taken to be the quantum yield of charge injection, which was inferred from the initial rate of xerographic discharge at high field assuming that other factors were negligible. A Marcus "inverted" region was observed and the data were fit with a reorganization energy of 0.14 eV and CGM oxidation potential of 0.79 V. The oxidation potential of TiOPc dissolved in dichloromethane (very low solubility) was found to be 1.04 V, but the discrepancy is perhaps understandable since in the OPC the phthalocyanine is in pigment form and the binder polymer and dichloromethane are very different.

OPCs with mixed phthalocyanine pigment-based CGLs have been reported. Hayashida and co-workers prepared dual-layer OPCs with CGLs containing TiOPc and ClInPc.[142] The pigment mixture was acid-pasted and treated with "organic solvent" to create a mixed crystal pigment. Dual-layer OPCs prepared from mixed crystals with varying content exhibited increasing sensitivity with increasing TiOPc content, although few details are provided. Molaire and co-workers have prepared OPCs with cocrystalline mixtures of TiOPc and TiO(F_4-Pc) by a combination of dry milling and solvent treatment.[143,144] Dual-layer OPCs prepared with the cocrystalline pigment exhibit enhanced photosensitivity. A detailed study of the effect of CGL binder polymer (polyvinyl butyrals of various compositions) on milling and pigment dispersion

preparation was reported by Molaire and co-workers.[145] By using blends of previously prepared dispersions containing TiO(F_4-Pc) and TiOPc/TiO(F_4-Pc), it is possible to prepare CGLs with tunable sensitivity over a wide range.

Suzuki and Takahashi have prepared interesting dual-layer photoreceptors where the CGM binder polymer is an organic−inorganic hybrid containing TiO_2 prepared by the sol−gel method.[146] To prepare the CGL, Ti-(i-OC_3H_7)$_4$ was hydrolyzed with ethanol followed by the addition of aqueous acidic ethanol. X-H_2Pc pigment was added and the mixture was dispersed by ball milling and coated on top of the previously coated CTL (∼0.4 μm). Curing was accomplished by heating to 150 °C for 30 min. The CTL (∼15 μm) was 25 wt % of 1,1-bis(p-diethylaminophenyl)-4,4-diphenyl-1,3-butadiene in polycarbonate. Dual-layer OPCs were prepared with both the standard and the inverted architecture. With the CGL on top (positive charging), the photodischarge exhibited a severe induction effect and the photodischarge rate was extremely slow. However, when the CTL was on top (the standard dual-layer architecture), the negatively charged OPC did not exhibit a photodischarge induction effect but required 100 μJ/cm^2 to photodischarge from −400 to −200 V with a 100 V residual potential.

5.2. Molecular Complexes

The charge-transfer complex between poly(*N*-vinyl carbazole) (PVK) and 2,4,7-trinitrofluorenone (TNF) and the complex between a pyrylium dye and bisphenol A polycarbonate are the most prominent examples of molecular complex-based charge-generation materials. The PVK−TNF complex was the first organic material brought to commercialization,[43] and many reviews are available.[9,147−152] Because of toxicity concerns around TNF, this OPC had a short commercial life. The sensitization of photogeneration in PVK by forming charge-transfer complexes with electron acceptors has been known for some time.[153−155] The carrier-generation mechanism in PVK films doped with electron acceptors has received considerable attention. Melz used the xerographic discharge technique to determine the field dependence of the photogeneration efficiency of a PVK−TNF film (molar ratio of TNF to PVK of 0.06).[156] For a 15 μm film with 550 nm irradiation (optical density of ∼0.6), the generation efficiency was independent of the surface charge polarity, indicating that, under these conditions, both holes and electrons are efficiently transported. The results were analyzed using the Onsager theory in which the initial step involves autoionization of the bound excited state to produce a geminate charge pair that separate by field-dependent diffusion in competition with Coulombic attraction and recombination. The limiting quantum efficiency was 0.23. When OPCs with a molar ratio of 1:1 were examined, the photogeneration efficiency increased significantly but the limiting quantum efficiency remained the same. The difference is attributed to weaker field dependence for charge separation, which in the Onsager model is an increase in the separation distance between the geminate charge pair, from 2.5 to 3.5 nm. Yokoyama and co-workers investigated the mechanism of charge generation in PVK doped with various electron acceptors.[157] The general mechanism shown in Figure 20 was proposed for charge generation in donor−acceptor systems.[158,159] A key feature of this mechanism is that thermalization of a higher excited state of the charge-transfer complex is the direct precursor of a "loose ion pair" with initial separation of 3 nm. The lower-energy

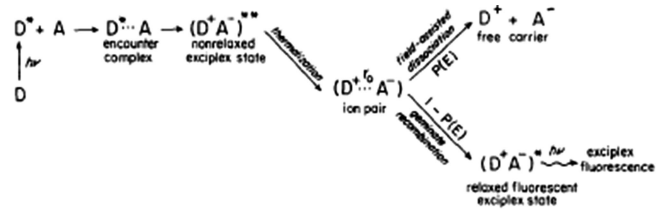

Figure 20. General mechanism for charge generation in charge-transfer systems with PVK as the electron donor. (Reprinted with permission from reference 158. Copyright 1982 American Institute of Physics.)

fluorescent charge-transfer state is not involved in charge generation. More recently, Abramavicius and co-workers have studied a similar system, poly-*N*-epoxypropylcarbazole doped with varying concentrations of TNF.[160] Charge-transfer absorption bands are observed at ∼460 and ∼550 nm. Fluorescence (maximum ∼640 nm) is assumed to arise from electron−hole recombination. In addition, excitation into the charge-transfer absorption gives rise to transient absorptions at ∼600 and ∼800 nm, which are assigned to the radical anion of TNF and the radical cation of the carbazole moiety, respectively. On the basis of the kinetic characteristics of the fluorescence and induced absorptions, it was concluded that there is a distribution of charge-transfer complexes and a corresponding distribution of initial charge-pair separation distances in this system. In PVK−TNF OPCs, photodischarge occurs by transport of both holes, through the PVK, and electrons, through the TNF.

Donor−acceptor charge-transfer complexes of PVK with fulleranes of various types have been investigated. Wang found that, with a positive surface charge, films of PVK doped with C_{60}/C_{70} (∼85:15) exhibited high photosensitivity compared to PVK-only films.[161] The field dependence of the charge-generation efficiency was fit to the Onsager model with a primary quantum yield of 0.9 and r_0 of 1.9 nm. The photodischarge occurred by hole transport through the PVK (photodischarge with a negative surface charge and strongly absorbed light was less efficient). The charge-transfer complex absorption maximum occurred ∼500 nm with absorption tailing to 700 nm, and the photosensitivity action spectrum (charges generated per photons incident) mirrored the film absorption. Chen and co-workers compared the photodischarge sensitivity of C_{60}-modified PVK (3.85% and 12.28% C_{60}), C_{60} doped PVK, and PVK.[162] The photosensitivity decreased in the following order (the numbers in parentheses are the relative initial slopes of the published photodischarge curves): 3.85% C_{60}-PVK (12), 12.28% C_{60}-PVK (5), 3.85% C_{60} doped PVK (2), and PVK (1). Itaya and co-workers used picosecond laser photolysis to study the mechanism of charge generation in films of 0.7 mol % C_{60} doped into PVK.[163] They concluded that the charge-separated state was produced immediately after excitation (532 nm, 1 ps) and decayed with a time constant of 1.2 ns via three paths: recombination, hole migration through carbazole moieties, and formation of the triplet state of C_{60}. The hole migration path was 30% and the authors proposed that this is the source of the enhanced photoconductivity in fullerene doped PVK. Wang and Suna examined the effect of applied electric and magnetic field and concluded that charge generation occurs through the singlet state of a weak charge-transfer complex between PVK and the fullerene.[164]

The dye−polymer based OPC was first described in 1978.[49] There have been some recent reports on the dye−polymer complex based OPC. A good illustration of

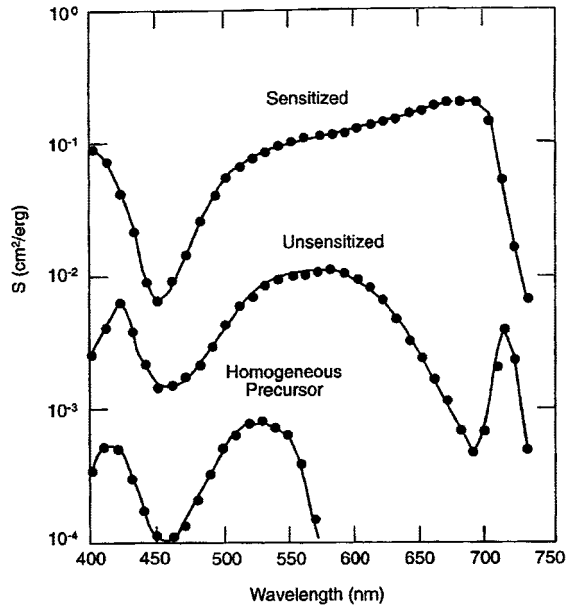

Figure 21. Comparison of the photosensitivity action spectra of three OPCs based on the dye−polymer aggregate (exposure through the positively charged surface). (Data in part from ref 10 in part).

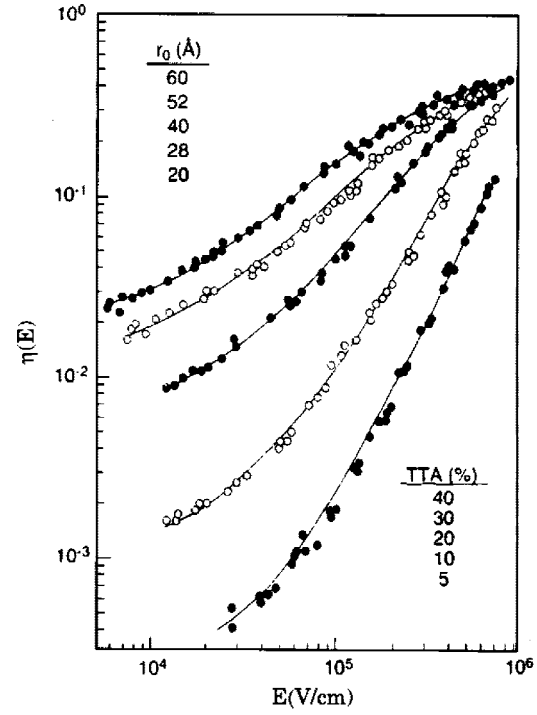

Figure 22. Dependence of the charge-generation efficiency of the aggregate-based CGM on field as a function of TTA concentration in the CTL. (Reprinted from ref 42 with permission of IS&T: The Society for Imaging Science and Technology, sole copyright owners of *Journal of Imaging Science and Technology.*)

the effect of sensitization is to compare the photosensitivity of the positive charged single-layer dye−polymer aggregate photoreceptor in three different forms: nonaggregated precursor, aggregated, and aggregated and sensitized by the addition of a hole-transport material and sensitizer, 4,4′-bis(diethylamino)-2,2′-dimethyltriphenylmethane (Figure 21).[10] The dye is 4-(4-dimethylaminophenyl)-2,6-diphenylthiapyrylium perchlorate and is present at ∼10 wt % in bisphenol A polycarbonate. When coated, the film absorption is that of the dye with a maximum at ∼580 nm. However, when the film is plasticized (as by exposure to dichloromethane vapors), the dye is able to diffuse and form an aggregate with the polymer and the absorption is shifted to 680 nm. The physical structure of the aggregate is that of fine filaments.[49] In the unsensitized form, the photosensitivity action spectrum actually exhibits a minimum at 680 nm. This behavior is consistent with electron transport through the filaments as being the primary mode of photodischarge of the OPC. On the addition of ∼40 wt % CTM, the photosensitivity is increased and mirrors the absorption spectrum.[50] In the presence of the CTM, the action spectra with positive and negative surface charging indicate that photodischarge occurs with similar contributions from hole and electron transport. Thus, the hole-transport material has both sensitized the photogeneration of charge and facilitated their transport through the OPC. The dependence of photogeneration on field and CTM content has been reported by O'Regan and co-workers.[42] The photoreceptor was dual-layer with a 2−3 μm CGL and 10−20 μm CTL. The CGL comprised the dye, bisphenol A polycarbonate, and tri-*p*-tolylamine (TTA) CTM. The CTL contained TTA in a polyester binder. Figure 22 shows the effect of TTA on the field dependence of generation. The solid lines are calculated based on the Onsager theory where r_0 is the electron−hole separation distance in the geminate pair, which is related to the field dependence of generation. The results were interpreted in terms of excition formation and diffusion to the interface between the dye−aggregate filament and the CTL followed by "surface-enhanced exciton dissociation" and charge formation. It was speculated that the decrease in the field dependence of charge generation with increasing TTA concentration in the CTL was related to the concentration dependence of hole mobility in the CTL. The limiting quantum yield for charge generation was about 0.6.

5.3. Azo Pigments

Azo pigments (molecules containing the "azo" functionality (−*N*═N−) are very popular charge-generation materials in OPCs. Bisazo (two azo units in the molecule) pigments strongly absorb visible light, and trisazo (three azo units in the molecule) pigments absorb into the near-infrared. Molecular structures of two typical examples are shown in Figures 5 and 6, and their photosensitivity action spectra are shown in Figures 8 and 9, respectively. Thus, this class of CGMs can be utilized in EP engines with either visible or near-infarared exposure systems. A bisazo pigment, chlorodiane blue (4,4′-bis(1″-azo-2″-hydroxy-3″-naphthanilide)-3,3′-dichlorobiphenyl), based dual-layer OPC was commercialized for the IBM 3800 Printing Subsystem model 3 and described in 1984.[165] This OPC had a 0.1 μm CGL and 16 μm CTL with DEH based CTM. The exposure system used a He−Ne laser, and the exposure requirement for imaging was 14 erg/cm^2. An OPC using the trisazo pigment shown in Figure 5 was described in 1989 for use in a Ricoh laser printer with a 780 nm exposure system.[166] The OPC was dual-layer with a 0.2 μm CGL with polyvinylbutyral as the binder and a 45 μm CTL with 4-*N*,*N*-bis(4-methylphenyl)amino-α-phenylstilbene as CTM in a polycarbonate binder polymer.

Since azo pigments are synthesized by azotization of an aromatic amine followed by reaction with an active coupling agent, such as a 2-hydroxy-3-naphthanilide (Naphthol AS), the molecule has a 1-azo-2-hydroxy structural unit. With this structure, two tautomers are possible, and according to Law:

"Without exception, all photoconductive azo pigments have been found to exist as ketohydrazones in solids."[1,167] Unlike the phthalocyanines, polymorphism is not a ubiquitous feature of azo pigments. However, Law has synthesized unsymmetrical bisazo pigments from a 2-nitro-4,4′-diaminodiphenylamine, where solid-state intermolecular donor−acceptor interactions are possible, and observed red-shifted absorption and enhanced photosensitivity.[168]

In 1977 Meltz showed that, for a dual-layer OPC with chlorodiane blue based CGL, the oxidation potential of the CTM was a dominant factor in the photogeneration efficiency as determined by the initial slope of the PIDC. The CTMs were 1-(4-X-phenylvinyl)-3-phenyl-4-(4-X-phenyl)-2-pyrazoline where X = H, methoxy, and diethylamino. OPCs with these CTMs were compared with an OPC with a PVK CTL. At a field of 2×10^5 V/cm and 550 nm exposure, the approximate efficiencies were 0.2 (diethylamino), 0.02 (methoxy), 0.01 (H), and 0.001 (PVK). A similar result was reported by Kakuta and co-workers, who examined OPCs formulated with a large variety of CTMs (with an oxidation potential range of ∼1 eV) and a chlorodiane blue based CGL.[169] For these OPCs, there was a linear correlation of the log of the photosensitivity (energy for a −800 to −400 V white light photodischarge) with CTM ionization potential. DiPaola-Baranyi and co-workers came to a similar conclusion in their investigation of dual-layer OPCs using four bisazo pigments and five CTMs.[170] Law and co-workers have synthesized a large number of bisazo pigments and compared their photosensitivities when used as CGMs in dual-layer OPCs with CTLs containing *N*,*N*′-diphenyl-*N*,*N*′-bis(3-methylphenyl)-1,1′-biphenyl-4,4′-diamine (TPD) as the CTM.[171−173] Substituent effects on photosensitivity were observed; after extensive study, it was concluded that the most likely explanation was that the substituents were influencing the size of the pigment in the CGL, and the smaller the size (larger surface are) the greater the photosensitivity.

Murayama has reviewed the process of designing bisazo pigments for OPCs with improved sensitivity and lightfastness.[174] The process is outlined in Figure 23. The aromatic diamino component chosen was 2,5-bis(4-aminophenyl)-1,3,4-oxadiazole and was coupled with 2-hydroxy-3-naphthoic acid anilide (Naphthol AS), which is C-1 in Figure 23. The resulting bisazo pigment (A-1) was used as the CGM, but the OPC exhibited poor cyclic stability due to light fatigue. Another coupler, C-2, was used to produce pigment A-2. The OPC with A-2 based CGM was Mitsubishi Chemical Corporation's first commercialized OPC. However, the lifetime was still only 10 000 copies because of poor cyclic stability due to light fatigue. Since perinone pigments have good lightfastness, a coupler, C-3, was prepared with similar chemical structure. Since C-3 has two isomers, coupling produces A-3, which is a mixture of three isomers. Compared with A-1, an OPC with A-3 CGM had three times the photosensitivity and had greatly improved stability to fluorescent light exposure. Solid state ^{13}C NMR analysis of these pigments indicated that A-1 and A-2 were ketohydrazone tautomers while A-3 was hydroxylazo, and this was suggested as the reason for improved light stability. On the basis of published work, it was reasoned that a large excited state dipole moment would lead to enhanced exciplex formation with the CTM and increased charge-generation efficiency. This led to the synthesis of the unsymmetrical pigment A-4. This pigment exhibited both hydroxylazo and ketohydrazone tautomers. The OPC with A-4 had doubled photosensitivity relative to A-3. In this work, it was also found that the charge-generation efficiency was dependent on the CTM used in the CTL.

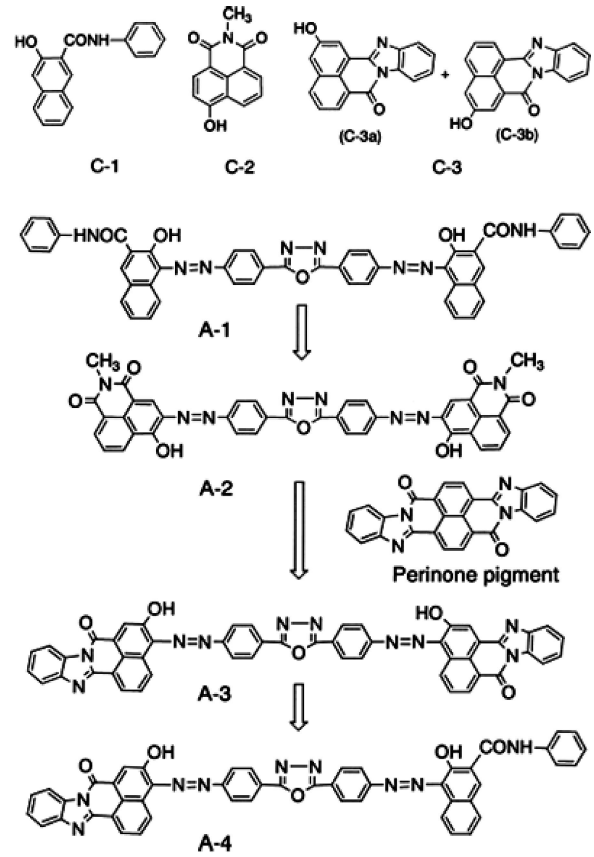

Figure 23. Design of bisazo pigments. (Reprinted from ref 174 with permission of IS&T: The Society for Imaging Science and Technology, sole copyright owners of *Journal of Imaging Science and Technology.*)

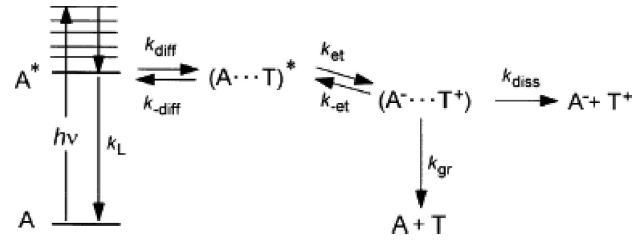

Figure 24. Mechanism for extrinsic charge generation in OPCs with azo pigment CGMs. (Reprinted from ref 175 with permission of IS&T: The Society for Imaging Science and Technology, sole copyright owners of *Journal of Imaging Science and Technology.*)

5.3.1. Charge-Generation Mechanisms

The mechanism of charge generation in azo pigment based OPCs has been extensively studied. Figure 24 shows a mechanistic scheme proposed by Umeda that summarizes an extensive body of research.[175] Charge generation is extrinsic, and following light absorption and relaxation to the first singlet state, the exciton diffuses from the site of absorption within the pigment to the surface of the pigment particle, where it forms an exciplex with adsorbed charge-transport molecules (T). The exciplex undergoes charge separation, and the charged species are separated under the influence of the applied field. One should keep in mind that, in a dual-layer OPC, when the CTL overcoats the CGL, the

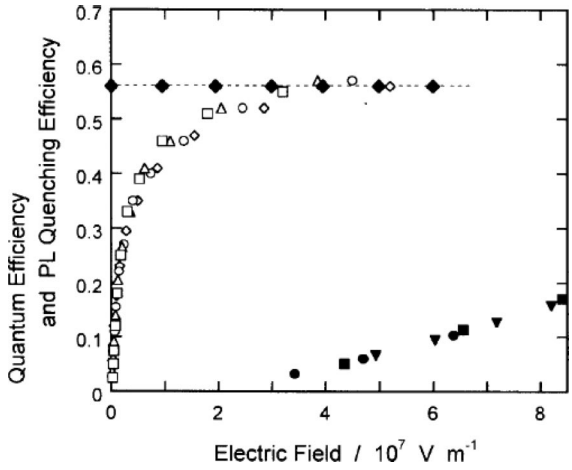

Figure 25. Quantum efficiency (symbols) and fluorescence quenching data (dashed line) for OPCs with a bisazo fluorenone based CGM (shown in Figure 5). Solid symbols are for a single-layer OPC (pigment and binder only) with varying thickness (0.15 and 0.27 μm), and open symbols are for a dual-layer OPC with varying CGL thickness (0.09−0.49 μm) and 22 μm CTL. The OPC used in the luminescence experiments had a 0.15 μm CGL and 1.9 μm CTL. (Reprinted from ref 175 with permission of IS&T: The Society for Imaging Science and Technology, sole copyright owners of *Journal of Imaging Science and Technology.*)

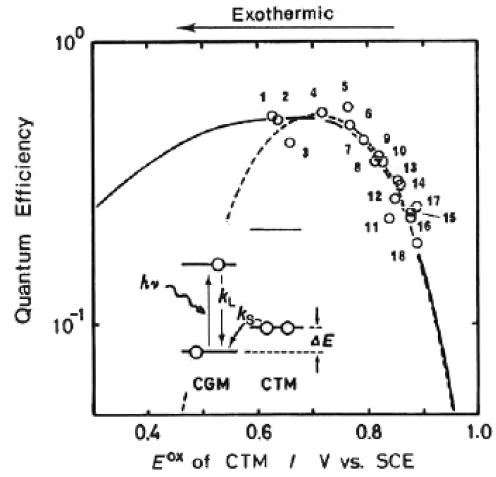

Figure 26. Effect of charge-transport material oxidation potential on the quantum efficiency for charge generation in a dual-layer OPC with a trisazo pigment CGL. Excitation was 700 nm, and the applied field 4×10^5 V/cm. (Reprinted with permission from ref 180. Copyright 1993 American Chemical Society.)

two-layer structure is preserved but the CTL solvent penetrates and swells the CGL, allowing the small-molecule transport materials to duffuse throughout the CGL.[176,177] Experiments were carried out on an OPC with the fluorenone bisazo pigment shown in Figure 5. The CGL was pigment and poly(vinyl butyral) (4:10 weight ratio), and the CTL was DEH CTM in polycarbonate (9:10 weight ratio). Layer thicknesses were as described in the caption of Figure 25. The single-layer OPC was pigment-only, and the effect of the addition of the hole-transport layer is very apparent. From this data, one can conclude that there is very little intrinsic charge generation. The fluorescence has a lifetime of 409 ps and was identified by electroabsorption experiments as a Frenkel exciton. Fluorescence quenching is observed to be independent of the applied field, and the generation efficiency increases with field and eventually becomes equal to the quenching efficiency. Also, the quantum efficiency for charge generation is independent of wavelength from 480 to 660 nm. These observations are incorporated into the mechanistic scheme in Figure 24. Since electron transfer occurs in charge generation, it was argued that the difference in ionization potentials between the pigment and CTM (0.47 eV for these materials) makes back electron transfer very inefficient. The fluorescence emissions from the oxadiazole-based pigments A-1, -2, and -3 shown in Figure 23 were found to have two components (50−60 and 130−200 ps), both of which were quenched by DEH.[178] Schreiber and co-workers examined the photoconductivity action spectra for a bisazo pigment and found over an order of magnitude increase in the charge-generation efficiency in the presence of a hole-transport molecule.[124]

The mechanism of charge generation in the trisazo pigment (Figure 6) has also been studied extensively. From electroabsorption, the first excited singlet state was identified as a charge-transfer exciton,[179] and doping the CGL with charge-transport material increased the photogeneration efficiency by an order of magnitude.[45] For electron-transfer reactions, Marcus theory predicts that the electron-transfer rate will depend upon the difference in oxidation potentials of the donor and acceptor components. Figure 26 shows this effect with an OPC having a CGL based on the trisazo pigment and CTL with transport materials having a range of oxidation potentials.[180] The two lines are fits assuming adiabatic (dashed line) or nonadiabatic electron transfer (solid). For the former case, the reorganization energy was 0.19 eV and the CGM oxidation potential was 0.90 V (vs SCE). The measured oxidation potential of 0.86 V agreed reasonably well with that obtained from the fit.

Charge generation in azo pigments has been studied using thermally stimulated current. In these experiments, the OPC sample is irradiated at low temperature, and a field is applied, and the current is monitored as the sample is heated. Dual-layer photoreceptors (CGL of 50 wt % bisazo A-3 in Figure 23 in poly(vinylbutyral), ~0.3 μm, CTL of 50 wt % hydrazone CTM in polycarbonate, ~16 μm) were used in these studies.[181] When the irradiation occurs with sample below 160 K, the amount of charge collected is independent of field or temperature. Above 160 K, the amount of charge increases with both increasing field and temperature. These results demonstrated that the efficiency of charge generation (exciton migration and charge-transfer interaction with the CTM) is independent of field and temperature. From the time dependence of the decay of collected charge, it was determined that there was some slow first-order decay (~1 s) of bound charge pairs but dissociated charge pairs were stable indefinitely below 160 K.[182] Above this temperature, which corresponds to energy of 0.014 eV, field- and temperature-dependent charge separation and charge recombination compete. Using an Arrhenius model, $k = k_0 \exp[-E_a/kT]$ where k is the rate, E_a is the activation energy, k is the Boltzmann constant, and T is the temperature, for the competition between charge separation and recombination, the data was fit with recombination $k_0 = 2.7 \times 10^6$ s^{-1} and $E_a = 0.25$ eV and separation $k_0 = 5.9 \times 10^3$ s^{-1} and $E_a = 0.15$ eV.[183] The generation efficiency was found to depend on the combination of CGM and CTM used in the OPC formulation. With this CGM and DEH CTM (oxidation potential vs SCE 0.52 V), the photosensitivity for photodischarge from −700 to −350 V was 2.3 cm^2/μJ, but with a CTM with higher oxidation potential (hydrazone CTM from diphenylhydrazone and 1-formylpyrene, 0.92 V vs SCE), the photosensitivity was 4.0 cm^2/μJ. When an asymmetric CGM

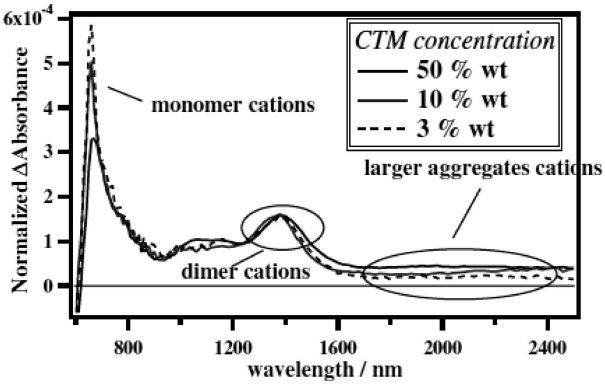

Figure 27. Transient absorptions of CTM cation radicals. (Reprinted from ref 185 with permission of IS&T: The Society for Imaging Science and Technology, sole copyright owners of IS&T's NIP19: International Conference on Digital Printing Technologies Proceedings.)

was used (A-4 in Figure 23), the photosensitivity with DEH was 3.3 $cm^2/\mu J$ and with the pyrene-based hydrazone was 4.8 $cm^2/\mu J$.

Conclusive evidence of the involvement of the CTM in charge generation comes from time-resolved absorption studies on OPCs with azo pigment CGMs. The OPCs studied included those mentioned above in connection with thermally stimulated current measurements. The transient absorption spectrum is collected after exposure (525 nm, 120 fs pulse) in the absence of an applied electric field.[184,185] Absorptions from an OPC with CGM A-3 (Figure 23) and the pyrene-based hydrazone mentioned above are shown in Figure 27. Broad absorptions are observed at 700, 1400, and 2000 nm, which are assigned to the CTM radical cation, CTM dimer cation, and the cation of larger CTM aggregates. As the CTM concentration increased, the 2000 nm absorption increased at the expense of the 700 nm absorption. The decay of the absorption at 1200 nm was fit to a double exponential with time constants of 6.1 μs (41%) and 69 μs (51%). The decay time of the 1200 nm absorption was increased in formulations containing a CTM with lower mobility. These observations were collected in a proposal for charge generation involving photoinduced electron transfer between the CGM and CTM to produce the CGM radical anion and CTM radical cation followed by a competition between recombination and free carrier formation. The latter process occurs within 1 ms. At zero applied field, the free carriers have a lifetime of several seconds, and they are mobilized on application of a field.

5.4. Perylene Pigments

Because the perylene molecule is relatively flat, diimides of perylene-3,4,9,10-tetracarboxylic acid exhibit polymorphism depending on the nature of the imide substituent. Figure 28a shows the solution and the vacuum-deposited film absorption spectra of *N*,*N*-bis(2-phenethyl)-perylene-3,4:9,10-bis(dicarboximide).[186] The thin film spectrum is broadened somewhat relative to solution, but when heated, or exposed to solvent vapors, a new red-shifted absorption appears (Figure 28b). Other, structurally related pigments with *N*,*N*-bis(methyl) and *N*,*N*-bis(3,5-dimethylphenyl) substituents have identical solution spectra but as films do not exhibit the intense absorption ~600 nm.[187] On the basis of crystal structure studies, it was concluded that the long-wavelength absorption is the result of intramolucar stacking, giving rise to exciton coupling, which varies depending on the imide

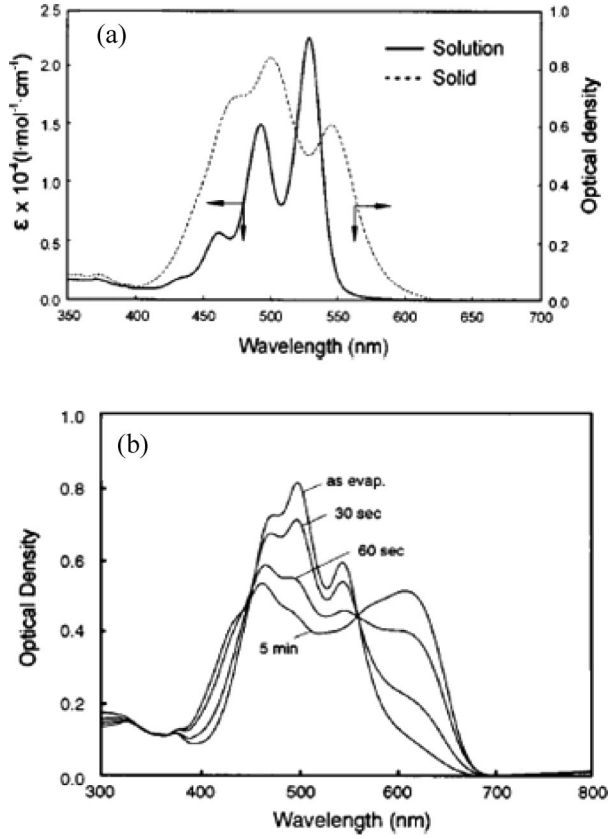

Figure 28. (a) Shows the absorption spectra of *N*,*N*-bis(2-phenethyl)-perylene-3,4:9,10-bis(dicarboximide) dissolved in dimethyl sulfoxide and as a thin film produced by vacuum deposition; (b) shows the effect of heating the evaporated film at 100 °C. (Reprinted with permission from ref 186. Copyright 1998 American Institute of Physics.)

substituents.[188] Since polymorphism in this class of pigments is associated with molecular planarity, Loutfy and co-workers examined several perylenes and observed a correlation between molecular planarity and OPC photosensitivity.[40] The OPC with the highest photosensitivity had a CGM (0.1 μm) of a cis- and trans-mixture of a bisbenzamidazole perylene (see Figures 5 and 6). The best performance was achieved with a dual-layer OPC having the following formulation and architecture: Mylar/Al/silane charge-blocking layer (0.1 μm)/perylene (vacuum deposited 0.1 μm)/35 wt % TPD in bisphenol A polycarbonate (~15 μm).

Kazmaier and co-workers have carried out extensive molecular modeling studies in an effort to identify highly photosensitive polymorphs and to extend the perylene absorption into the near-infrared. Dreiding force-field calculations were found to be useful for studying polymorphism in perylene pigments.[189] Pariser−Parr−Pople calculations predicted that the perylenebisimide absorption at 469 nm would be red-shifted by 136 nm by going to a dibenzoperylene structure.[190] This material was synthesized, and the actual red shift was 160 nm. Unfortunately, the absorption was weak above 750 nm and OPCs prepared with this CGM had low photosensitivity. Similar results on this CGM had been previously reported.[191] Extended Hückel semiempirical molecular orbital calculations were carried out on one-dimensional stacks of perylene.[192] Because the highest occupied molecular orbital (HOMO) and the lowest unoccupied molecular orbital (LUMO) of the individual molecules have nodal characteristics, when one molecule is displaced relative to another, either transversely or longitudinally, the

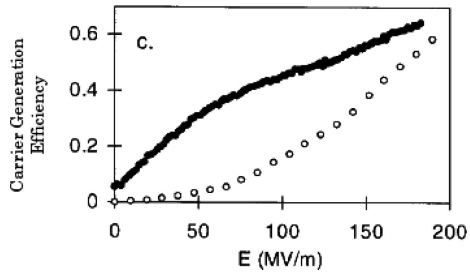

Figure 29. Carrier-generation efficiency as a function of field for samples having CTLs with 0 wt % TTA (open circles) and 20 wt % TTA (filled circles).[198] (Reprinted from ref 194 with permission of IS&T: The Society for Imaging Science and Technology, sole copyright owners of *Journal of Imaging Science and Technology.*)

wave function overlap does not decrease monotonically with decreasing overlap but will oscillate due to quantum mechanical interference.

5.4.1. Carrier Generation

Carrier generation in OPCs containing perylene as the CGM has been studied by Popovic and co-workers. The benzimidazole perylene CGM (Figure 5) as an evaporated film (0.2 μm) was found to have high photogeneration efficiency when overcoated with a CTL containing TPD as the CTM, and the pigment fluorescence was quenched.[47] When overcoated with a polymer-only CTL, the efficiency was almost 50-fold lower (at 20 V/μm). Interestingly, the CGL, although coated from dichloromethane solution, apparently did not penetrate the perylene CGL as the efficiency was higher with exposure at the CGL/CTL interface (quantum efficiency of 0.36) relative to exposure from the opposite side (quantum efficiency of 0.20). Similarly, the fluorescence from a film of the pigment was quenched after dipping into a dilute solution of TPD in dichloromethane but recovered on rinsing with pure solvent. The mechanism proposed was exciton diffusion and formation of a charge-transfer state, which dissociates under the influence of the applied field. The extent of fluorescence quenching depended on the CTM oxidation potential such that a low oxidation potential hydrazone (0.53 V vs SCE) did little quenching but extensive quenching was observed with PVK (0.79 V vs SCE). This data was consistent with the proposed mechanism in that efficient charge transfer requires the CTM HOMO, which is related to the solution oxidation potential, to be higher in energy than the pigment HOMO.

Several studies have been carried out on the charge-generation mechanism with *N*,*N*-bis(2-phenethyl)perylene-3,4:9,10-bis(dicarboximide). As mentioned above, this pigment exhibits a long-wavelength absorbing polymorph (Figure 28).[186] OPCs prepared with a thin film CGM of this polymorph exhibited a 3-fold enhancement in charge-generation efficiency relative to an OPC where the pigment was amorphous.[193] Subsequently, Popovic and co-workers examined field-induced fluorescence quenching as a function of the amount of CTM (TTA) in the CTL and concluded that both intrinsic and extrinsic (involving CTM) charge generation were important.[194] At low fields (<1 V/μm), extrinsic generation dominates, but this saturates at higher fields and intrinsic charge generation becomes more important. The carrier generation efficiencies for OPCs with 0 and 20 wt % TTA in the CTL are shown in Figure 29. The samples used in this study were prepared in a manner that differs from the usual method of OPC construction. A thin charge-injection blocking layer of hexamethyldisilazane was spin-coated on a NESA glass substrate. This was followed by spin-coating a 1 μm CTL layer of TTA in bisphenol A polycarbonate and vacuum depositing a 0.1 μm layer of pigment. The sample was subsequently exposed to dichloromethane vapors to convert the pigment to the photoactive form. The solvent treatment may also enable CTM to diffuse into the pigment layer, although the typical OPC construction procedure of overcoating the pigment layer with the CTL solution would be much more effective in that regard. It is not known how the different construction methods might affect charge generation.

5.5. Charge Generation in Other Pigments

The preceding discussion highlights most of the recent activity around pigments commonly used as the CGMs in OPCs. However, there are many, many examples of other pigments that have been tried as CGMs. One such class of materials is the squaraines (Figure 6). This class received considerable attention in Law's 1993 review,[1] and not a great deal of new information has been obtained since then.

Mixed-pigment CGM systems have been mentioned previously in connection with the phthalocyanines, and in this section, we will discuss some other OPCs in which the CGM is a mixture of different classes of pigments. Mixing pigments would seem to be a natural direction since charge generation is facilitated by having sites within or on a pigment particle where exciton localization and charge transfer can occur. One might imagine that, in a mixed crystal or even two crystals in intimate contact, where the components had different electron affinities, it would provide such sites. Kawahara and co-workers have demonstrated that this is indeed the case in their studies of single-layer OPCs with CGM comprising a mixture of H_2Pc and *N*,*N*′-bis(3,5-dimethylphenyl)-3,4:9,10-perylene bis(dicarboximido) and a CTM (40 wt %) of 9-isopropyl-9H-carbazole-3-carbaldehyde diphenylhydrazone in bisphenol A polycarbonate.[195] The OPC (~20 μm) had a CGM of 5 wt % perylene or 0.4 wt % phthalocyanine, or a mixture of the two. Figure 30 shows the absorption spectra of the two pigments in polycarbonate films, and the spectral sensitivities for these three OPCs for 50% photodischarge from an initial surface potential of 700 V. The perylene OPC has spectra sensitivity only in the visible as expected but the addition of a small amount of phthalocyanine results in a dramatic increase in photosensitivity in the near-infrared. Particle-size analysis of dispersions and SEM analysis of the mixed pigment film showed that the mixed system has pigment aggregates, and it was suggested that the p-type phthalocyanine and n-type perylene aggregate due to an opposite sign of surface charge and form a p/n junction at the point of contact. Thus, the contact point will be a site for efficient charge generation. Chen and co-workers have similarly reported that dual-layer OPCs with mixed TiOPc and azo pigments exhibit enhanced photosensitivity.[196]

Hiramoto and co-workers have studied the charge-generation mechanism in films comprising 5 wt % pigment in polycarbonate.[197] The pigment, *N*,*N*-bis(methyl)-perylene-3,4:9,10-bis(dicarboximide) with or without added H_2Pc, was dispersed in polycarbonate. The interesting observation was made that the addition of H_2Pc increased the carrier-generation efficiency but the field-dependent quenching of perylene fluorescence was reduced. The mechanism proposed, Figure 31, invokes a dual path for charge generation.

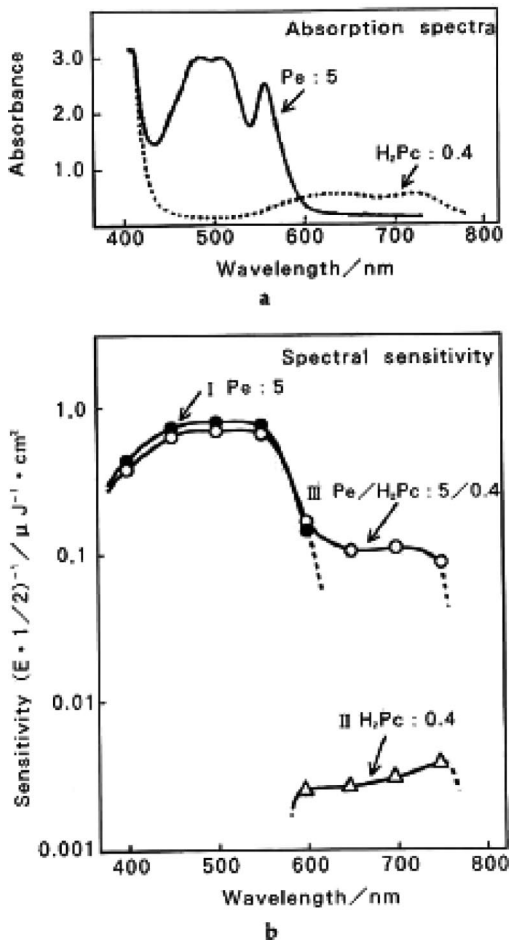

Figure 30. (a) Absorption spectra of 5 wt % *N,N′*-bis(3,5-dimethylphenyl)-3,4:9,10-perylene bis(carboximido) and 0.4 wt % H_2Pc in bisphenol A polycarbonate. (b) Spectral sensitivity of three single-layer OPCs with CGM of (I) 5 wt % perylene or (II) 0.4 wt % phthalocyanine or (III) a mixture of the two. (Reprinted from ref 195 with permission of IS&T: The Society for Imaging Science and Technology, sole copyright owners of *Journal of Imaging Science and Technology.*)

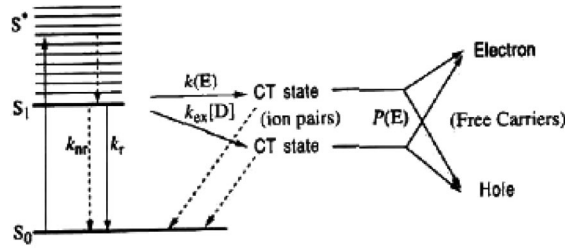

Figure 31. Two channel route for charge generation in *N,N*-bis(methyl)-perylene-3,4:9,10-bis(dicarboximide) doped with H_2Pc. The rate constants refer to radiative (r) and nonradiative (nr) decay.[197] (Reprinted with permission from ref 197. Copyright 1994 Chemical Society of Japan.)

One route is intrinsic through a charge-transfer state associated with the perylene, and the other is extrinsic through a charge-transfer state associated with where perylene and phthalocyanine particles are in contact. An interesting feature of this model is the proposal for a field-dependent rate of formation of a charge-transfer state for intrinsic charge generation.

Fullerenes, C_{60} and C_{70}, have been examined as charge-generation materials by Hosoya and co-workers.[198] A dual-layer OPC comprised a 1 μm vacuum-deposited layer of C_{70} overcoated with a 15 μm CTL of 30 wt % TPD hole-transport material in polystyrene. A photodischarge of −500 to −250 V required 0.5 $\mu J/cm^2$ over the wavelength range of 400−675 nm. The photosensitivity of C_{60} based photoreceptors was much lower. This was taken one step further by Yasuda and Takeuchi who studied the photoconductivity of vacuum-deposited mixtures of C_{60} and α-H_2Pc.[199] They concluded that, at phthalocyanine concentrations above ~60 wt %, the conduction changed from n- to p-type. OPCs containing fullerenes have not yet been studied, but Kessler has determined the valence band energies of several pigments; reasoning from the energetics of electron transfer from the HOMO of the pigment to the LUMO of the fullerene has predicted enhanced photogeneration of charge with all the standard phthalocyanine pigment CGMs.[200]

In summary, the mechanism that has emerged to explain charge generation in OPCs is complex and depends on the materials (pigments or molecular complexes), the class of pigment and chemical structure (azo pigment tautomerism for example), the pigment polymorph, and the presence of additives (electron donors or acceptors, pigments, water, etc.). Figure 31 shows the basics although it appears that intrinsic generation may or may not be field-dependent depending on the material. Charge generation occurs from the lowest-energy excited state(s) and is either intrinsic involving charge-transfer states associated with the generation material (crystal defects, surface-adsorbed oxygen, or water) or extrinsic involving charge-transfer states associated with additives. Other factors that are important with respect to OPC performance include the method of CGL preparation (pigment size, size distribution, and dispersion characteristics), formulation (pigment type and concentration, binder polymer(s), additives), and how the OPC is fabricated (CGL thickness and extent of CGL−CTL mixing, for example).

6. Charge-Transport Layer: Transport Models, Performance, and Materials

As discussed in section 4, successful electrophotographic imaging requires that charge transport through the CTL occur with little trapping in the time scale of the electrophotographic cycle. Here we discuss how this is accomplished in an "impure" organic chemical based CTL. There are several informative reviews on this topic.[201−204]

6.1. Charge-Transport Models

The CTL of an OPC is a glassy solid solution of a charge-transport active moiety in a polymer binder. The charge-transport moiety can be molecular or a polymer component. The molecular solutions are called molecularly doped polymers, MDP. The transport active component is typically 40−50% weight fraction of the CTL. Thus, "doping" in the present context is decidedly different from what doping refers to in conventional semiconductor physics.[205,206] In the latter case, the dopant is typically introduced at very low concentration to control the relative proportion of electrons and holes in the bands of a semiconductor crystal, leaving optical properties largely unaffected. In a semiconductor crystal at ambient temperature, the dominant field-driven transport mechanism is scattering-perturbed motion of charge carriers in the bands. Under these circumstances, mobility decreases algebraically with increasing temperature, while carrier population in the bands is thermally activated. The convolution of these processes manifests in a thermally activated conductivity. On the other hand, in MDPs under equilibrium

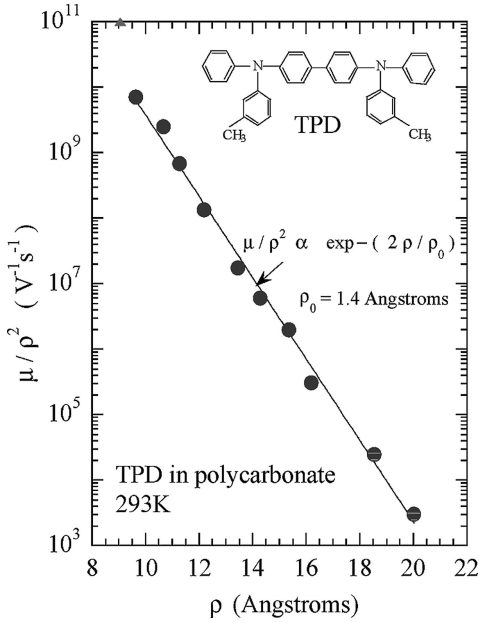

Figure 32. Variation of the mobility $\mu/(\rho)^2$ of TPD in bisphenol A polycarbonate as a function of intersite separation ρ at 293 K. (Reprinted with permission from ref 210. Copyright 2004 Elsevier B.V.)

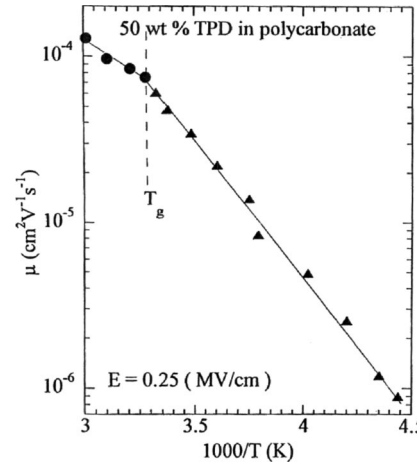

Figure 33. Dependence of the drift mobility for a MDP of 50 wt % TPD in bisphenol A polycarbonate (2.5×10^5 V/cm) on reciprocal temperature. A discontinuity occurs at the glass transition temperature (T_g) of the film. (Reprinted with permission from ref 210. Copyright 2004 Elsevier B.V.)

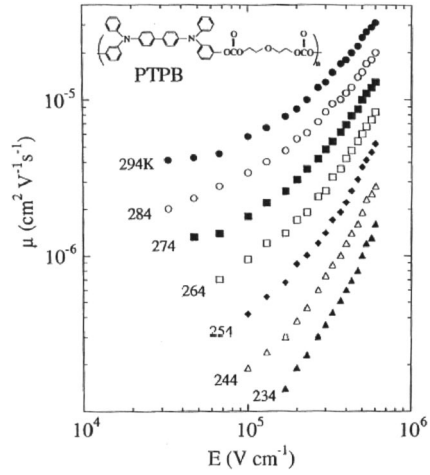

Figure 34. Field dependence of the hole mobility of the polymeric CTM PTPB parametric in temperature. (Reprinted with permission from ref 210. Copyright 2004 Elsevier B.V.)

conditions, the transport-active molecule is in the neutral state, and the glassy films are perfect insulators, that is, there are no free carriers present in thermal equilibrium.[207] These systems can nevertheless support relatively efficient charge transport under the action of an applied field when in contact with a charge reservoir. At fixed temperature, the drift mobility of extrinsic carriers decreases exponentially with increasing average intersite separation of the active molecule (ρ), so the drift mobility of MDPs can be tuned over a broad range by simply adjusting concentration.[208,209] This feature of tunability can readily accommodate a wide range of xerographic process speeds as described above and is therefore advantaged from a technological point of view. This is illustrated in Figure 32 for a common hole-transport material, TPD.[210] The data is in conformity with a simple tunneling model where ρ_0 is the wave function localization radius and the transport states are sited on the TPD molecules. At 40−50 wt % doping, approximately 10^4 "hops" are required for the hole to transit a 20 μm photoreceptor. The drift mobility in MDPs always has a thermally activated temperature dependence; thus, the log of the drift mobility scales with inverse temperature as illustrated in Figure 33, where earlier measurements[208] have been extended[210,211] to encompass the characteristic slope change displayed in the glass-transition region.[212] However, in a significant number of cases cited in the literature,[9] the analogous scaling is with the square of the inverse temperature, (i.e., nonsimple activation), as predicted by the disorder model.[213] The experimentally observed scaling with intersite separation, the temperature dependence, and the high degree of disorder in these systems clearly indicate that electronic transport must involve the field-biased hopping of carriers in an energetically inequivalent manifold of states sited on the transport active molecules. Apart from their technological importance in electrophotography[214] and light-emitting displays,[215] what has made MDPs a laboratory for the study of hopping transport is that a number of key secondary features in their transport behavior are in fact pervasive in other disordered molecular media.[216] There is then the suggestion of a common underlying mechanism susceptible to theoretical treatment. Thus, the field and temperature-dependent behavior of molecular dispersions is also observed in polymers with transport-active pendant groups like poly(*N*-vinylcarbazole),[217] in polymers in which small-molecule moieties are incorporated in a main chain[218] in sigma-conjugated polymers,[219,220] and most recently in certain poly π-conjugated systems.[221,222] Figure 34 is a plot of the field dependence of hole drift mobility in the polymer PTPB parametric in temperature over a 60 K range.[223] PTPB is a glassy polymer in which TPD moieties are covalently bonded into a main chain.[218] The data is replotted in Figure 35 to show the explicit dependence of the log mobility on the square root of the applied field. The field dependence is itself temperature-dependent and clearly becomes stronger with decreasing temperature. The two TPD-based hole-transport media are closely related, but qualitatively identical results are reproduced in polysilylenes and polygermylenes that have a sigma-conjugated backbone capable of supporting electron delocalization as inferred from analysis of absorption and emission spectra.[224,225] For example, hole transport in PTPB can be represented in an Arrhenius plot over the temperature range illustrated in Figure 36.[210] In this purely phenomenological description, the activation decreases with the square

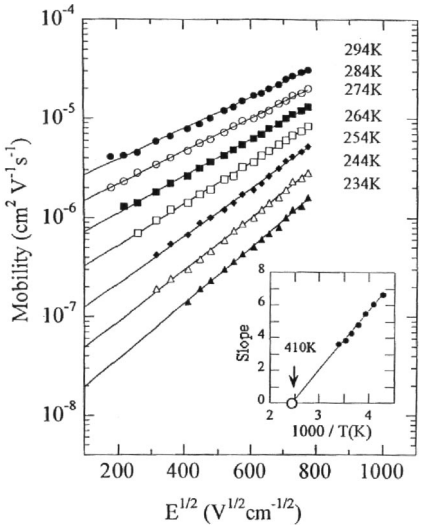

Figure 35. Data of Figure 34 replotted as a function of $E^{1/2}$. The insert shows the temperature dependence of the slope of each data set. (Reprinted with permission from ref 210. Copyright 2004 Elsevier B.V.)

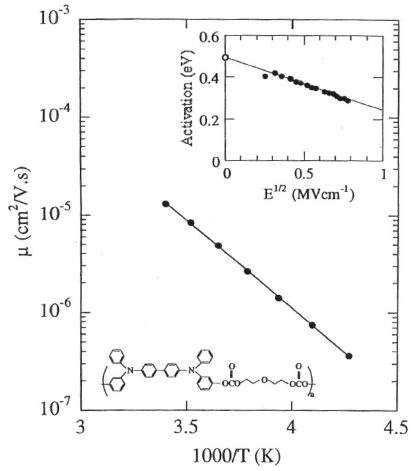

Figure 36. Arrhenius plot of the reciprocal temperature dependence of the hole mobility in PTPB. The field dependence of activation is shown in the insert. (Reprinted with permission from ref 210. Copyright 2004 Elsevier B.V.)

root of the applied field as displayed in the insert. Precisely the same behavior is exhibited when the same phenomenological description is applied to hole-drift mobility data in poly(methylphenylsilylene), PMPS, as shown in Figure 37. Combining drift mobility[226] and spectroscopic data[227] has in fact suggested that transport in these sigma-conjugated polymers involves the hopping of holes among chromophore-like main chain segments of varying length whose function for transport is therefore analogous to the TPD sites in PTPB. More recently, the convoluted pattern of behavior first identified in MDPs and, therefore, clearly characteristic of hopping among discrete energetically inequivalent molecular sites has been reported in TOF experiments on π-conjugated systems, notably the phenylene vinylenes. The sites, like those in polysilylenes, are interpreted to be domain-like backbone segments of varying conjugation length.[221,222] These combined results and the recurrent pattern of behavior they reveal in systems of widely varying composition and morphology suggest that a transport theory must be founded on universally shared characteristics.[228] The theoretical literature stimulated by these observations is in fact extensive and far too detailed to be adequately described here. In the

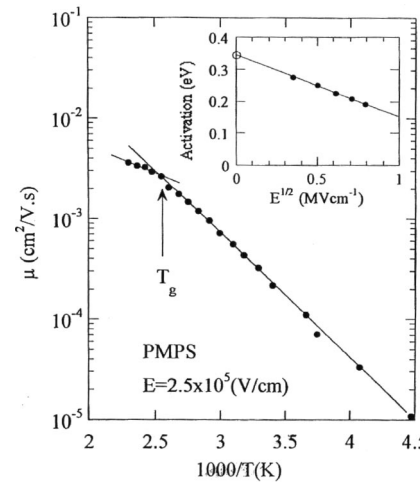

Figure 37. Arrhenius plot of the reciprocal temperature dependence of the hole mobility in poly(methylphenylsilylene), PMPS (T_g is the glass-transition temperature). The field dependence of activation is shown in the insert. (Reprinted with permission from ref 210. Copyright 2004 Elsevier B.V.)

present context, it suffices to briefly comment on certain general trends. The activated temperature dependence universal to all these materials systems arises because states in the hopping manifold are energetically inequivalent. Energetic inequivalence can be understood on the basis of site relaxation accompanying polaron formation.[229−231] Energetic inequivalence of sites is also a common feature of disordered solids resulting from site-to-site fluctuation of the static and dynamic electrostatic potential.[213,232,233] There is no excluding some combination of both effects. In fact, there is a general need to develop the framework for distinguishing the relative contributions of these key processes in the analysis of experimental data.[234,235] A particularly challenging issue has been the attempt to account for the special features of the Poole-Frenkel-like field dependence illustrated in Figure 35. Polaron models typically predict that the log mobility should scale linearly with applied field.[229,236] The disorder model based on analysis of Monte Carlo computer simulation of hopping on a finite lattice as originally proposed by Bässler was in fact able to self-consistently account for a number of key experimental features in terms of a limited set of disorder parameters.[213,232,237,238] On the other hand, it could only model the observed field dependence over a very narrow range. It was later recognized, in the formulation of dipole disorder models,[239−241] that slow site-to-site variation as distinct from fully random fluctuation in the effective electrostatic potential could more properly account for the field-dependent behavior of mobility commonly observed over several orders of magnitude.[241−244] The more general formulation of the disorder model developed by Dunlap and co-workers treats the disorder potential as fully correlated and, therefore, slowly varying, and argues that such a supposition is physically plausible on general grounds in glassy solids. Young and co-workers published a series of papers that have included the effects of group and net dipole moments, due to the polymer binder or the transport material itself, on charge transport.[245−250] Nevertheless, questions remain and a complete description of charge transport in MDPs remains elusive.[251−253]

If every chemical impurity remaining in even the most scrupulously processed polymer film could act as a trap, organics as a materials class would be completely excluded as a basis for the design of xerographic photoreceptors. Trap-

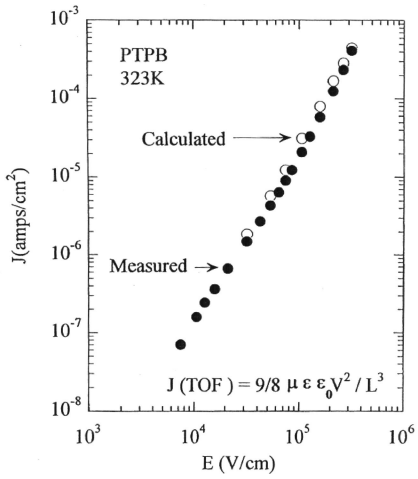

Figure 38. Field dependence of the dark current for a PTPB film at 323 K. Positive bias is applied to an Au coated mica substrate (filled circles), and the trap-free space-charge-limited current (open circles) is calculated from the hole-drift mobilities obtained by the time-of-flight technique. (Reprinted with permission from ref 210. Copyright 2004 Elsevier B.V.)

free transport in CTLs was achieved not by entirely eliminating impurities but by properly designing the transport-active moiety.[254,255] The associated studies first carried out in this technologically critical context on molecularly doped systems[256] were instrumental in generally elucidating trap interactions in hopping systems and in first unambiguously illustrating and analyzing the mechanism of trap-controlled hopping transport.[257] It was already pointed out that hole transport is supported in MDPs when the neutral transport molecule is donor-like. For electrons, the corresponding neutral transport molecule is acceptor-like in character. In each case, the CTLs are typically unipolar when analyzed by TOF or xerographic techniques. As it turns out, the principle (simple in hindsight), which applies, for example, to hole-transport CTLs, is to make the transport molecule significantly more donor-like than any of the resident impurity species. The limit is that the material must be stable to air oxidation. From an energetic point of view, the impurity levels which then lie above the hole-transport states are antitraps. An important class of small molecules that have these desired characteristics are the aromatic amines, and TPD is a prime example of a particularly strong donor in this class of molecules. The trap-free nature of these transport layers is xerographically apparent because there is no buildup of bulk space charge as measured by Kelvin probe techniques even after tens of thousands of CVs of holes are discharged through a photoreceptor with this CTL as a component.[258] The trap-free nature of hole transport can also be independently demonstrated by combining TOF drift mobility and analysis of current voltage measurements carried out on any transport layer fitted with a semitransparent blocking contact on one surface and an ohmic contact on the opposite face.[72,259,260] Figure 38 illustrates the result for the polymer PTPB in which TPD is covalently incorporated as the transport-active unit.[259] Semitransparent Al on the films exposed surface is used for the TOF measurements of drift mobility. Dark injection occurs under positive bias from the gold coated mica substrate onto which the PTPB film had initially been deposited. PTPB is highly insulating so that the bulk dielectric relaxation time is always much longer than the transit time of any excess injected carrier at all applied voltages. With the Al contact under positive bias, hole-drift mobility is measured as a function of applied voltage V. From the measured drift mobility, the trap-free space-charge-limited current density (TFSCLC), J,[261] that would be sustained by an ohmic contact under positive bias can be calculated to a good approximation, even when the drift mobility is itself field dependent,[262,263] using the expression $J = 9\varepsilon\,\varepsilon_0 V^2/8L^3$. These values are represented by open circles in Figure 38. The electric field in the film is, of course, nonuniform, and E in plots of this sort is simply shorthand for V/L, where V is the externally applied voltage. It should be noted that, under the present conditions, the TFSCLC is, in principle, the maximum current that the bulk of a transport medium like PTPB can demand from a contact in the steady state. It should also be noted that the observation that an injecting contact under test is capable of sustaining a space-charge limited dark current is a *prima facie* demonstration of ohmicity.[89] Filled circles represent the steady-state current measured when positive bias is applied to the substrate. That these calculated and measured currents coincide demonstrates that the injecting Au contact is ohmic and that the PTPB film is trap-free. Similar results have been obtained for other commonly used CTL MDPs such as TPD in bisphenol A polycarbonate and in films of poly(methylphenylsilylene).

6.2. Charge-Transport Layer Performance and Materials

Virtually all useful hole-transport materials are aromatic amines with oxidation potentials between 0.6 and 1.2 eV (vs SCE). Hole-transport materials with oxidation potentials below about 0.5 eV are sensitive to oxidation by air and the oxidizing effluents from corona chargers, and when the oxidation potential is greater than about 1.2 eV, hole injection from the charge-generation material can become inefficient.

Some typical molecules are shown in Figure 39, and Appendix 3 of ref 9 has a relatively complete listing of hole-transporting materials, their chemical structures, and common acronyms. Unfortunately, the literature for hole-transporting materials is littered with acronyms often based on inaccurate or home-grown nomenclature. In addition, hole-transport materials are also usually classified according to a specific functionality present in the molecule: hydrazone, triarylamine, butadiene, biphenyl, etc. Borsenberger and coworkers have contributed extensively to the literature on hole transport, and Weiss has published a summary of these publications.[264]

In section 3.4, we discussed some examples of OPCs with CTLs, which have superior performance in the EP process. Literally thousands of hole-transport materials have been developed, but only a very few actually make it into a commercialized OPC. The available charge-transport models have not been particularly helpful in assisting the chemist in the design of CTMs with superior characteristics. Thus, there has been considerable study of those factors that might affect CTM performance including layer mixing, binder polymer(s), and CTM characteristics such as molecular structure, polarizability, HOMO energy, and oxidation potential. Some of these factors were discussed above in connection with the development of transport models.

The key performance attribute for a CTL is to transport charge without trapping in the time scale of the EP process. The symptom of charge-transport limitation or trapping is an increasing residual potential with EP cycling. In the fabrication of a dual-layer OPC, the CTL solution, with

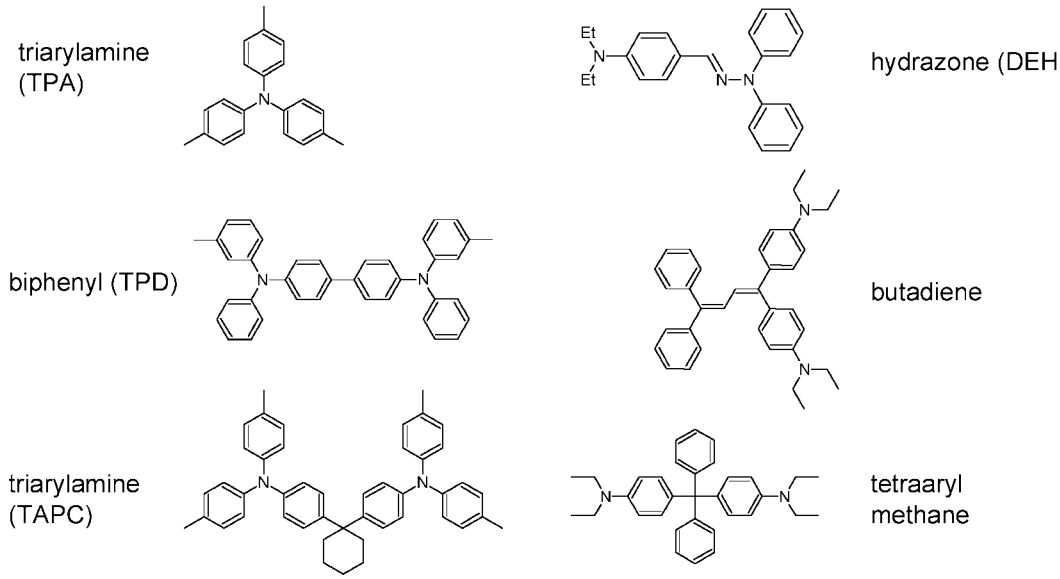

Figure 39. Molecular structures, and commonly used molecular class names and acronyms, of some typical hole-transport materials.

~40−50 wt % CTM, is coated over the previously coated and dried CGL. As mentioned previously, some interlayer mixing is generally desired because the CTM must associate with the CGM to facilitate charge generation. Also, if no mixing occurs, the layers will not adhere. It is not obvious, but too much mixing may also lead to performance degradation if particles of the CGM are dispersed into the CTL. If this occurs, negative charge generated in these particles will be trapped. In addition, based on changes in the shape of the time-of-flight transients of a CTL (1:1 DEH in polyester) with the addition of small amounts of x-H_2Pc, Macartney and co-workers suggested the formation of deep hole-trapping sites.[265] Kanemitsu and co-workers observed that electron trapping in the CGL can lead to hole trapping at the CGL−CTL interface.[91] A combination of photoacoustic spectroscopy and xerographic discharge was used to study charge generation and trapping in OPCs with an H_2Pc based CGL and DEH based CTL.[139,266]

To be effective as a sensitizer for charge generation, the CTM must have a HOMO level lower than that of the CGM. Russell and co-workers have suggested the use of cyclic votammetry for screening CTMs for oxidation potential as well as the stability of the CTM radical cation.[267] Kakuta and co-workers found a correlation between the CTM ionization potential, determined by calculation as well as cyclic voltammetry, and photosensitivity in an OPC with a bisazo pigment CGM.[169]

There are many studies in which molecular orbital calculations have been carried out on CTMs to determine HOMO level, polarizability, dipole moment, etc. For example, Kitamura and Yokoyama carried out calculations and time-of-flight mobility measurements on six aminophenylhydrazone CTMs and came to the conclusion that, for high mobility, a well-balanced positive charge distribution was important.[268] Huang and co-workers found that, for a series of hydrazone-based CTMs, the HOMO level and the number of active hole-transport nitrogen atoms were both important.[269] Similarly, Aratani and co-workers found that, for a series of triarylamine CTMs in bisphenol A polycarbonate, the mobility was increased when most of the HOMO electron density was on the triarylamine moiety and there was no correlation with ionization potential.[270] Kanemitsu and Sugimoto have found that the hole mobility among eight CTMs of varying chemical class decreased linearly with the calculated dipole moments of the neutral molecules.[271] Shoda and co-workers measured and calculated the polarizabilities and dipole moments for a large series of CTMs and found that smaller dipole moment and high polarizability were desirable CTM features.[272−274] Figure 40 shows the field dependence of the mobilities and the compounds used in these studies. Mobilities were determined using the time-of-flight method on dual-layer OPCs with a CGL of β-TiOPc and CTL of 1:1 CTM in bisphenol A polycarbonate (10−15 μm). It would seem reasonable that a large geometry change on going from the neutral CTM to the radical cation would produce an energy barrier to hole transport. Sakanoue and co-workers found such a correlation,[275] but Shoda and Murayama used an improved method of calculation on an expanded set of molecules and found no correlation between the reorganization energy and the hole mobility.[276] Thus, the group and molecular dipole moments of CTMs are a dominant factor in determining hole mobility, and this has been explained in terms of the disorder model as described in the previous section.

The CTLs of OPCs are usually MDPs in that they comprise a high concentration (40−50 wt %) of hole-transport molecule dissolved in an "inert" polymeric binder. However, the binder polymer can play an important role in determining the CTL transport characteristics. An example is shown in Figure 41 for 40 wt % TTA in various polymers.[277] A major contributor to this effect is believed to be the effects of the group dipole moments on the energetic disorder in the transport manifold as discussed in the previous section. Kochelev and co-workers have found that the mobility of MDPs of DEH in bisphenol A polycarbonate decreases with increasing polymer molecular weight.[278] The authors suggest that "free volume" trapping as described by Molaire might be involved.[279] According to this model, if a film is heated above the T_g and rapidly cooled, the excess free volume can cause a hole range limitation. Slow cooling or subsequent annealing can reduce the free volume with a subsequent improvement in hole transport.[280]

This discussion would not be complete without some mention of hole-transporting polymers where the hole-transport moieties are either pendant or part of the polymer backbone. Such a system was discussed in the previous

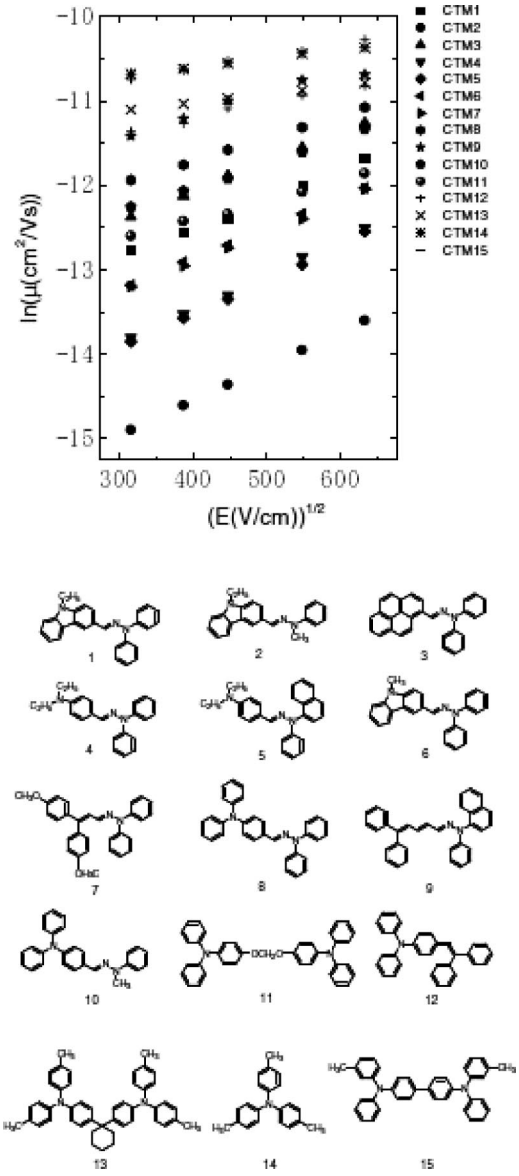

Figure 40. Hole-drift mobility as a function of square root of field for the CTMs shown. (Reprinted from ref 273 with permission of IS&T: The Society for Imaging Science and Technology, sole copyright owners of IS&T's NIP17: International Conference on Digital Printing Technologies Proceedings.)

section. Polymeric hole-transport materials as CTLs would provide several advantages. They would be tougher because they would not be "molecularly doped" and they would be suited for use in a liquid toner EP process because the CTM could not leach from the film. Such polymers have been and remain an active topic of research.[281] However, to date, polymeric CTLs have not been developed which have the combination of wear resistance and inexpensive synthesis.

6.3. Electron and Bipolar Transport Materials

In all OPCs, some of the photodischarge occurs via electron transport. In a single-layer OPC, if the light is uniformly absorbed throughout the film, electron and hole transport each account for 50% of the photodischarge. However, as mentioned previously, in dual-layer OPCs the electron-transport component is minimized with a thin CGL and thick hole-transporting CTL. Figure 42 shows the chemical structures of some typical electron-transport materials and their acronyms. The chemical names are as follows:

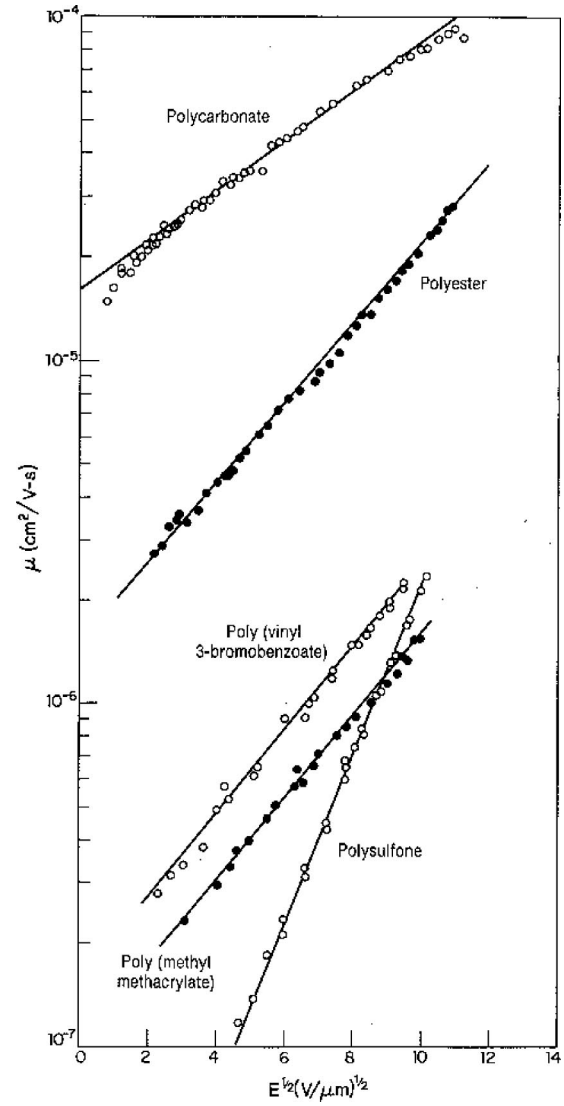

Figure 41. Hole mobility as a function of square root of field for 40 wt % TTA in various polymeric binders. (Reprinted with permission from ref 277. Copyright 1990 American Institute of Physics.)

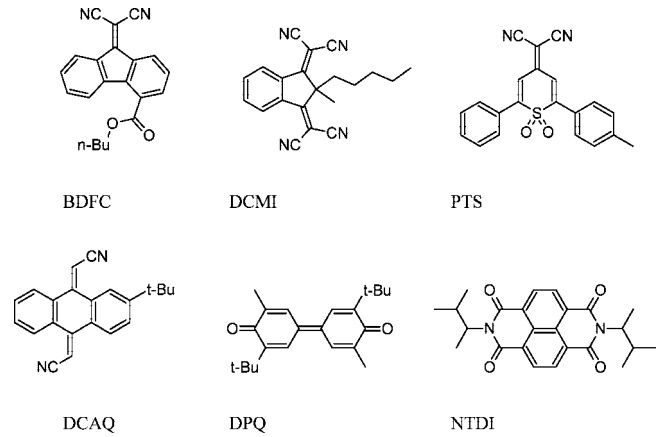

Figure 42. Chemical structures and common acronym for electron-transport molecules. See the text for the chemical names.

n-butyl 9-dicyanomethylenefluorene-4-carboxylate (BCMF aka BDFC); 2-methyl-2-pentyl-1,3-bis(dicyanomethylene)indane (DCMI); 4*H*-1,1-dioxo-4-dicyanomethylidene-2-*p*-tolyl-6-phenylthiopyran (PTS); *N*,*N*′-dicyano-2-*t*-butyl-9,10-anthraquinonediimine (DCAQ); 3,5-dimethyl-3′,5′-di-*t*-butyl-

4,4′-diphenoquinone (DPQ): *N*,*N*′-bis(1,2-dimethylpropyl)-1,4,5,8-naphthalenetetracarboxylic diimide (NTDI). A more complete list of electron-transport materials is available.[9] There is a large body of literature on electron-mobility characteristics but few papers where the materials are the main charge-transport components of an OPC. Borsenberger and co-workers carried out extensive studies on many types of electron-transport materials, and a compilation of these publications is available.[264]

As with hole transport, electron transport occurs via electron hopping; however, in this case, the transport-active species is the radical anion of the charge-transport moiety. Thus, the key requirement for an electron-transport molecule is that it is easily and reversibly reduced. In general, the mobilities of electron-transport materials are much lower than hole-transport materials, and electron-mobility limitations and trapping are commonly observed when these materials are used in CTLs. This is why OPCs based on mainly electron transport have not been commercialized. The reasons for the poor transport characteristics are not well-understood. To obtain low reduction potentials, electron-transport molecules typically have one or more electronegative substituents, which lowers their solubility in the typical polymeric binders such that the required 40−60 wt % transport moiety cannot be attained. In addition, since these molecules are highly polar, they may themselves act as polar "dopants" and reduce the transport efficiency.[245,282−284] Another possible factor is that the reduction potential of oxygen in a polymeric binder is thought to be ∼0.5 eV, and therefore, it may serve as an electron trap in these systems.[285] Finally, low reduction potential molecules, such as TNF, can give a positive Ames test for mutagenicity.[286]

Single-layer OPCs must transport electrons to function, and we have previously discussed PVK−TNF and the dye−polymer aggregate (sections 2.5 and 5.2, respectively). In OPCs using PVK−TNF, electron transport occurs via the TNF, and in the dye−polymer aggregate it occurs through the dye. The electrophotographic characteristics of PVK−TNF OPCs have been described by Schaffert.[43] A PVK−TNF molar ratio of 1:1 (62 wt % TNF) was found to give optimum photosensitivity for white light exposure with either positive or negative surface charging. Exposure at 404 nm gave equivalent photodischarge rates independent of surface polarity and thickness (8 and 15 μm), indicating that both holes and electrons were transported with equal efficiency. However, for a 20 μm film sensitivity at this wavelength, the photosensitivity was much greater with a negative surface potential. On the other hand, Gill determined the hole and electron mobilities in films (10 μm) of PVK−TNF as a function of molar ratio.[217] At a 1:1 molar ratio and a field of 5×10^5 V/cm, the hole and electron mobilities are 5×10^{-9} and 6×10^{-7} cm^2 V^{-1} s^{-1}, respectively. These low mobilities are insufficient for OPCs in today's electrophotographic engines.

A natural extension of PVK−TNF was to examine TNF as a stand-alone electron-transport material in a dual-layer OPC. Gill reported that the electron mobility in a film of 30 wt % TNF in a phthalate-based polyester was $\sim 5 \times 10^{-6}$ cm^2/(V s) (10^6 V/cm).[287] Kuder and co-workers prepared a variety of compounds with low reduction potentials such as 2-carboethoxy-4,5,7-trinitrofluorene-9-one and nitrated 9-dicyanomethylenefluorenes.[285] In this work, it was noted that many electron-transport compounds exhibit poor solubility and incompatibility with many polymer binders. The exception was PVK, where charge-transfer complex formation occurs. In addition, doped films prepared with compounds having electron affinities below ∼2.1 eV exhibit decreased mobility, and it was suggested that oxygen (electron affinity 0.44 eV) might interfere with electron transport. Finally, it was noted that those compounds that exhibited irreversible cyclic voltammetry in solution also exhibited mobility limitations for electron transport. To address the problem of poor solubility and polymer compatibility of TNF, Ong and co-workers synthesized trinitrofluorene-9-ones with a 2-alkyl substituent.[288] The photodischarge characteristics of an OPC with a CTL containing 2-(1,1-dimethylbutyl)-4,5,7-trinitrofluoren-9-one in PVK indicated an electron mobility about 2 times that of TNF. Turner prepared OPCs using *n*-butyl 4,5,7-trinitro-9-fluorenone-2-carboxylate and compared it with a polymer having this electron-transport moiety as a pendant group in poly(methylmethacrylate).[289] From the photodischarge rates, electron mobilities were estimated to be 3×10^{-8} cm^2/(V s) (10^5 V/cm).

Murti and co-workers investigated *n*-butyl 9-dicyanomethylenefluorene-4-carboxylate (BDFC) as an electron-transport material in dual-layer OPCs.[290] When doped into bisphenol A polycarbonate at >40 wt %, changes in the absorption spectrum with time suggested aggregation and crystallization. However, when doped with a small amount of TPD (∼13 wt %), a charge-transfer complex formed and the film was stable. At a field of 4×10^5 V/cm, the mobility with a film with 40 wt % BDFC was 4×10^{-7} cm^2/(V s). A dual-layer OPC with a squaraine CGM and an electron-transporting CTL containing BDFC (35 wt %) and TPD (15 wt %) in bisphenol A polycarbonate exhibited a residual potential of 70 V when photodischarged from an initial potential of +600 V. From the residual potential data as a function of surface potential, the deep trapping lifetime was found to be 48.8 ms (see section 6 for an explanation).

Polymers with pendant 9-dicyanomethylene-9-fluoenone were synthesized by Sim and co-workers.[291] Both a homopolymer of 4-vinylbenzyl-9-dicyanomethylenefluorene-4-carboxylate and a copolymer with butyl acrylate (or methacrylate) were prepared. The electron mobility in the copolymer was high 3.5×10^{-6} cm^2/(V s) (4.3×10^5 V/cm). These polymers were tested as electron-transport CTLs in dual-layer OPCs with a TiOPc based CGL. Although the CTLs were relatively thin (∼15 μm), the homopolymer based OPC only photodischarged to 46% of the initial potenial (∼600 V). The best photodischarge performance was with a CTL of a copolymer with *n*-butyl acrylate.

Tokarski and co-workers synthesized dimers of 9-dicyanomethylene 4-carboxylate with a variety of bridging groups.[292] Many of the compounds were incompatible with bisphenol-Z polycarbonate at a 1:1 weight ratio and could not be tested. The electron mobility with the bridging group $-O-(CH_2)_{10}-O-$ was 1.4×10^{-7} cm^2/(V s) at a field of 6.4×10^5 V/cm. At this field, the mobility of a 1:1 film with BDFC in bisphenol-Z polycarbonate was 2×10^{-6} cm^2/(V s). Single-layer OPCs were prepared with the composition CGM (4.3)/h-CTM (52)/e-CTM (15)/polyvinylbutyral (28.7) at a thickness of 10 μm. These had acceptable performance when evaluated in an electrical-only testing apparatus (charge/expose/erase) for over 500 cycles.

Zhang and co-workers reported that a single-layer OPC with 2,2′,5′-tri-*t*-butyl diphenoquinone, a hole-CTM, phthalocyanine CGM, in a polyester binder, exhibited satisfactory single-cycle electrophotographic performance for hole-

dominated photodischarge but had a large residual potential with electron-dominated photodischarge even at a concentration of 40 wt % (−172 V).[293] Under the same conditions, an OPC formulated with 40 wt % TNF had a residual potential of −157 V.

Mizuta and co-workers prepared single-layer OPCs with several naphthoquinones including 2-phenyl-3-benzoyl-1,4-naphthoquinone.[54] High residual potentials (−150 V) were observed when these OPCs were formulated for electron-transport-dominated photodischarge. In another report, Mizuta and co-workers synthesized a series of 6,13-diazanaphtho[2,3-b]fluorine-5-arylimino-7,12 diones and used them as electron-CTMs in dual-layer OPCs.[294] The electron mobility was low (10^{-7} cm^2/(V s)), but an OPC (0.5 μm CGL of X-form metal-free phthalocyanine in polyvinylbutyral, and a 20 μm CTL of 40 wt % electron-CTM in bisphenol A polycarbonate) exhibited satisfactory cycling performance.

Matsui and co-workers synthesized a series of *N*-(2,4,7-trinitrofluorenylidene)-2,6-dialkylanilines and examined them as electron-transporting CTLs with a bisphenol A polycarbonate binder (1:1 weight ratio).[295] A near-infrared sensitive CGL was used and the OPC with CTM of 2,6-diethyl exhibited high photosensitivity and low residual potential (one charge−expose cycle).

Since single-layer OPCs require the presence of both hole- and electron-transporting functionalities, it is interesting to note that it is possible to combine both functionalities into one molecule: *N*-(*p*-(di-*p*-tolylamino)phenyl)-*N*′-(1,2-dimethylpropyl-1,4,5,8-naphthalenetetracarboxylic diimide (TAND).[296] This molecule combines the TTA hole-transporting functionality with the NTDI electron-transporting functionality. In films of 40 wt % TAND in bisphenol A polycarbonate, the hole and electron mobilities were 10^{-7} and 5×10^{-8} cm^2/(V s), respectively, at 3.6×10^5 V/cm. For comparison at the same field and concentration, the hole mobility of TTA in bisphenol A polycarbonate is 5×10^{-5} cm^2/(V s)[297] and the electron mobility of NTDI in polystyrene is 10^{-6} cm^2/(V s).[298] Thus, placing both transport molecules in the same molecule has dramatically lowered both the hole and electron mobilities. These mobilities are too low for this material to be used in an OPC.

7. Undercoat Layer

An OPC will typically have an undercoat layer (UCL) to prevent unwanted charge injection from the electrode. Since OPCs usually have a negative surface charge, holes injected from the electrode into the CGL will be transported by the CTMs through the CTL and result in decreased surface potential. Abkowitz and co-workers have done extensive research and have found that ohmic contacts are formed between a typical CTL layer (TPD in polycarbonate) and many electrodes.[299] The details of the dark hole injection are complex, and in some investigations the electrodes under investigation were applied by vacuum deposition to the CTL, which causes surface "damage".[300] However, a carbon-filled polymer has been shown to form an ohmic contact with an overcoated polymeric CTL.[301] Further studies using CTL (TPD in polycarbonate) solution coated onto various electrodes showed that the injection efficiency scaled with the estimated interfacial barrier height which is related to the work function of the electrode.[302] The injection efficiency decreased in the order: carbon-filled polymer > Au > glassy carbon > Ag > Cr. However, substantial variability was observed with Ag and Cr and ascribed to the presence of surface oxides.

The work functions of the metals commonly used as OPC electrodes (Ni, Cr, Fe, Ti) are all around 4 eV except for Al, which is ~3 eV. Thus, the lower work function Al is obviously the metal of choice to minimize dark hole injection, and it comes as no surprise that Al tubes and Al coated polymer films are standard OPC substrates. However, metals other than Al are found in commercial OPC loops. One reason is that it is difficult to prepare semitransparent Al, so if the OPC is exposed through the polymeric substrate (imaging or erase), some other electrode is needed. A field of 2×10^5 V/cm is formed across an OPC of 20 μm with a surface charge of −500 V. At this field, ohmic hole injection would produce a current density of 10^{-4} amp/cm^2 in the OPC.[302] At this current density, it would take ~0.7 ms for the surface charge (4×10^{11} charges/cm^2) to be neutralized. Obviously, ohmic hole injection into the OPC is incompatible with the electrophotographic process. Thus, OPCs generally have a hole-injection barrier layer coated on top of the electrode. Even Al drums are often anodized, or overcoated, to prevent unwanted charge injection. An undercoat material might be an insulating polymer but it must be insoluble in the solvents used in the CGL and CTL formulations to remain effective. Polyamides (Nylons) are often chosen, as are cross-linked polymers of all types. A disadvantage of an insulating polymer undercoat is that, as the OPC undergoes charge/expose cycling, charge will not transit the layer and a residual potential will build up. This residual potential will increase until the field across the layer becomes so large that tunneling transport finally occurs. Literature values for the breakdown fields of insulating polymers are not accurate, but residual potentials can be built up across insulating layers in OPCs that correspond to fields of >10^6 V/cm.[303] The residual potential due to an insulating blocking layer places limitations on the electrophotographic process, which may or may not be acceptable. For this reason, these layers are coated as thinly as possible, <1 μm.

Another important issue is that the efficiency of charge injection will be enhanced where structures exist that can concentrate charge and create very small and localized charge-injection sites. Such structures might be micrometer-sized defects in the electrode (Al tubes often have turning lines from surface processing) or coated-in debris. In the typical digital electrophotographic process, toner is developed in discharged areas of the OPC. Thus, in those nonexposed regions where localized charge injection occurs, small clumps of toner will be developed. These are commonly called "charge-deficient spots" and at some level represent an objectionable print defect. To prevent coated-in debris, it is necessary to filter all solutions before coating. Filtration of the CGL can be problematic because typically this is a dispersion of pigment particles. In any case, a pigment particle in direct contact with the metal will serve as a charge-injection site. Usually the most satisfactory solution is to coat a charge-injection blocking layer as described.

Surface potential mapping of an OPC has been carried out using a biased stylus.[304] Using this technique it was shown that 90% of the spots with reduced surface potential are toned in the electrophotographic process. It was estimated that the actual defect size in this sample was <4 μm. Focusing on a single microscopic charge-injection site, it was shown that the current was space charge limited.[305,306] The biased stylus technique, although elegant, is not suitable for testing

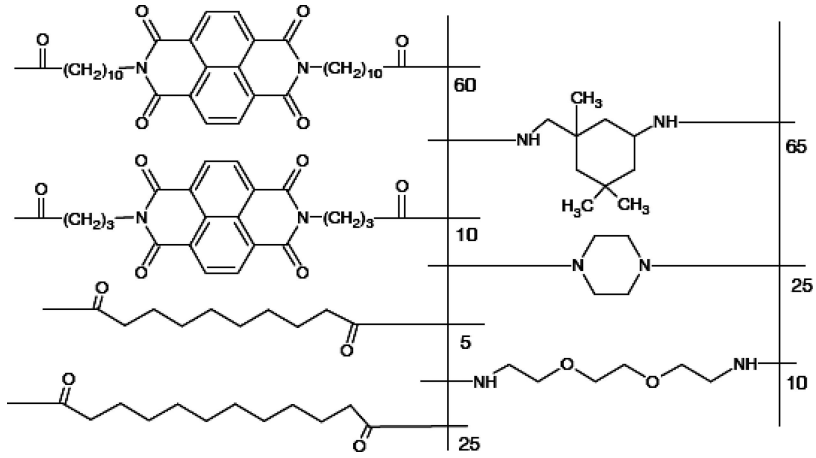

Figure 43. Chemical structure of an electron-transporting naphthalene bisimide polymer useful as an OPC undercoat layer. (Reprinted from ref 313 with permission of IS&T: The Society for Imaging Science and Technology, sole copyright owners of IS&T's NIP24: International Conference on Digital Printing Technologies Proceeding and Digital Fabrication 2008.)

a full-size OPC in a reasonable period of time. To this end, commercial "defect" test machines have been introduced. One technique is to image the toner developed on a drum OPC with a charge-coupled device (CCD) line camera.[307,308] Another technique uses a "transparent" surface voltmeter capacitively coupled to the OPC to detect differences between areas of the OPC that photodischarge efficiently and those that do not (because of the presence of a charge-injection spot or some other defect).[309] Finally, Tse and co-workers have reviewed various approaches and determined that surface potential mapping using standard probes has high sensitivity and has the capability of detecting defects as small as 100 μm.[310] This is an important manufacturing problem. Because microscopic defects are not detectable by visible inspection; and test printing with image analysis[311] or defect scanning as described above, is only practical on a limited basis, the manufacturing process has to ensure that such defects are never produced.

To avoid the residual potentials associated with insulating polymer undercoats, it is necessary to have a layer that is somewhat conductive. One approach is to fill an insulating polymer with semiconductor metal oxide particles as reported by Molaire.[312] These can be relatively thick and therefore also serve as smoothing layers on an Al drum. Toda and co-workers have recently described a commercial OPC that has both an undercoat layer on top of the Al electrode and a smoothing layer on top of the undercoat layer.[66] The OPC has a smoothing layer composed of inorganic pigment in resin, but without the undercoat layer, objectionable "background fouling" was observed that increased with increasing field. It is not clear if the authors are referring to "background", which is a uniform distribution of toner in nonexposed areas of the OPC, or "charge-deficient spots" as described above. In either case, this problem was solved with a multipronged approach. By adding a "resin" blocking layer and by increasing the CTL thickness (to reduce the field at the aim surface potential), the "background fowling" was reduced to an acceptable level. However, this improved photoreceptor had a reduced first-cycle surface potential, and this was solved by increasing the pigment content of the smoothing layer, thereby increasing its ability to transport electrons to the UCL.

A more recent approach has been to prepare insulating layers, which can accept and transport electrons from the pigment in the CGL. This is, therefore, essentially a thin electron-transporting CTL, and to prepare such layers, electron-transporting CTMs have been incorporated into polymers. Naphthalene bisimides are a class of electron-transporting materials that have been incorporated into polyamides[313] as shown in Figure 43, as well as in thermally cross-linkable systems formulated with diethyl malonate and blocked isocyanates.[314] The former polymers are soluble in chlorinated solvents only if alcohol is present, and in the latter systems, deblocking and cross-linking occur at 120 °C.

8. Overcoat Layer

In the electrophotographic process, the surface of the OPC is exposed to many insults, which may eventually result in performance degradation. For example, the OPC surface is in contact with potentially abrasive materials: metal carrier particles during image development, cleaning brush or cleaning blade, and paper or some intermediate receiver in the process of transferring the toned image. In addition, the environment associated with corona or roller charging contains corrosive chemicals: ozone, oxides of nitrogen, and their associated acids. Finally, although the OPC is exposed to light during image creation and erase, the intensities are low and the exposures are in the visible and near-infrared spectral regions. Depending on the formulation, even low levels of exposure to ultraviolet light, as emitted from cool-white fluorescent lighting, can cause performance degradation due to CTL photochemical damage. Thus, physical, chemical, and photochemical processes can cause the performance of the OPC to degrade either slowly or rapidly and need to be minimized as much as possible. This is especially critical in high-speed, high-volume machines and not as critical in low-volume home and small-office machines.

The CTL of a dual-layer OPC is relatively soft because it is plasticized by the presence of up to 50 wt % CTM. It is possible to increase the hardness to some degree by lowering the CTM concentration, but efficient hole transport requires >30 wt % CTM. The OPC surface can be chemically modified such that it has optimized characteristics. For example, Satoh and co-workers have prepared an OPC with fluorinated surface by exposing the OPC to an RF plasma using CF_4.[315] Carbon−fluorine bonding was confirmed by X-ray photoelectron spectroscopy (XPS) analysis, and the fluorinated surface had increased hydrophobicity for use in a novel contact-charging process.

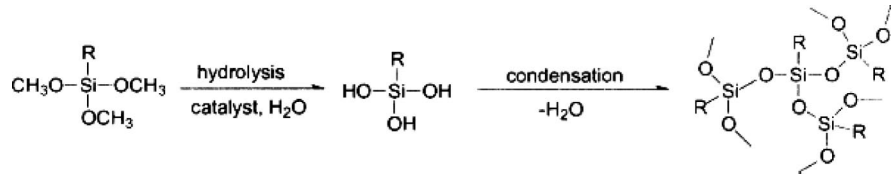

Figure 44. Silsesquioxane sol−gel preparation. (Reprinted from ref 331 with permission of IS&T: The Society for Imaging Science and Technology, sole copyright owners of *Journal of Imaging Science and Technology.*)

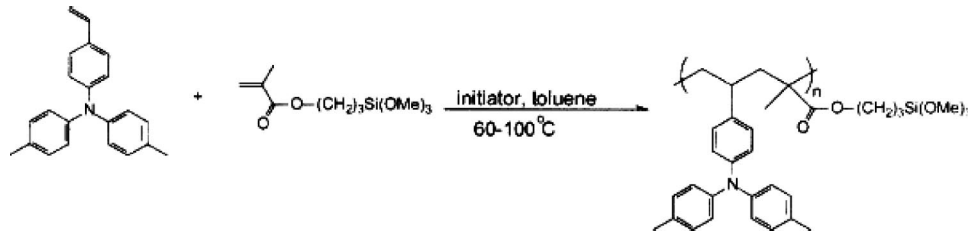

Figure 45. Charge-transport monomer for a silsesquioxane film prepared by radical polymerization. (Reprinted from ref 331 with permission of IS&T: The Society for Imaging Science and Technology, sole copyright owners of *Journal of Imaging Science and Technology.*)

Thus, overcoating the CTL with a protective layer, OCL, has been the preferred approach. As with the undercoat layer, an overcoat layer must be very thin, if insulating and noncharge transporting, to prevent the build up of an objectionable residual potential.

Vacuum deposition of very thin, hard materials (diamond-like carbon, silicon carbide, etc.) onto the OPC surface is one overcoat approach. Thus, a sputtered 18 nm film of AlZrN affords a very hard transparent layer and has been shown to improve OPC performance.[316] Similar results were obtained with overcoats of AlCrN[317] and AlN.[318] The use of hydrogenated SiC (SiC_X:H) as an overcoat has been discussed by Stahr and co-workers.[319] One problem with his material is that it reacts with ozone (from corona charging), and the surface becomes hydrophilic and the surface energy increases. The increase in lateral surface conductivity causes unacceptable image blurring. By optimizing the carbon content of the material, this tendency can be minimized. Seino and Ebisu have demonstrated that SiO (and not Al_2O_3, SiC, SiO_2 or Si_3N_4) is effective in protecting an OPC surface from damage due to NO_2 from corona chargers.[320]

Diamond-like carbon is another material that has been used as a protective OPC overcoat.[321] He and co-workers found that an optimized coating of 150 nm could be prepared by electron cyclotron resonance plasma deposition to form an overcoat with high transparency and $>10^{14}$ Ω cm resistivity. Kochelev and co-workers found that, by overcoating an OPC with 100 nm diamond-like carbon, the service life was extended by a factor of 2−5.[322]

Silsesquioxane sol−gel materials have been extensively studied for use as OPC overcoats.[323−325] Silsesquioxanes are highly cross-linked silicon-based polymers where the monomer unit has the structure $R\text{-}SiO_{1.5}$. Figure 44 shows the sol−gel process used to create a silsesquioxane film. A solution of trialkoxysilanes is hydrolyzed and partially polymerized to produce a sol. At this stage, polymerization continues slowly but the formulation has enough stability for subsequent coating onto an OPC. Following coating, the polymerization is thermally driven to completion. The effects of extent of cross-linking, formulation, and thickness on conductivity, scratch resistance, hardness, and brittleness have been described in detail. The alkyltrimethoxysilane substituent (R) was varied to affect the characteristics of the final film. For example, methyl imparts hardness, propyl imparts plasticity, 3-aminopropyl effects curing and bulk conductivity, 3-glycidoxypropyl effects cross-linking and bulk conductivity. Lithium iodide was added to the formulation to control the bulk conductivity. The interplay between all these factors was studied to optimize both the physical and electrical characteristics of the overcoat.[326] A deficiency of this approach was that the salts added to increase the bulk conductivity made the overcoat sensitive to corona effluents at high humidity. The result was that image blurring occurred under these conditions. A technique was developed to analyze image blurring on an OPC in terms of surface resistivity, which entailed analysis of the time-dependent spreading of the OPC surface potential after exposing through a slit to produce a square well exposure.[327] Chen and co-workers used a similar technique to study the effect of liquid toner on latent image spreading.[328] Previously, such analyses required high-resolution single-point surface potential measurements with the OPC on a stepping table with micrometer resolution.[329,330] To avoid the deleterious effects of ionic materials in the silsesquioxane formulation, copolymers were prepared from methyltrimethoxysilane and another component with hole-transport functionality.[331,332] In this case, the hole-transporting monomer component was prepared by radical polymerization as shown in Figure 45. OPCs were prepared where this coating was the only CTL and where it was coated on an existing CTL as a protective overcoat. In both cases, the decreasing residual potential with increasing CTM content demonstrated that holes were injected into and transported through this layer. However, as the CTM content increased, scratch resistance decreased. Overcoats were also prepared with formulations containing a hydroxylated hole-transport material, 9,9-bis{4-[*N*-ethyl-*N*-(2-hydroxyethyl)]aniline}fluorine, which is incorporated into the silsesquioxane polymer in the curing process.[333] A TiO_2-gel overcoat prepared from $Ti(i\text{-}OC_3H_7)_4$ has been described by Suzuki.[146] This was coated on a single-layer OPC with H_2Pc CGM.

Another approach is to have two CTLs where the uppermost, protective, CTL provides the desired characteristics. A recently commercialized OPC illustrates this concept.[67] The dual-layer photoreceptor was overcoated with a "filler-reinforced layer". This layer contained dissolved CTM and dispersed Al_2O_3 in a polycarbonate binder. To achieve the desired dispersion quality, it was necessary to add a stabilizer to the formulation. In addition, when an OPC having the overcoat was exposed to NO_x from the corona charger, image

spreading was observed due to an increase in the OPC surface conductivity. This was reduced by the incorporation of an antioxidant. At 55 wt % alumina loading, the OPC wear rate (in a specific process) was less than 0.1 μm per 20 000 prints. However, when tested in the EP process in a high-temperature, high-humidity environment, wear-resistant OPCs exhibited image blurring. Reasoning that some wear was desirable to refresh the OPC surface, the alumina concentration was adjusted and an optimum was found where image blurring was not observed. This example demonstrates that formulating an overcoat is an optimization process that is best carried out by testing in the specific electrophotographic process for which the OPC is destined.

9. OPC Fatigue

OPC fatigue describes the deterioration of physical and/or electrical characteristics with use. Physical changes such as abrasive wear, scratching, delamination, etc. are typical modes of OPC degradation that will eventually lead to OPC replacement. Cais and co-workers studied the effect of CTL composition on mechanical characteristics and abrasive wear.[334] The investigation compared the characteristics of three polycarbonate binder polymers doped with three hydrazone CTMs at concentrations from 0 to 50 wt %. As expected, doping with the monomeric components lowers the glass-transition temperature. Thus, the T_g of bisphenol A polycarbonate decreases from 150 °C to ~70 °C depending on the dopant CTM. Tensile strength and modulus increased at all but the highest doping concentration, indicating that the dopants are antiplasticizers. Resistance to abrasion with "carbide" decreased with CTM concentration. This effect was minimized with bisphenol A polycarbonate binder polymer, but at the same time abrasive wear with Kraft paper was the greatest with this polymer. In a subsequent study, a correlation was found between entanglement density (increases with molecular weight of the polymer) and resistance to permanent deformation with wear.[61] These characteristics were related to the strength and position of the sub-T_g dynamic mechanical relaxation.[335]

In this section, we will concentrate on two factors that may lead to degradation of electrical performance: exposure to corona and exposure to light.

9.1. Corona Exposure

In the electrophotographic process, the OPC receives a surface charge, sometimes more than once, each imaging cycle. The charge is created by forming an air corona using a wire or pin, or a conductive roller, maintained at a high voltage.[336] Because ozone is one of the byproducts, the charging devices have received considerable attention. Commercial EP printers must meet ozone emission requirements, so machines typically have ozone filters to reduce such emissions to the outside. The charged species in an air corona, which are attracted to the OPC ground layer and end up on the OPC surface, are hydrated protons, $(H_20)_nH^+$,[337] with positive charging, and reaction products from O^- (mainly CO_3^- and O_3^-)[338] with negative charging. The vibrationally excited states of nitrogen and NO have been identified as molecules capable of injecting charge into polymers.[339] Other neutral species produced are nitrogen oxides (NO_x), the corresponding acids depending on the water content of the atmosphere, and ozone. This mix of highly oxidizing chemicals has been termed a "gaseous electrolyte" by Goldman and Sigmond, who studied their corrosive effects on Al.[340] Thus, there has been considerable work to understand and reduce ozone generation in an air corona. This includes both modeling[341,342] and study of the effects of gas flow,[343] humidity,[344,345] temperature,[346] and corona electrode.[347] The development of reduced ozone charging systems follows naturally.[348] In spite of these efforts, in high speed EP processes, the corona charger technology is essentially unchanged over many years.

Given the nature of the chemicals generated in an air corona, one expects that exposure of the OPC will result in chemistry that has deleterious effects on photoelectrical performance. This is indeed the case, and specific examples will be discussed below. In addition, since the corona deposits ionic species on the OPC surface under the appropriate conditions, high humidity for example, the OPC surface will become conductive and the electrostatic latent image will become unstable. As with all OPC characteristics, acceptable performance depends on the requirements of the printer. For low-volume applications, the chemical exposure may be modest and small changes in OPC performance may be acceptable. However, in high-volume applications, it is generally necessary to reduce the chemical exposure by actively venting the chargers to reduce the OPC exposure, modifying the OPC formulation with additives, and/or utilizing a protective OPC overcoat.

In the subsequent discussion, we will focus on the CTL of dual-layer OPCs because there are few publications on corona interactions with single-layer or inverted dual-layer OPCs. However, these latter structures will be very sensitive to exposure to corona gases because the CGM will not be "protected" by the thick CTL. All of the pigments and complexes used as CGMs will react with ozone, NO_x, and HNO_x, and the OPC performance will rapidly be severely impacted. Seino and Ebisu reported that exposure of a single-layer OPC with CuPc CGM to NO_x causes a rapid decrease in the OPC charge acceptance, which necessitated the development of a protective overcoat of vacuum-deposited SiO (0.3 μm).[349] This is one of the reasons why single-layer, or inverted dual-layer, OPCs are difficult to implement in an EP process. Although a single-layer OPC appears attractive from many viewpoints, implementation would almost require the development of a protective overcoat layer, and the value proposition is not as strong.

Some time ago, Takenouchi and co-workers reported that, on exposure to an air corona, a dual-layer OPC with CTMs containing a stilbene functionality underwent ozonolysis to the corresponding aldehydes, which had lower oxidation potential than the starting CTMs, were hole traps, and caused a residual potential with EP cycling.[350]

Weiss demonstrated that exposure of a CTL containing tri-*p*-tolylamine (TTA) CTM to either corona gases, NO_2, or the vapors over concentrated nitric acid resulted in initial formation of the TTA radical cation (maximum absorption at 680 nm) followed by its decay and formation of nitrated TTA.[74] The creation of the CTM radical cation is one reason why single-layer positive-charging OPCs exhibit rapid degradation of charge acceptance when exposed to a positive corona. It was also shown that exposure of an OPC to corona gases results in an increased surface conductivity and spreading of the electrostatic latent image.[328] Kobayashi and co-workers found that exposure of a dual-layer OPC with DEH CTM to ozone did not cause image spreading.[351] However, with charge/expose EP cycling, a significant

decrease in image resolution was observed. They identified nitrate salts and the DEH radical cation and suggested that the image spreading was due to an accumulation of these near the OPC surface. Formation of the CTM radical cation would increase the CTL conductivity and result in increased dark decay, and chemical alteration of the CTM could lead to hole-transport limitations and increased residual potential.

Image spreading caused by surface conduction was examined by Yarmchuck and Keefe using sequential point-by-point measurements of surface charge with 10 μm resolution.[329,330] Corona contamination was identified as the cause, and wiping the OPC surface with methanol eliminated the effect. Tokarski and co-workers found that another source of image spreading, and image ghosting (vestages of prior images in an EP print), in dual-layer OPCs is the exposure-related accumulation of positive charge carriers at a subsurface layer in the CTL or at the UCL−CGL interface.[352] In the full EP process described in a subsequent paper, the dual-layer OPC is negatively charged then exposed and developed.[353] Developed toner is transferred to paper using a positively biased transfer roller which, if paper is not present, will leave a positive charge on the OPC. Using the incremental charging technique, the charging characteristics of new and used (40 000 printed pages) OPCs were compared. It was found that, in the EP process, the CTL surface is damaged, allowing positive charge injection. The damage was permanent in that there was no recovery after a dark rest or annealing at 120 °C. However, the charging characteristics were restored after abrasive wear of the CTL surface to remove the source of positive charge injection.

The use of stabilizing additives has been the focus of much study, and the addition of antioxidants to both single- and dual-layer OPCs is standard. The trick is to find a material that can be added in sufficient amounts to stabilize the OPC, yet have no deleterious effects on any OPC physical and/or electrical characteristics. Kobayashi and co-workers found that, for a positive charging single-layer OPC, the addition of 3,5-di-*t*-butyl-4-hydroxybenzylphosphonate diethylester was a satisfactory stabilizing additive for corona exposure.[131] Endo and co-workers showed that adding an antioxidant to the CTL of dual-layer OPCs was necessary to maintain image resolution.[354] Kochelev and co-workers investigated a large number of dual-layer OPC formulations and found that the addition of antioxidants and/or electron acceptors in both the CTL and CGL helped to stabilize the OPCs from the deleterious effects of exposure to light and to corona gases.[355] Thus, interactions of the OPC surface with corona chemicals can lead to OPC fatigue that can take the form of latent image blurring, increased dark decay (decreased charge acceptance), and increased residual potential.

9.2. Light Exposure

OPCs are designed such that the CGMs are selected to strongly absorb the imaging and erase light exposures with little or no competition for the light from the CTMs or the CGL and CTL binder polymers. CTMs generally absorb in the ultraviolet but some have absorptions that extend into the blue. Problems can arise if the OPC is exposed to light that is absorbed by the CTM, which subsequently undergoes photochemistry. For example, bisphenol A polycarbonate is a common CTL binder polymer and has very little absorption beyond 300 nm. Typical CTMs, TTA and DEH, dissolved in this polymer have absorption maxima of TTA 300 and 370 nm, respectively. Thus, exposure of the OPC to light,

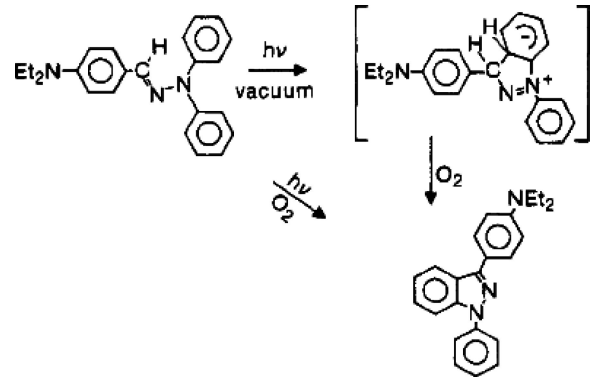

Figure 46. Photocyclization of DEH to an indazole derivative. (Reprinted with permission from ref 359. Copyright 1991 American Chemical Society.)

except what is involved in the EP process, is to be avoided, and the packaging material of all commercial OPCs has such a warning. Fluorescent light, cool-white in particular, has a significant UV component. In any case, unexpected exposures of an OPC to light absorbed by the CTMs will often lead to electrical performance degradation or photofatigue.

It is well-known that irradiation of molecularly doped films of CTMs gives rise to field-dependent generation of mobile holes in relatively low yield. Photogeneration in poly-*N*-vinylcarbazole (PVK) has been the subject of many reviews.[9] Borsenberger and co-workers reported a photogeneration efficiency of ~0.01 for 40 wt % triphenylamine in bisphenol A polycarbonate at 10^6 V/cm with 300 nm irradiation.[356] Thus UV irradiation of CTL films leads to increased conductivity due to the formation of photogenerated holes (CTM radical cations).[357] The effects of fluorescent light exposure on the electrical characteristics of a dual-layer OPC with H_2Pc CGM were found to depend on the binder polymer and the CTM. An OPC with a CTL composition of DEH in bisphenol A polycarbonate was found to have an improved charge acceptance after irradiation, while an OPC with another CTM had decreased charge acceptance.[358] The effects of CTL irradiation were clarified when it was found by Pacansky and co-workers that DEH underwent an efficient photocyclization to an indazole derivative, 1-phenyl-3-(4-(diethylamino)-1-phenyl)-1,3-indazole, when exposed to light with wavelength <480 nm (Figure 46).[359] The presumed intermediate is the dihydroindazole shown, and this is subsequently oxidized by molecular oxygen. Electrophotographic studies were carried out on a dual-layer OPC with a bisazo pigment based CGL and CTL of 40 wt % DEH in bisphenol A polycarbonate. A high residual potential was observed on electrophotographic charge/expose cycling of the OPC after irradiation of the CTL with light absorbed by DEH. The dark-decay characteristics were changed very little. The indazole has an oxidation potential that is higher than DEH (5.3 vs 4.3 eV), so as DEH near the surface of the CTL undergoes photochemistry, this region is less able to transport the photogenerated positive charge and a residual potential is observed. In an interesting twist, DEH photosensitivity has been utilized to determine the effects on hole transport of selectively decreasing the DEH concentration near the OPC surface.[360] Annealing the OPC near the glass-transition temperature of the CTL allows the DEH to diffuse back into the photolyzed areas, and the OPC performance recovers. When the chemical structure of DEH is modified to prevent the photocyclization reaction, the photochemical reaction, and the associated photofatigue, is prevented.[361]

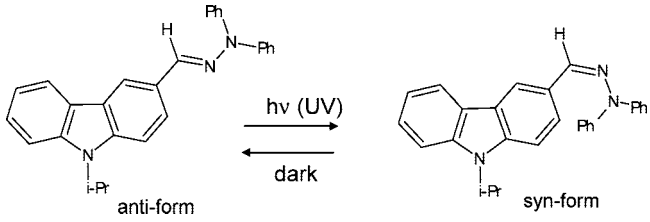

Figure 47. Photoreactions of anti-9-isopropylcarbazole-3-carbaldehyde diphenylhydrazone.[368]

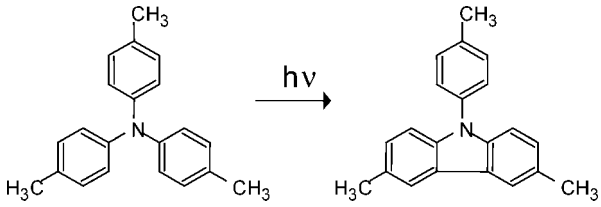

Figure 48. Photocyclization of tri-*p*-tolylamine.[370]

When polyester is used as the CTL binder polymer, irradiation with longer wavelength light (520−800 nm) causes an increase in the OPC dark decay and bleaching of the bisazo CGM.[362] These characteristics were correlated with the polymer acid number. In a subsequent paper, it was noted that DEH photochemistry is very efficient in bisphenol A polycarbonate and poly(methylmethacrylate); in polyesters containing terephthalate linkages, the photochemistry is quenched but the dark conductivity increases with irradiation, and the OPC becomes persistently conductive.[363] It was suggested that the quenching involved triplet energy transfer from DEH to the terephthalate. However, the possibility of nonradiative decay of an exciplex was also mentioned, and in the light of past research on charge generation involving exciplexes in PVK doped with dimethyl terephthalate,[364] as well as more recent data (to be discussed later in this section), this seems the more likely mechanism for both the quenching of DEH photochemistry and the photoinduced persistent conductivity.

Kanemitsu and co-workers reported that, in molecularly doped polymer films, the chemical nature of the binder polymer and its interactions with the CTM to form charge-transfer states had a large effect on photoinduced conductivity.[365] Wong and co-workers studied the effect of UV irradiation on the performance of commercially available OPCs and concluded that CTM photochemistry was involved.[366,367]

Another example of hydrazone CTM photochemistry is shown in Figure 47.[368] In this case, *anti*-9-isopropylcarbazole-3-carbaldehyde diphenylhydrazone, a CTM, isomerized to two syn-isomers of differing conformation.[369] Both syn-isomers have ionization potentials lower than the anti-isomer by ∼0.1 eV and are, thus, CTL hole traps. Irradiation of an OPC having a CTL with this CTM resulted in a residual potential with charge/expose cycling.

Weiss and Chen reported that exposing an OPC (vacuum-deposited CGL of *N*,*N*′-bis(2-phenethyl)perylene-3,4:9,10-bis(dicarboximide), ∼0.2 μm, and CTL of 40 wt % tri-*p*-tolylamine (TTA) in bisphenol A polycarbonate, 15−20 μm) to cool-white fluorescent light caused a residual potential to develop on subsequent electrical-only electrophotographic cycling.[370] Irradiated CTLs were found to contain the *N*-aryl carbazole shown in Figure 48. The quantum yield was ∼0.05 for 300 nm irradiation of a film of 10 wt % TTA in bisphenol A polycarbonate. Other lower-yield products were also identified including di-*p*-tolylamine, hydroxyl-substituted TTA, hydroxyl-substituted *N*-arylcarbazole, and a product giving rise to absorption at ∼500 nm. The *N*-arylcarbazole has an oxidation potential of 1.25 eV (the oxidation potential of TTA is 0.89 eV vs SCE), so the residual potential was ascribed to either the loss of TTA near the CTL surface or hole trapping by any of the minor products or a combination of these. The absorption at ∼500 nm was a convenient chemical marker, and it was found that the addition of the weak electron acceptor phthalic anhydride (reduction potential −1.16 eV vs SCE) to the CTL resulted in a charge-transfer absorption (∼400 nm) and essentially identical quenching of the residual potential, 500 nm absorption, and TTA fluorescence (maximum ∼375 nm) with concomitant formation of the TTA radical cation. Static quenching analysis indicated a quenching sphere radius of 2.8 nm. CTM radical cation formation occurred on irradiation of polymer films of *N*-isopropylcarbazole,[371] PVK,[372] and related polymers[373] doped with weak electron acceptors. In these systems, the carbazole fluorescence was quenched by exciton migration to charge-transfer sites with the appearance of a new charge-transfer emission. In more recent work, Weiss and Gruenbaum have shown that other classes of weak electron acceptors can be doped into the CTL of an OPC to afford protection from exposure to UV light.[374] Polyesters containing the terephthalate moiety and *N*-aryl trimellitimide esters (reduction potential ≈ −1.3 eV) had the same effect in terms of producing a new charge-transfer complex absorption and quenching the UV-exposure-induced residual potential and the 500 nm absorption. However, with these materials, the TTA radical cation was not produced and a new charge-transfer emission was observed. Static quenching analysis indicated a quenching sphere radius of ∼2 nm. To rationalize these observations, a mechanism was proposed in which the donor−acceptor charge-transfer sites act as energy sinks and effectively quench the excited singlet state of the CTM.

Kochelev and co-workers have suggested that much of the instability of OPCs occurs when the CTM radical cations are exposed to light, have published results for a large number of OPC formulations,[375,376] and have found that the addition of 2,3,5,6-tetramethylpyrazine increases the stability of CTLs with a variety of CTMs to UV exposure.[377] Because present day OPCs are highly photosensitive, exposure to very high light intensities can induce fatigue even if the wavelengths are the same as the imaging or erase exposure in the EP process. Kanemitsu and Imamura used a photoacoustic method and found that an OPC (vacuum-deposited H_2Pc (200 nm) overcoated with a 10 μm CTL of DEH in a polyester binder) exhibited enhanced charge generation after prolonged exposure (700 nm) in the presence of an applied field. This effect was ascribed to the formation of a high field region in the CGL due to the presence of trapped electrons.[378]

In summary, irradiation of an OPC with light absorbed by the charge transport and/or the charge-generation component can lead to performance changes. Improved photostability has been obtained by modifing the CTM molecular structure or making changes to the formulation such as the addition of stabilizing components.

10. Summary and Outlook

OPCs are a maturing technology, but companies continue to invest heavily in research and development for improvements. In 2008 there were 1675 United States patents issued in Class 399 (electrophotography), and approximately 7% were OPC related. Patent analysis is problematic. It may take

several years for a patent to issue and companies use patents as strategic tools for a variety of purposes. For example, a patent may be designed to block others from using a technology that the assignee has no intention of using. Also, one must keep in mind that the contents of patents are not scientifically rigorous, so misleading and even incorrect information may be present. Patents are also bargaining chips and a company with a large patent portfolio is in a strong position with respect to cross-licensing of technologies. Nevertheless, the percentage of OPC-related patents in Class 399 has remained relatively constant since the year 2000. Looking a little deeper (and subjectively determining the thrust of the patent), about 20% deal with charge-transport materials, and 10% each deal with overcoat layers, charge-injection blocking/smoothing layers, and charge-generation materials. The remaining 50% deal with additives of various sorts: antioxidants in the CTL, electron-transport materials in the CGL, and other materials that, it is claimed, improve performance. There are also a small number of virtually useless patents that claim an OPC characteristic that may have no obvious connection with performance or any clear indication of how the desirable features are obtained. Nevertheless, it is clear from the point of view of patents that OPC technology continues to progress at a steady pace.

Predicting the future directions for maturing technologies is difficult because a successful technology needs to satisfy the business demands for profit. Therefore, the success of an OPC technology depends not only on how well it performs but also on integrating it into a profitable business plan that is accepted by the corporate management. With this in mind, we should divide electrophotographic printing into its two distinct classes: consumer and commercial. On the consumer side are the desktop printers in which the OPC substrate is an aluminum drum of ~25 mm diameter. In these printers, the OPC is part of a cartridge assembly containing the entire electrophotographic engine. Such cartridges are user replaceable at modest cost (<$100). The usual reason for replacing a cartridge is that the toner supply is exhausted. A toner load of ~100 g will last for one year at a printing rate of 7 pages per day (assuming ~5% toner coverage). For monochrome black printing, this corresponds to about 2 500 pages or 9 000 cycles of the OPC (3.6 OPC cycles are needed for an 11 in. page). This is only a small fraction of the expected OPC life, and a large industry has developed for toner refilling and cartridge recycling by the original manufacturer as well as by remanufacturers. With a color laser printer, a separate EP cycle is required for each of the four subtractive colors (C, M, Y, K). OPCs in this market are commodities manufactured by the millions at very low cost (<$1). These OPCs are manufactured by dip-coating of large batches, and the materials costs are a minor component of the manufacturing cost. Here, the desire is to minimize the number of coated layers so single-layer OPCs should reign. However, because of the deficiencies of single-layer OPC performance, dual-layers remain commonplace.

The commercial printer market is dominated by high-speed, high-volume machines with very large area OPCs (drums or seamed belts). For example, the OPC belt in the Xerox iGen3 has a surface area of approximately 12 000 cm^2 and a printing speed of about 100 copies per minute (this depends on the paper size). A single OPC revolution may produce 10 printed pages, and for each page, the OPC experiences four charge/expose/develop cycles. Since these machines are designed to maximize throughput, an OPC life of around one million "impressions" is desirable. The OPC in these, and related, machines is an expensive component, and the business model in large measure determines what is desired in terms of OPC "life". Machines such as this are often leased rather than purchased, and a service contract may not include OPC replacement. For the iGen3 and related machines, the belt is not user-replaceable (a large belt is very easy to damage during installation) and long life may be paramount. On the other hand, the OPC drums used in the Kodak NexPress printers are purchased by the user and easily replaced, so in this case, there is a business conflict between the desire of the user to minimize cost and the manufacturer to maximize profits. OPCs for these machines retail for over $1000. As with other devices requiring a surface with no defects, the manufacturing cost increases almost exponentially with surface area. Clearly, in this market, the business model will determine the OPC replacement strategy. In any case, at the high end, there is a continuous push toward optimum quality images and longer OPC life. For example, a commercial print shop will not accept image defects that a lower-end user might not notice.

Tracing the history of OPC development, we see that the first OPCs were single-layer, but with the advent of laser printers in the early 1980s, it was necessary to separate the charge-generation and charge-transport functions to satisfy requirements posed by near-infrared laser-exposure systems. These dual-layer OPCs remain commonplace, but with the demands of the consumer for improved image quality and longer life, extra layers have been added with specific optimized functionalities. What can we expect for future OPCs? Since ultimately one of the limiting factors for image resolution is the OPC thickness, as the exposure resolutions increase (2 400 dots-per-inch corresponds to an exposed area of 10 μm), thinner OPCs might be required. Furthermore, since manufacturing cost is always an issue, decreasing the number of functional layers is desirable. Perhaps with the development of newer, better functioning materials, such changes may become possible. For example, electron-transporting materials with improved transport characteristics might facilitate the shift back to single-layer OPCs, especially if the OPC thickness is decreased. Furthermore, a charge-transport layer with ceramer-like hardness might negate the need for a separate overcoat layer.

OPC technology is maturing, yet the cost and performance improvements driven by the continued development of new materials will yield competitive advantage in the marketplace. This we believe will fuel continued OPC development in what remains a scientifically stimulating and commercially important technology. Finally, it should be emphasized that the underlying materials research has in turn driven major advances in development of organic light-emitting diodes (OLEDs) and flexible broadband photodetectors.

11. References

(1) Law, K.-Y. *Chem. Rev.* **1993**, *93*, 449.
(2) Stockman, D. L. *Current Problems in Electrophotography*; Walter de Gruyter: New York1972; p 194.
(3) Stolka, M.; Pai, D. M. *Adv. Polym. Sci.* **1978**, *29*, 1.
(4) Pai, D. M. *Frontiers of Polymer Research*; Prasad, P. N., Nigam, J. K., Eds.; Plenum Press: New York, 1991; p 315.
(5) Pai, D. M. *J. Non-Cryst. Solids* **1983**, *59 & 60*, 1255.
(6) Nguyen, K. C.; Weiss, D. S. *J. Imaging Soc.* **1989**, *15*, 158.
(7) Borsenberger, P. M.; Weiss, D. S. *Handbook of Imaging Materials*; Diamond, A., Ed.; Marcel Dekker: New York, 1991; p 379.
(8) Pai, D. M.; Springett, B. E. *Rev. Mod. Phys.* **1993**, *65*, 163.
(9) Borsenberger, P. M.; Weiss, D. S. *Organic Photoreceptors for Xerography*; Marcel Dekker: New York, 1998.

(10) Borsenberger, P. M.; Weiss, D. S. *Handbook of Imaging Materials*; Diamond, A. S., Weiss, D. S., Eds.; Marcel Dekker: New York, 2002; p 369.
(11) Weiss D. S.; Cowdery, J. R.; Young R. H. *Electron Transfer in Chemistry: Volume 5: Molecular-Level Electronics, Part 2; Imaging and Information, Energy and Environment*; Balzani V., Ed.; Wiley-VCH: Weinheim, Germany, 2001; p 379.
(12) Melnyk, A. *Encyclopedia of Imaging Science and Technology*; Wiley: Hoboken, NJ, 2002; p 1169.
(13) Weiss, D. S.; Abkowitz, M. *Handbook of Electronic and Photonic Materials*; Kasap, S.,Capper, P., Eds.; Springer: New York, 2006; p 953.
(14) Fritz, G. F.; Hoesterey, D. C.; Brady, L. E. *Appl. Phys. Lett.* **1971**, *19*, 277.
(15) Schaffert, R. M.; Oughton, C. D. *J. Opt. Soc. Am.* **1948**, *38*, 991.
(16) Dessauer, J. H.; Mott, G. R.; Bogdonoff, H. *Photogr. Eng.* **1955**, *6*, 250.
(17) Dinsdale, A. *Photogr. Sci. Eng.* **1963**, *7*, 1.
(18) Mort, J. *The Anatomy of Xerography*; McFarland: Jefferson, NC, 1989.
(19) Owen, D. *Smithsonian* **2004**, *August*, 91.
(20) Mort, J. *Phys. Today* **1994**, *April*, 32.
(21) Golembeski, D. J. *Invention Technol.* **1989**, *Winter*, 8.
(22) Dessauer, J. H. *My Years with Xerox: The Billions Nobody Wanted*; Manor: New York, 1971.
(23) Owen, D. *Copies in Seconds: How a Lone Inventor and an Unknown Company Created the Biggest Communication Breakthrough Since Gutenberg—Chester Carlson and the Birth of the Xerox Machine*; Simon and Schuster: New York, 2005.
(24) Williams, E. M. *The Physics & Technology of Xerographic Processes*; Wiley: New York; 1984.
(25) Schaffert, R. M. *Electrophotography*, 2nd ed.; Focal Press: London, 1975.
(26) Schein, L. B. *Electrophotography and Development Physics*, 2nd ed.; Laplacian Press: Morgan Hill, CA, 1996.
(27) Julien, P. C.; Gruber, R. J. *Handbook of Imaging Materials*, 2nd ed.; Diamond, A. S., Weiss, D. S., Eds.; Marcel Dekker: New York, 1992; p 173.
(28) Chen, I. *J. Appl. Phys.* **1972**, *43*, 1137.
(29) Chen, I. *J. Appl. Phys.* **1978**, *49*, 1162.
(30) Buettner, A. V.; Mey, W. *Photogr. Sci. Eng.* **1982**, *26*, 80.
(31) Young, R. H. *J. Appl. Phys.* **1986**, *60*, 272.
(32) Lin, L.-B.; Young, R. H.; Weiss, D. S.; Molaire, M. F.; Jenekhe, S. A.; Borsenberger, P. M. *Proc. SPIE* **1998**, *3422*, 27.
(33) Lutz, M. *Proceedings IS&T's Eleventh International Congress on Advances in Non-Impact Printing technologies* **1995**, 23.
(34) Weiss, D. S.; Nguyen, K. C. *J. Imaging Sci.* **1989**, *15*, 158.
(35) Chen, I. *J. Imaging Sci.* **1990**, *34*, 15.
(36) Jeyadev, S.; Pai, D. M. *J. Imaging Sci. Technol.* **1996**, *40*, 327.
(37) Murayama, T. *Proceedings IS&T's NIP17: International Conference on Digital Printing Technologies* **2001**, 557.
(38) Enokida, T. *Jpn. J. Appl. Phys.* **1992**, *31*, L1135.
(39) Fujimaki, Y.; Tadokoro, H.; Oda, Y.; Yoshioka, H.; Homma, T.; Moriguchi, H.; Watanabe, K.; Konishita, A.; Hirose, N.; Itami, A.; Ikeuchi, S. *J. Imaging Tech.* **1991**, *17*, 202.
(40) Loutfy, R. O.; Hor, A. M.; Kazmaier, P.; Tam, M. *J. Imaging Sci.* **1989**, *33*, 151.
(41) Umeda, M.; Niimi, T.; Hashimoto, M. *Jpn. J. Appl. Phys.* **1990**, *29*, 2746.
(42) O'Regan, M. B.; Borsenberger, P. M; Magin, E. H.; Zubil, T. *J. Imaging Sci. Technol.* **1996**, *40*, 1.
(43) Schaffert, R. M. *IBM J. Res. Dev.* **1971**, *15*, 75.
(44) Law, K.-Y. *Chem. Mater.* **1992**, *4*, 605.
(45) Umeda, M; Hashimoto, M. *J. Appl. Phys.* **1992**, *72*, 117.
(46) Loutfy, R. O.; Menzel, E. R. *J. Am. Chem. Soc.* **1980**, *102*, 4967.
(47) Popovic, Z. D.; Hor, A. M.; Loutfy, R. O. *Chem. Phys.* **1988**, *127*, 451.
(48) Vahtra, U.; Wolter, R. F. *IBM J. Res. Dev.* **1978**, *22*, 34.
(49) Dulmage, W. J.; Light, W. A.; Marino, S. J.; Salzberg, C. D.; Smith, D. L.; Staudenmayer, W. J. *J. Appl. Phys.* **1978**, *49*, 5543.
(50) Borsenberger, P. M.; Chowdry, A.; Hoesterey, D.C.; Mey, W. *J. Appl. Phys.* **1978**, *49*, 5555.
(51) Borsenberger, P. M.; Hoesterey, D. C. *J. Appl. Phys.* **1980**, *51*, 4248.
(52) Tam, A. C.; Balanson, R. D. *IBM J. Res. Dev.* **1982**, *26*, 186.
(53) Adam, D.; Humpert, H.-J.; Dreihöfer, S.; Pinsler, H.; Lutz, M. *Proceedings IS&T's NIP13: 1997 International Conference on Digital Printing Technologies* **1997**, 245.
(54) Mizuta, Y.; Akiba, N.; Watanabe, Y.; Sugai, F.; Matsumoto, S.; Nakamori, H.; Miyamoto, E.; Nakazawa, T. *Proceedings IS&T's NIP13: 1997 International Conference on Digital Printing Technologies* **1997**, 197.
(55) Miyamoto, E.; Mizuta, Y.; Nakazawa, T. *Proceedings IS&T's NIP20: 2004 International Conference on Digital Printing Technologies* **2004**, 497.
(56) Montrimas, E.; Sidaravicius, J.; Lozovski, T.; Maldzius, R.; Jubran, N.; Tokarski, Z. *Proceedings IS&T's NIP20: 2004 International Conference on Digital Printing Technologies* **2004**, 562.
(57) Iwamatsu, T.; Toyoshima, T.; Azuma, N.; Mutou, Y.; Nakajima, Y. *Proceedings IS&T's NIP15: 1999 International Conference on Digital Printing Technologies* **1999**, 732.
(58) Chen, I. *Proceedings IS&T's NIP18: 2002 International Conference on Digital Printing Technologies* **2002**, 404.
(59) Mizuta, Y.; Miyamoto, E.; Azuma, J.; Nakazawa, T. *Proceedings IS&T's NIP20: International Conference on Digital Printing Technologies* **2004**, 501.
(60) Aizawa, K.; Takeshima, M.; Kawakami, H. *Proceedings IS&T's NIP17: International Conference on Digital Printing Technologies* **2001**, 572.
(61) Kawai, M.; Toriumi, A.; Nozomi, M.; Murakami, O.; Fujioka, K.; Cias, R. E. *Proceedings IS&T's Tenth International Congress on Advances in Non-Impact Printing Technologies* **1994**, 265.
(62) Molaire, M. F. *Proceedings IS&T's 21st International Conference on Digital Printing Technologies* **2005**, 17.
(63) Chen, I. *J. Imaging Sci. Technol.* **1993**, *37*, 396.
(64) Ritchie, I.; Fenn, J. B. *Proc. SPIE* **1987**, *759*, 30.
(65) Katsen, J. J.; Himmerwright, R. S.; Taylor, D. H. *Proceedings IS&T's Tenth International Congress on Advances in Non-Impact Printing Technologies* **1994**, 506.
(66) Toda, N.; Kitajima, R.; Niimi, T.; Tamoto, N.; Orito, T.; Yamashita, Y.; Koeda, M.; Shimeki, I. *Proceedings IS&T's NIP23* **2007**, 639.
(67) Nohsho, S.; Kitajima, R.; Ikegami, T.; Suzuki, T.; Niimi, T.; Kojima, N. *Proceedings IS&T's NIP22* **2006**, 4.
(68) Lee, N.-J.-; Joo, H.-R.; Yon, K.-Y.; No, Y. *Proceedings IS&T's NIP19: 2003 International Conference on Digital Printing Technologies* **2003**, 670.
(69) Mort, J.; Chen, I. *Appl. Solid State Sci.* **1975**, *5*, 69.
(70) Weigl, J. W. *Angew. Chem., Int. Ed. Engl.* **1977**, *16*, 374.
(71) Mort, J.; Pfister, G. *Polym.-Plast. Technol. Eng.* **1979**, *12*, 89.
(72) Abkowitz, M.; Facci, J. S.; Stolka, M. *Appl. Phys. Lett.* **1993**, *63*, 1892.
(73) Abkowitz, M. A.; Antoniadis, H.; Facci, J. S.; Hsieh, B. R.; Stolka, M. *Synth. Met.* **1994**, *67*, 187.
(74) Weiss, D. S. *J. Imaging Sci. Technol.* **1990**, *34*, 132.
(75) Mishra, S.; Pai, D. M. *Proceedings IS&T's NIP12: International Conference on Digital Printing Technologies* **1996**, 464.
(76) Scott, J. C.; Lo, G. S. *IS&T's Proceedings 6th International Congress on Advances in Non-Impact Printing Technologies* **1990**, 403.
(77) Lin, C.-W.; Nozaki, N.; Hoshino, Y. *Proceedings IS&T's NIP 13: 1997 International Conference on Digital Printing Technologies* **1997**, 270.
(78) Lin, C.-W.; Nozaki, N.; Hoshino, Y. *Proceedings IS&T's NIP 14: 1998 International Conference on Digital Printing Technologies* **1998**, 548.
(79) Lin, C.-W.; Hoshino, Y.; Kitakubo, S. *Proceedings IS&T's NIP 15: 1999 International Conference on Digital Printing Technologies* **1999**, 707.
(80) Montrimas, E.; Lozovski, T.; Sidaravicius, J.; Tokarski, Z. *J. Imaging Sci. Technol.* **2005**, *49*, 326.
(81) Weiss, D. S.; Benwood, B. R.; Troendle, D. L. *J. Imaging Sci. Technol.* **2007**, *51*, 520.
(82) Grum, F.; Costa, L. F. *Appl. Opt.* **1976**, *15*, 76.
(83) Gallo, C. F.; Legia, A. G.; McInally, J. A. *Photogr. Sci. Eng.* **1967**, *11*, 11.
(84) Pai, D. M. *SPSEs Fourth International Conference on Electrophotography* **1981**, 121.
(85) Pai, D. M.; Janus, J. *Photogr. Sci. Eng.* **1983**, *27*, 14.
(86) Dolezalek, F. K. *Photoconductivity and Related Phenomena*; Mort, J., Pai, D. M., Eds.; Elsevier: New York, 1976; p 71.
(87) Melnyk, A. R.; Pai, D. M. *Phys. Methods Chem.*, 2nd ed.; Rossiter, B. W., Hamilton, J. F., Baetzold, R. C., Eds.; John Wiley: New York, 1992; p 321.
(88) Chen, I.; Mort, J. *J. Appl. Phys.* **1972**, *43*, 1164.
(89) Rose, A. *Photoconductivity and Related Processes*; Interscience: New York, 1963.
(90) Bube, R. H. *Photoelectronic Properties of Semiconductors*; Cambridge University Press: Cambridge, U.K., 1992.
(91) Kanemitsu, Y.; Funada, H.; Imamura, S. *J. Appl. Phys.* **1990**, *67*, 4152.
(92) Tse, M.-K.; She, K. Y.; Slack, E.; Forrest, D. *Proceedings IS&T's NIP12: International Conference on Digital Printing Technologies* **1996**, 343.
(93) Pai, D. M. *Physics of Disordered Materials*; Adler, D., Fritzsche, H., Ovshinsky, S. R., Eds.; Plenum: New York, 1985; p 579.
(94) Onsager, L. *Phys. Rev.* **1938**, *54*, 554.

(95) Braun, C. L. *J. Chem. Phys.* **1984**, *80*, 4157.
(96) Smirnov, S. N.; Braun, C. L. *J. Imaging Sci. Technol.* **1999**, *43*, 425.
(97) Noolandi, J.; Hong, K. M. *J. Chem. Phys.* **1979**, *70*, 3230.
(98) Mayo, J. D. *Proceedings IS&T's NIP9* **1993**, 652.
(99) Martin, T. I.; Mayo, J. D.; Jennings, C. A.; Gardner, S.; Hsiao, C. K. *Proceedings IS&T's Eleventh International Congress on Advances in Non-Impact Printing Technologies* **1995**, 30.
(100) Watanabe, K.; Itami, A.; Kinoshita, A.; Fujimaki, Y *Proceedings IS&T's NIP9* **1993**, 659.
(101) Daimon, K.; Nukada, K.; Sakaguchi, Y.; Igarashi, R. *J. Imaging Sci. Technol.* **1996**, *40*, 249.
(102) Mayo, J. D.; Keoshkerian, B.; Hsiao, C.-K.; Gaynor, R. E.; Gardner, S. J. *Proceedings IS&T's Tenth International Congress on Advances in Non-Impact Printing Technologies* **1994**, 223.
(103) Mizuguchi, J.; Rihs, G.; Karfunkel, H. R. *J. Phys. Chem.* **1995**, *99*, 16217.
(104) Hinch, G.; Haggquist, G. W. *Proceedings IS&T's NIP13: 1997 International Conference on Digital Printing Technologies* **1997**, 202.
(105) Fujimaki, Y. *Proceedings IS&T's Seventh International Congress on Advances in Non-Impact Printing Technologies* **1991**, 269.
(106) Okada, O.; Klein, M. L. *Proceedings IS&T's NIP14: 1998 International Conference on Digital Printing Technologies* **1998**, 512.
(107) Yamakami, H.; Mizuguchi, J. *Proceedings IS&T's NIP18: 2002 International Conference on Digital Printing Technologies* **2002**, 666.
(108) Kubiak, R.; Janczak, J.; Ejsmont, K. *Chem. Phys. Lett.* **1995**, *245*, 249.
(109) Whitlock, J. B.; Bird, G. R.; Cox, M. D.; Panayotatos, P. *Thin Solid Films* **1992**, *215*, 84.
(110) Mizuguchi, J.; Takahashi, H.; Shiokawa, K. *Proceedings IS&T's NIP19: 2003 International Conference on Digital Printing Technologies* **2003**, 693.
(111) Menzel, E. R.; Jordan, K. *J. Chem. Phys.* **1978**, *32*, 223.
(112) Kitamura, T.; Tan-o, A. *Proceedings IS&T's Tenth International Congress on Advances in Non-Impact Printing Technologies* **1994**, 271.
(113) Popovic, Z. D. *Proceedings IS&T's 9th International Congress on Advances in Non-Impact Printing Technologies/Japan Hardcopy '93* **1993**, 591.
(114) Popovic, Z. D. *Chem. Phys.* **1984**, *86*, 311.
(115) Popovic, Z. D. *J. Chem. Phys.* **1982**, *76*, 2714.
(116) Popovic, Z. D.; Khan, M. I.; Hor, A.-M.; Goodman, J. L.; Graham, J. F. *Proceedings IS&T's NIP19: 2003 International Conference on Digital Printing Technologies* **2003**, 687.
(117) Popovic, Z. D.; Khan, M. I.; Atherton, S. J.; Hor, A.-M.; Goodman, J. L. *J. Phys. Chem. B* **1998**, *102*, 657.
(118) Saito, T.; Sisk, W.; Kobayashi, T.; Suzuki, S.; Iwayanagi, T. *J. Phys. Chem.* **1993**, *97*, 8026.
(119) Gulbinas, V.; Jakubenas, R.; Pakalnis, S.; Undzenas, A. *J. Chem. Phys.* **1997**, *107*, 4927.
(120) Yamaguchi, S.; Sasaki, Y. *J. Phys. Chem. B* **1999**, *103*, 6835.
(121) Tsuchiya, S.; Omote, A. *J. Imaging Sci. Technol.* **2003**, *47*, 366.
(122) Hackett, C. F. *J. Chem. Phys.* **1971**, *55*, 3178.
(123) Takeshita, K.; Sasaki, Y.; Murayama, T. *Proceedings IS&T's NIP20: International Conference on Digital Printing Technologies* **2004**, 493.
(124) Schreiber, A.; Bilke, R.; Pan, J.; Bleyl, I.; Bondkowski, J.; Adam, D.; Haarer, D. *Proc. SPIE* **1998**, *3471*, 224.
(125) Kitamura, T.; Miyazawa, Y. *IS&T's Proceedings NIP9* **1993**, 619.
(126) Kitamura, T.; Miyazawa, Y.; Yoshimura, H. *J. Imaging Sci. Technol.* **1996**, *40*, 171.
(127) Kubo, K.; Kobayashi, T.; Nagae, S.; Fujimoto, T. *J. Imaging Sci. Technol.* **1999**, *43*, 248.
(128) Hoshino, Y. *IS&T's Proceedings NIP17: International Conference on Digital Printing Technologies* **2001**, 772.
(129) Omote, A.; Itoh, Y.; Tsuchiya, S. *J. Imaging Sci. Technol.* **1995**, *39*, 271.
(130) Enokida, T. *Proceedings IS&T's NIP9* **1993**, 615.
(131) Kobayashi, T.; Wakita, K.; Kubo, K.; Nagae, S.; Fujimoto, T.; Koezuka, H. *Proceedings NIP12: International Conference on Digital Printing Technologies* **1996**, 480.
(132) Nishino, T.; Nogami, K.; Hiramoto, M.; Yokoyama, M. *Proceedings IS&T's Eleventh International Congress on Advances in Non-Impact Printing Technologies* **1995**, 152.
(133) Yokota, S.; Lee, H.-K.; Kim, B.-J.; Kim, S.-J.; Yon, K.-Y.; No, Y. *Proceedings IS&T's NIP20: 2004 International Conference on Digital Printing Technologies* **2004**, 509.
(134) Yokata, S. *J. Imaging Sci. Technol.* **2005**, *49*, 629.
(135) Yokoto, S. *J. Imaging Sci. Technol.* **2006**, *50*, 503.
(136) Kanemitsu, Y.; Yamamoto, A.; Funada, H.; Masumoto, Y. *J. Appl. Phys.* **1991**, *69*, 7333.
(137) Enokida, T.; Hirohashi, R.; Mizukami, S. *J. Imaging Sci.* **1991**, *35*, 235.
(138) Kanemitsu, Y.; Imamura, S. *Appl. Phys. Lett.* **1989**, *54*, 872.
(139) Kanemitsu, Y.; Imamura, S. *J. Appl. Phys.* **1990**, *67*, 3728.
(140) Marcus, R. A. *J. Chem. Phys.* **1956**, *24*, 966.
(141) Randolph, C.; Neely, J. *Proceedings IS&T's NIP 13: 1997 International Conference on Digital Printing Technologies* **1997**, 274.
(142) Hayashida, S.; Akimoto, T.; Morishita, Y.; Itagaki, M.; Matsui, M. *Proceedings IS&T's Tenth International Congress on Advances in Non-Impact Printing Technologies* **1994**, 249.
(143) Molaire, M. F.; Henry, J. T.; Zubil, T.; Kaeding, J. E. *Proceedings IS&T's NIP13: International Conference on Digital Printing Technologies* **1997**, 799.
(144) Molaire, M. F.; Zubil, T. *Proceedings IS&T's NIP20: 2004 International Conference on Digital Printing Technologies* **2004**, 487.
(145) Molaire, M. F.; Lobo, L.; Zubil, T.; VanEpps, L.; Sykes, M. *Proceedings IS&T's NIP22: International Conference on Digital Printing Technologies* **2006**, 12.
(146) Suzuki, T.; Takahashi, Y. *Proceedings IS&T's NIP 13: 1997 International Conference on Digital Printing Technologies* **1997**, 279.
(147) Schaffert, R. M. *Electrophotography*; Focal Press: New York, 1975; p 380.
(148) Gill, W. D. *Photoconductivity and Related Phenomena*; Mort, J., Pai, D. M., Eds.; Elsevier: New York, 1976; p 303.
(149) Penwell, R. C.; Ganguly, B. N.; Smith, T. W. *J. Polym. Sci., Makromol. Rev.* **1978**, *13*, 63.
(150) Pearson, J. M. *Pure Appl. Chem.* **1977**, *49*, 463.
(151) Hatano, M.; Tanikawa, K. *Prog. Org. Coat.* **1978**, *6*, 65.
(152) Grazulevicius, J. V.; Strohriegl, P.; Pielichowski, J.; Pielichowski, K. *Prog. Polym. Sci.* **2003**, *28*, 1297.
(153) Hayashi, Y.; Kuroda, M.; Inami, A. *Bull. Chem. Soc. Jpn.* **1966**, *39*, 1660.
(154) Hoegl, H. *J. Phys. Chem.* **1965**, *69*, 755.
(155) Lardon, M.; Lell-Döller, E.; Weigl, J. W. *Mol. Cryst.* **1967**, *2*, 241.
(156) Melz, P. J. *J. Chem. Phys.* **1972**, *57*, 1694.
(157) Yokoyama, M; Endo, Y.; Matsubara, A.; Mikawa, H. *J. Chem. Phys.* **1981**, *75*, 3006.
(158) Yokoyama, M.; Shimokihara, S.; Matsubara, A.; Mikawa, H. *J. Chem. Phys.* **1982**, *76*, 724.
(159) Yokoyama, M.; Mikawa, H. *Photogr. Sci. Eng.* **1982**, *26*, 143.
(160) Abramavicius, D.; Gulbinas, V.; Ruseckas, A.; Undzenas, A.; Valkunas, L. *J. Chem. Phys.* **1999**, *111*, 5611.
(161) Wang, Y. *Nature* **1992**, *356*, 585.
(162) Chen, Y.; Cai, R.-F.; Huang, Z.-E.; Bai, X.; Yu, B.-C.; Jin, W.; Pan, D.-C.; Wang, S.-T. *Polym. Bull.* **1996**, *36*, 203.
(163) Itaya, A.; Suzuki, I.; Tsuboi, Y.; Miyasaka, H. *J. Phys. Chem. B.* **1997**, *101*, 5118.
(164) Wang, Y.; Suna, A. *J. Phys. Chem. B.* **1997**, *101*, 5627.
(165) McMurtry, D.; Tinghitella, M.; Svendsen, R. *IBM J. Res. Dev.* **1984**, *28*, 257.
(166) Seki, K.; Suzuki, Y.; Yamanami, H. *SPSE Proceedings, the Fifth International Congress on Advances in Non-Impact Printing Technologies* **1989**, 60.
(167) Law, K.-Y.; Kaplan, S.; Crandall, R.; Tarnawskyj, I. W. *Chem. Mater.* **1993**, *5*, 557.
(168) Law, K.-Y.; Tarnawskyj, I. W. *J. Imaging Sci. Technol.* **1995**, *39*, 126.
(169) Kakuta, A.; Mori, Y.; Morishita, H. *IEEE Trans. Ind. Appl.* **1981**, *1A−17*, 382.
(170) DiPaola-Baranyi, G.; Hsiao, C. K.; Hor, A. M. *J. Imaging Sci.* **1990**, *34*, 224.
(171) Law, K.-Y.; Tarnawskyj, I. W. *J. Imaging Sci. Technol.* **1993**, *37*, 22.
(172) Law, K.-Y.; Tarnawskyj, I. W.; Popovic, Z. D. *J. Imaging Sci. Technol.* **1994**, *38*, 118.
(173) Law, K.-Y.; Tarnawskyj, I. W. *J. Imaging Sci. Technol.* **1995**, *39*, 1.
(174) Murayama, T. *J. Imaging Sci. Technol.* **2002**, *46*, 285.
(175) Umeda, M. *J. Imaging Sci. Technol.* **1999**, *43*, 254.
(176) Niimi, T.; Umeda, M. *J. Appl. Phys.* **1994**, *76*, 1269.
(177) Umeda, M.; Niimi, T. *J. Imaging Sci. Technol.* **1994**, *38*, 281.
(178) Sasaki, Y; Yamaguchi, S.; Shoda, T.; Aramaki, S.; Murayama, T. *Proceedings NIP17: International Conference on Digital Printing Technologies* **2001**, 568.
(179) Umeda, M.; Yokoyama, M. *Jpn. J. Appl. Phys.* **1995**, *34*, L44.
(180) Umeda, M.; Shimada, T.; Aruga, T.; Niimi, T.; Sasaki, M. *J. Phys. Chem.* **1993**, *97*, 8531.
(181) Aramaki, S.; Murayama, T. *Proceedings IS&T's Eleventh International Congress on Advances on Non-Impact Printing Technologies* **1995**, 26.
(182) Shoda, T.; Aramaki, S.; Murayama, T. *Proceedings IS&T's NIP 13: 1997 International Conference on Digital Printing Technologies* **1997**, 220.
(183) Shoda, T.; Aramaki, S.; Murayama, T. *Proceedings IS&T's NIP 14: 1998 International Conference on Digital Printing Technologies* **1998**, 508.

(184) Sasaki, Y.; Takeshita, K.; Shoda, T.; Murayama, T. *Proceedings IS&T's NIP 18: 2002 International Conference on Digital Printing Technologies* **2002**, 400.
(185) Takeshita, K.; Sasaki, Y.; Shoda, T.; Murayama, T. *Proceedings IS&T's NIP 19: 2003 International Conference on Digital Printing Technologies* **2003**, 683.
(186) Mizuguchi, J. *J. Appl. Phys.* **1998**, *84*, 4479.
(187) Tojo, K.; Mizuguchi, J. *Proceedings IS&T's NIP17: International Conference on Digital Printing Technologies* **2001**, 564.
(188) Hino, K.; Mizuguchi, J. *Proceedings IS&T's NIP20: 2004 International Conference on Digital Printing Technologies* **2004**, 558.
(189) McKerrow, A. J.; Buncel, E.; Kazmaier, P. M. *Can. J. Chem.* **1993**, *71*, 390.
(190) Désilets, D.; Kazmaier, P. M.; Burt, R. A. *Can. J. Chem.* **1995**, *73*, 319.
(191) Richter, A. M.; Ackermann, R. *Proceedings IS&T's Tenth International Congress on Advances in Non-Impact Printing Technologies* **1994**, 246.
(192) Kazmaier, P. M.; Hoffmann, R. *J. Am. Chem. Soc.* **1994**, *116*, 9684.
(193) Magin, E. H.; Borsenberger, P. M. *Proceedings IS&T's Eighth International Congress on Advances in Non-Impact Printing Materials* **1992**, 243.
(194) Popovic, Z. D.; Cowdery, R.; Khan, I. J.; Hor, A.-M.; Goodman, J. *J. Imaging Sci. Technol.* **1999**, *43*, 266.
(195) Nakazawa, T.; Kawahara, A.; Watanabe, Y.; Mizuta, Y. *J. Imaging Sci. Technol.* **1994**, *38*, 421.
(196) Chen, H.-Z.; Jiang, K.-J.; Wang, M. *J. Photochem. Photobiol., A* **1999**, *120*, 211.
(197) Hiramoto, M.; Sakaue, Y.; Yokoyama, M. *Bull. Chem. Soc. Jpn.* **1994**, *67*, 2011.
(198) Hosoya, M.; Miyamoto, H. ; Nishizawa, H.; Hirao, A. *Proceedings IS&T's Eleventh International Congress on Advances in Non-Impact Printing Technologies* **1995**, 51.
(199) Yasuda, R.; Takeuchi, M. *Proceedings IS&T's NIP 14: 1998 International Conference on Digital Printing Technologies* **1998**, 552.
(200) Kessler, B. *Appl. Phys. A: Mater. Sci. Process.* **1998**, *67*, 125.
(201) Abkowitz, M. A.; Stolka, M. *IUPAC International Symposium on Polymers for Advanced Technologies*; VCH: New York, 1987; p 225.
(202) Maruyama, Y. *Mol. Cryst. Liq. Cryst.* **1989**, *171*, 287.
(203) Shirota, Y.; Kageyama, H. *Chem. Rev.* **2007**, *107*, 953.
(204) Baranovskii, S. D.; Rubel, R. *Handbook of Electronic and Photonic Materials*; Kasap, S., Capper, P., Eds.; Springer: New York, 2006; p 161.
(205) Sze, S. M. *Physics of Semiconductor Devices*, 2nd ed.; Wiley: New York, 1981.
(206) Coropceanu, V.; Cornil, J.; da Silva Filho, D. A.; Olivier, Y.; Sibey, R.; Bredas, J.-L. *Chem. Rev.* **2007**, *107*, 926.
(207) Abkowitz, M. A.; Stolka, M. *Int. Symp. Polym. Adv. Technol.*; Lewin, M., Ed.; VCH: New York, 1988; p 225.
(208) Pai, D. M.; Yanus, J. F.; Stolka, M. *J. Phys. Chem.* **1984**, *88*, 4714.
(209) Stolka, M.; Yanus, J. F.; Pai, D. M. *J. Phys. Chem.* **1984**, *88*, 4707.
(210) Abkowitz, M. A. *Synth. Met.* **2004**, *141*, 29.
(211) Abkowitz, M. *J. Reinf. Plast. Compos.* **1997**, *16*, 1303.
(212) Abkowitz, M. A.; Stolka, M.; Morgan, M. *J. Appl. Phys.* **1981**, *52*, 3453.
(213) Bässler, H. *Phys. Status Solidi B* **1984**, *107*, 9.
(214) Stolka, M.; Abkowitz, M. A. *Practical Applications of Organic Electronic Materials*; Iwamoto, M., Pu, I. S., Taniguchi, S., Eds.; Science Forum: Tokyo, 1994; p 265.
(215) Tang, C. W.; VanSlyke, S. A. *Appl. Phys. Lett.* **1987**, *51*, 913.
(216) Abkowitz, M. A.; Bässler, H.; Stolka, M. *Philos. Mag. B* **1991**, *63*, 201.
(217) Gill, W. D. *J. Appl. Phys.* **1972**, *43*, 5033.
(218) Abkowitz, M. A.; Facci, J. S.; Limburg, W. W.; Janus, J. *Phys. Rev. B: Condens. Matter* **1992**, *46*, 6705.
(219) Kepler, R. G.; Zeigler, J. M.; Harrah, L. A.; Kurtz, S. R. *Phys. Rev. B* **1987**, *35*, 2818.
(220) Abkowitz, M. A.; Stolka, M. *Synth. Met.* **1992**, *50*, 395.
(221) Hertel, D.; Baessler, H.; Scherf, U.; Horhold, H. H. *J. Chem. Phys.* **1999**, *110*, 9214.
(222) Im, C.; Baessler, H.; Rost, H.; Horhold, H. H. *J. Chem. Phys.* **2000**, *113*, 3802.
(223) Facci, J. S.; Abkowitz, M. A.; Limburg, W. W.; Renfer, D.; Yanus, J. *Mol. Cryst. Liq. Cryst.* **1991**, *194*, 55.
(224) Michl, J.; Downing, J.; W.; Karatsu, T.; McKinley, A. J.; Poggi, G.; Wallraff, G. M.; Sooriyakumaran, R. *Pure Appl. Chem.* **1988**, *60*, 959.
(225) Miller, R. D.; Michl, J. *Chem. Rev.* **1989**, *89*, 1359.
(226) Abkowitz, M. A.; Stolka, M. *Polym. Prepr.* **1990**, *31*, 254.
(227) Miller, R. D.; Rabolt, J. R.; Sooriyakumaran, R.; Fickes, G. N; Farmer, B. L.; Kuzmany, H *Polym. Prepr.* **1987**, *28*, 422.
(228) Abkowitz, M. A.; Stolka, M. *Philos. Mag. Lett.* **1988**, *58*, 239.
(229) Emin, D. *Adv. Phys.* **1975**, *24*, 305.
(230) Schein, L. B.; Rosenberg, A.; Rice, S. L. *J. Appl. Phys.* **1986**, *60*, 4287.
(231) Schein, L. B. *Mol. Cryst. Liq. Cryst.* **1990**, *183*, 41.
(232) Bässler, H. *Phys. Status Solidi* **1993**, *175*, 15.
(233) Baessler, H.; Schoenherr, G.; Abkowitz, M. A.; Pai, D. M. *Phys. Rev. B: Condens. Matter* **1982**, *26*, 3105.
(234) Dunlap, D. E.; Parris, P. E.; Kenkre, V. M. *Proc. SPIE* **1999**, *3799*, 88.
(235) Parris, P. E.; Kenkre, V. M.; Dunlap, D. H. *Phys. Rev. Lett.* **2001**, *87*, 126601.
(236) Schein, L. B. *Philos. Mag. B.* **1992**, *65*, 795.
(237) Bassler, H. *Mol. Cryst. Liq. Cryst.* **1994**, *252*, 11.
(238) Borsenberger, P. M.; Magin, E. H.; Van der Auweraer, M.; De Schryver, F. C. *Phys. Status Solidi A* **1993**, *140*, 9.
(239) Novikov, S. V.; Vannikov, A. V. *J. Phys. Chem.* **1995**, *99*, 14573.
(240) Novikov, S. V.; Dunlap, D. H.; Kenkre, V. M.; Parris, P. E.; Vannikov, A. V. *Phys. Rev. Lett.* **1998b**, *81*, 4472.
(241) Novikov, S. V.; Dunlap, D. H.; Kenkre, V. M. *Proc. SPIE* **1998a**, *3471*, 181.
(242) Dunlap, D. H. *Phys. Rev. B* **1995**, *52*, 939.
(243) Dunlap, D. H.; Parris, P. E.; Kenkre, V. M. *Phys. Rev. Lett.* **1996**, *77*, 542.
(244) Dunlap, D. H. *Proc. SPIE* **1996**, *2850*, 110.
(245) Young, R. H.; Kung, T.-M.; Sinicropi, J. A.; Fitzgerald, J. J.; Eilers, J. E.; Chen, C. H.; Boaz, N. W. *J. Phys. Chem.* **1996**, *100*, 17923.
(246) Young, R. H.; Fitzgerald, J. J. *J. Chem. Phys.* **1995**, *102*, 2209.
(247) Young, R. H.; Fitzgerald, J. J. *J. Chem. Phys.* **1995**, *102*, 6290.
(248) Young, R. H.; Fitzgerald, J. J. *J. Chem. Phys.* **1995**, *102*, 9380.
(249) Young, R. H.; Fitzgerald, J. J. *J. Phys. Chem.* **1995**, *99*, 4230.
(250) Young, R. H.; Sinicropi, J. A.; Fitzgerald, J. J. *J. Phys. Chem.* **1995**, *99*, 9497.
(251) Young, R. H. *J. Chem. Phys.* **1995**, *103*, 6749.
(252) Schein, L. B.; Tyutnev, A. *J. Phys. Chem. C* **2008**, *112*, 7295.
(253) Schein, L. B.; Saenko, V.; Pozhidaev, E. D.; Tyutnev, A.; Weiss, D. S. *J. Phys. Chem. C* **2009**, *113*, 1067.
(254) Abkowitz, M. A. *Philos. Mag. B* **1992**, *65*, 817.
(255) Stolka, M.; Abkowitz, M. A. *Synth. Met.* **1993**, *54*, 417.
(256) Yuh, H. J.; Abramsohn, D.; Stolka, M. *Philos. Mag. Lett.* **1987**, *55*, 277.
(257) Schmidlin, F. W. *Phys. Rev. B.* **1977**, *16*, 2362.
(258) Abkowitz, M. A.; Enck, R. C. *J. Phys. Colloq., C4, Pt. 1* **1981**, 443.
(259) Abkowitz, M. A.; Facci, J. S.; Stolka, M. *Chem. Phys.* **1993**, *177*, 783.
(260) Abkowitz, M. A. *Conjugated Polymer and Molecular Interfaces*; Salaneck, W. R., Seki, K, Kahn, A., Pireaux, J.-J., Eds.; Marcel Dekker: New York, 2002; p 545.
(261) Lampert, M. A.; Mark, P. *Current Injection in Solids*; Academic Press: New York, 1970; p 17.
(262) Murgatroyd, P. N. *J. Phys. D* **1970**, *3*, 151.
(263) Young, R. H. *Philos. Mag. Lett.* **1994**, *70*, 331.
(264) Weiss, D. S. *Proceedings of the 10th Annual Symposium of the NSF Center: Photoinduced Charge Transfer*; Rothberg, L., Ed.; World Scientific: Singapore, 2000; p 1.
(265) Macartney, A. A. W.; Goldie, D. M.; Gibson, R. A. G.; Gairns, R. S. *Synth. Met.* **1994**, *67*, 201.
(266) Kanemitsu, Y.; Imamura, S. *J. Appl. Phys.* **1989**, *66*, 997.
(267) Russell, D. D.; Meyer, R. L.; Davis, N. G.; Moudry, R.; Jubran, N.; Tokarski, Z.; Lee, H.-K. *IS&T's NIP20: 2004 International Conference on Digital Printing Technologies* **2004**, 538.
(268) Kitamura, T.; Yokoyama, M. *J. Appl. Phys.* **1991**, *69*, 821.
(269) Huang, Z.; Yu, Q.; Pan, J.; Lin, R.; Zong, H. *Proceedings IS&T's NIP15: 1999 International Conference on Digital Printing Technologies* **1999**, 699.
(270) Aratani, S.; Kawanishi, T.; Kakuta, A. *Jpn. J. Appl. Phys.* **1996**, *35*, 2184.
(271) Kanemitsu, Y.; Sugimoto, Y. *Phys. Rev. B* **1992**, *46*, 14182.
(272) Shoda, T.; Fujii, A.; Murayama, T.; Aramaki, S. *Proceedings IS&T's NIP15: 1999 International Conference on Digital Printing Technologies* **1999**, 651.
(273) Shoda, T.; Murayama, T.; Fujii, A. *Proceedings IS&T's NIP17: International Conference on Digital Printing Technologies* **2001**, 550.
(274) Fujii, A.; Shoda, T.; Aramaki, S.; Murayama, T. *J. Imaging Sci. Technol.* **1999**, *43*, 430.
(275) Sakanoue, K.; Motoda, M.; Sugimoto, M.; Sakaki, S. *J. Phys. Chem. A* **1999**, *103*, 5551.
(276) Shoda, T.; Murayama, T. *Proceedings IS&T's NIP16: 2000 International Conference on Digital Printing Technologies* **2000**, 443.
(277) Borsenberger, P. M. *J. Appl. Phys.* **1990**, *68*, 5188.
(278) Kochelev, K. K.; Kocheleva, O. K.; Kuts, S; Tameev, A. R.; Kozlov, A. A.; Vannikov, A. V. *Proceedings IS&T's NIP16: 2000 International Conference on Digital Printing Technologies* **2000**, 133.
(279) Molaire, M. F.; Zubil, T. *Proceedings IS&T's NIP15: 1999 International Conference on Digital Printing Technologies* **1999**, 668.

(280) Molaire, M. F. *Proceedings IS&T's NIP8: International Congress on Advances in Non-Impact Printing* **1992**, 219.
(281) Stolka, M.; Pai, D. M.; Renfer, D. S.; Yanus, J. F. *J. Polym. Sci., Part A: Polym. Chem.* **1983**, *21*, 969.
(282) Borsenberger, P. M.; Rossi, L. J. *J. Chem. Phys.* **1992**, *96*, 2390.
(283) Borsenberger, P. M; Gruenbaum, W. T.; O'Regan, M. B.; Rossi, L. J. *J. Polym. Sci, Part B: Polym. Phys.* **1995**, *33*, 2143.
(284) Borsenberger, P. M.; Gruenbaum, W. T.; Magin, E. H. *Proc. SPIE* **1995**, *2526*, 63.
(285) Kuder, J. E.; Pochan, J. M.; Turner, S. R.; Hinman, D. F. *J. Electrochem. Soc.: Electrochem. Sci. Tech.* **1978**, *125*, 1750.
(286) Matsui, M.; Fukuyasu, K.; Shibata, K.; Muramatsu, H. *J. Chem. Soc., Perkin Trans.* **1993**, *2*, 1107.
(287) Gill, W. D. *Proceedings 5th International Conference on Amorphous and Liquid Semiconductors* **1973**, 901.
(288) Ong, B. S.; Keoshkerian, B.; Martin, T. I.; Hamer, G. K. *Can. J. Chem.* **1985**, *63*, 147.
(289) Turner, S. R. *Macromolecules* **1980**, *13*, 782.
(290) Murti, D. K.; McAneney, T. B.; Popovic, Z. D.; Ong, B. S.; Loutfy, R. O. *J. Phys. D: Appl. Phys.* **1991**, *24*, 953.
(291) Sim, J. H.; Ogino, K.; Sato, H. *J. Imaging Sci. Technol.* **1996**, *40*, 164.
(292) Tokarski, Z.; Moudry, R.; Law, K.; Jubran, N.; Getautis, V.; Jankauskas, V.; Gaidelis, V.; Montrimas, E.; Sidaravicius, J. *Proceedings IS&T's NIP19: 2003 International Conference on Digital Printing Technologies* **2003**, 708.
(293) Zhang, W.; Wu, T.; Want, W.; Pu, J. *Proceedings IS&T's NIP23* **2007**, 661.
(294) Mizuta, Y.; Watanabe, Y.; Sugai, F.; Matsumoto, S.; Kawaguchi, H.; Akiba, N.; Saitou, S.; Okada, H.; Goto, M.; Nakazawa, T. *Proceedings IS&T's NIP12: International Conference on Digital Printing Technologies* **1996**, 429.
(295) Matsui, M.; Shibata, K.; Muramatsu, H.; Nakazumi, H. *J. Mater. Chem.* **1996**, *6*, 1113.
(296) Kaeding, J. E.; Murray, B. J.; Gruenbaum, W. T.; Borsenberger, P. M. *J. Imaging Sci. Technol.* **1996**, *40*, 245.
(297) Borsenberger, P. M. *J. Appl. Phys.* **1990**, *68*, 6263.
(298) Borsenberger, P. M.; Gruenbaum, W. T.; Magin, E. H.; Visser, S. A. *Phys. Status Solidi A* **1998**, *166*, 835.
(299) Abkowitz, M.; Pai, D. M. *Philos. Mag.* **1986**, *53*, 193.
(300) Ioannidis, A.; Facci, J. S.; Abkowitz, M. A. *J. Imaging Sci. Technol.* **1999**, *43*, 242.
(301) Abkowitz, M. A. *J. Imaging Sci. Technol.* **1996**, *40*, 318.
(302) Abkowitz, M. A.; J. Facci, J. S.; Rehm, J. *J. Appl. Phys.* **1998**, *83*, 2670.
(303) Weiss, D. S. unpublished results.
(304) Popovic, Z. D.; Iglesias, P.; Parco, D.; Robinette, S. *J. Imaging Technol.* **1991**, *17*, 71.
(305) Popovic, Z. D. *Proceedings IS&T's NIP 13: 1997 International Conference on Digital Printing Technologies* **1997**, 238.
(306) Jeyadev, S.; Ramesh, P.; Popovic, Z. D.; Maitra, S. *Proceedings IS&T's NIP 13: 1997 International Conference on Digital Printing Technologies* **1997**, 241.
(307) Lin, C.-W.; Kutsuwada, N.; Nakamura, Y.; Shohdohji, T.; Nozaki, T.; Tanzawa, H. *IS&T SEPJ Proceedings 9th International Congress on Advances in Non-Impact Printing Technologies/Japan Hardcopy '93* **1993**, 689.
(308) Lin, C.-W.; Nozaki, T.; Kutsuwada, N.; Nakamura, Y. *Proceedings IS&T's Tenth International Conference on Advances in Non-Impact Printing Technologies* **1994**, 286.
(309) Lin, C.-W.; Kutsuwada, N.; Nakamura, Y. *J. Imaging Sci. Technol.* **1993**, *37*, 476.
(310) Tse, M.-K.; Forrest, D. J.; Wong, F. Y. *Proceedings IS&T's NIP14: 1998 International Conference on Digital Printing Technologies* **1998**, 615.
(311) Tse, M.-K.; Forrest, D. J.; She, K. Y. *Proceedings IS&T's Eleventh International Congress on Advances in Non-Impact Printing Technologies* **1995**, 251.
(312) Molaire, M. F. *Proceedings IS&T's NIP23: 23rd International Conference on Digital Printing Technologies* **2007**, 653.
(313) Ferrar, W. T.; Weiss, D. S.; Molaire, M. F.; Jin, X.; Sorriero, L. J. *Proceedings IS&T's NIP24: 24th International Conference on Digital Printing Technologies* **2008**, 176.
(314) Molaire, M. F.; Ferrar, W. T.; Galipo, R. G.; Sykes, M. *Proceedings IS&T's NIP24: 24th International Conference on Digital Printing Technologies* **2008**, 184.
(315) Satoh, M.; Matsumoto, S.; Higashiguchi, T.; Matsuda, M.; Muranoi, T.; Kikuma, I.; Momose, Y.; Takeuchi, M. *Appl. Surf. Sci.* **1996**, *92*, 635.
(316) Chan, Y. C.; Miao, X. S.; Pun, E. Y. B. *J. Mater. Res.* **1998**, *13*, 2042.
(317) Miao, X. S.; Chan, Y. C.; Pun, E. Y. B. *Thin Solid Films* **1998**, *324*, 180.
(318) Miao, X. S.; Chan, Y. C.; Pun, E. Y. B. *Thin Solid Films* **1998**, *315*, 123.
(319) Stahr, F.; Kottwitz, A.; Röhlecke, S.; Schade, K.; Lutz, M. *Proceedings IS&T's NIP13: 1997 International Conference on Digital Printing Technologies* **1997**, 233.
(320) Seino, K.; Ebisu, O. *J. Imaging Sci. Technol.* **2000**, *44*, 523.
(321) Nakaue, H.; Mitani, T.; Kurokawa, H. *Diamond Films Technol.* **1993**, *3*, 45.
(322) Kochelev, K.; Zhylina, V. I.; Khots, G. E.; Kocheleva, O.; Sleptsov, V. V. *Proceedings IS&T's NIP12: International Conference on Digital Printing Technologies* **1996**, 483.
(323) Cornelius, L. *R&R News* **1994**, *July*, 34.
(324) Weiss, D. S.; Ferrar, W. T.; Cowdery-Corvan, R. *Proceedings IS&T's NIP 14: 1998 International Conference on Digital Printing Technologies* **1998**, 520.
(325) Weiss, D. S.; Ferrar, W. T.; Corvan, J. R.; Parton, L. G.; Miller, G. J. *Imaging Sci. Technol.* **1999**, *43*, 280.
(326) Ferrar, W. T.; Weiss, D. S.; Cowdery, J. R.; Parton, L. G. *J. Imaging. Sci. Technol.* **2000**, *44*, 429.
(327) Weiss, D. S.; Cowdery, J. R.; Ferrar, W. T.; Young, R. H. *J. Imaging Sci. Technol.* **1996**, *40*, 322.
(328) Chen, I.; Mort, J.; Machonkin, M. A.; Larson, J. R. *J. Imaging Sci. Technol.* **1996**, *40*, 431.
(329) Yarmchuk, E. J.; Keefe, G. E. *J. Appl. Phys.* **1989**, *66*, 5435.
(330) Yarmchuk, E. J.; Keefe, G. E. *J. Imaging Sci.* **1991**, *35*, 231.
(331) Jin, X.; Weiss, D. S.; Sorriero, L. J.; Ferrar, W. T. *J. Imaging Sci. Technol.* **2003**, *47*, 361.
(332) Jin, X.; Weiss, D. S.; Ferrar, W. T. *Proceedings IS&T's NIP 19: 2003 International Conference on Digital Printing Technologies* **2003**, 674.
(333) Ferrar, W. T.; Gruenbaum, W. T.; Jin, X.; Molaire, M. F.; Cowdery, J. R.; Weiss, D. S. *Silicon* **2009**, *1*, 13.
(334) Cais, R. E.; Nozomi, M.; Murakami, O.; Kawai, M. *Proceedings IS&T's Eighth International Congress on Advances in Non-Impact Printing Technologies* **1992**, 253.
(335) Cais, R. E.; Nozomi, M.; Kawai, M.; Miyake, A. *Macromolecules* **1992**, *25*, 4588.
(336) Shahin, M. M. *Photogr. Sci. Eng.* **1971**, *15*, 322.
(337) Shahin, M. M. *J. Chem. Phys.* **1966**, *45*, 2600.
(338) Shahin, M. M. *Appl. Opt. Suppl.* **1969**, *3*, 106.
(339) Haridoss, S.; Perlman, M. M.; Carlone, C. *J. Appl. Phys.* **1982**, *53*, 6106.
(340) Goldman, A.; Sigmond, R. S. *J. Electrochem. Soc.* **1985**, *132*, 2842.
(341) Kawamoto, H. *J. Imaging Sci. Technol.* **1995**, *39*, 267.
(342) Kawamoto, H. *J. Imaging Sci. Technol.* **1995**, *39*, 439.
(343) Abdel-Salam, M.; Mizuno, A.; Shimizu, K. *J. Phys. D, Appl. Phys.* **1997**, *30*, 864.
(344) Frank, C. W.; Buchacek, R.; Dreher, G.; Green, E.; Shiffman, S. *Proceedings Soc. Photographic Scientists and Engineers Second International Conference on Electrophotography* **1974**, 52.
(345) Jiang, S.; Huang, J.; Hoshino, Y. *Proceedings IS&T's NIP23 and Digital Fabrication* **2007**, 57.
(346) Gallo, C. F.; Germanos, J. E.; Courtney, J. E. *Appl. Opt. Suppl.* **1969**, *3*, 111.
(347) Nashimoto, K. *J. Imaging Sci.* **1986**, *32*, 205.
(348) Hosaka, Y.; Nakao, H. *Proceedings IS&T's NIP 12: International Conference on Digital Printing Technologies* **1996**, 339.
(349) Seino, K.; Ebisu, O. *Proceedings IS&T's NIP 15: 1999 International Conference on Digital Printing Technologies* **1999**, 675.
(350) Takenouchi, S.; Hirano, A.; Yoshioka, H.; Fujimaki, Y.; Moriguchi, H. *Proceedings IS&T's Fourth International Congress on Advances in Non-Impact Printing Technologies* **1988**, 22.
(351) Kobayashi, T.; Saito, T.; Aratani, S.; Suzuki, S.; Iwayanagi, T. *J. Imaging Sci. Technol.* **1995**, *39*, 485.
(352) Tokarski, Z.; Ahn, Y.-J.; Gaidelis, V.; Maldzius, R; Lozovski, T.; Sidaravicius, J. *Proceedings IS&T's NIP23 and Digital Fabrication* **2007**, 643.
(353) Tokarski, Z; Ahn, Y.-J. *J. Imaging Soc. Jpn.* **2008**, *47*, 494.
(354) Endo, K.; Miyaoka, S.; Katsuya, Y. *Proceedings IS&T's Tenth International Conference on Advances in Non-Impact Printing Technologies* **1994**, 279.
(355) Kochelev, K. K.; Tameev, A. R.; Kocheleva, G. A.; Kozlov, A. A.; Kocheleva, O. K.; Golovin, V. E.; Vannikov, A. V. *Proceedings IS&T's NIP 14: 1998 International Conference on Digital Printing Technologies* **1998**, 524.
(356) Borsenberger, P. M.; Contois, L. E.; Hoesterey, D. C. *J. Chem. Phys.* **1978**, *68*, 637.
(357) Hirao, A.; Nishizawa, H.; Hosoya, M. *Jpn. J. Appl. Phys.* **1994**, *33*, 1944.
(358) Nabeta., O.; Kuroda, M.; Furusho, N. *Proc. SPIE* **1990**, *1235*, 155.
(359) Pacansky, J.; Waltman, R. J.; Grygier, R.; Cox, R. *Chem. Mater.* **1991**, *3*, 454.

(360) Stasiak, J. W.; Storch, T. J.; Mao, E. *Proceedings IS&T's Eleventh International Congress on Advances in Non-Impact Printing Technologies* **1995**, 147.
(361) Pacansky, J.; Waltman, R. J.; Cox, R. *Chem. Mater.* **1992**, *4*, 401.
(362) Pacansky, J.; Waltman, R. J.; Cox, R. *Chem. Mater.* **1991**, *3*, 903.
(363) Pacansky, J.; Waltman, R. J. *Chem. Mater.* **1991**, *3*, 912.
(364) Yokoyama, M.; Endo, Y.; Mikawa, H. *Bull. Chem. Soc. Jpn.* **1976**, *49*, 1538.
(365) Kanemitsu, Y.; Imanishi, D.; Imamura, S. *J. Appl. Phys.* **1989**, *66*, 4526.
(366) Wong, C. K. H.; Chan, Y. C.; Lam, Y. W.; Webb, D. P.; Leung, K. M.; Chiu, D. S. *J. Electron. Mater.* **1996**, *25*, 1451.
(367) Wong, C. K. H.; Chan, Y. C.; Pfleger, J.; Lam, Y. W.; Leung, K. M.; Chiu, D. S. *J. Mater. Res.* **1997**, *12*, 106.
(368) Nakazawa, T.; Mizuta, Y.; Kawahara, A.; Miyamoto, E.; Muto, N. *Chem. Lett.* **1992**, 1125.
(369) Mizuta, Y.; Kawahara, A.; Miyamoto, E.; Mutoh, N.; Nakazawa, T. *Proceedings IS&T's 9th International Congress on Advances in Non-Impact Printing Technologies/Japan Hardcopy '93* **1993**, 663.
(370) Weiss, D. S.; Chen, D. A. *J. Imaging Sci. Technol.* **1995**, *39*, 425.
(371) Johnson, G. E. *Macromolecules* **1980**, *13*, 145.
(372) Okamoto, K.; Kusabayashi, S.; Mikawa, H. *Bull. Chem. Soc. Jpn.* **1973**, *46*, 2613.
(373) Okamoto, K.; Yano, A.; Kusabayashi, S.; Mikawa, H. *Bull. Chem. Soc. Jpn.* **1974**, *47*, 749.
(374) Weiss, D. S.; Gruenbaum, W. T. *J. Imaging Soc. Jpn.* **2008**, *47*, 501.
(375) Kochelev, K. K.; Kocheleva, O. K.; Golovin, V. E.; Kocheleva, G. A. *Proceedings IS&T's NIP 15: 1999 International Conference on Digital Printing Technologies* **1999**, 718.
(376) Kochelev, K. K.; Bulavka, V. N.; Kocheleva, O. K.; Golovin, V. E.; Kocheleva, G. A. *Proceedings IS&T's NIP 16: 2000 International Conference on Digital Printing Technologies* **2000**, 160.
(377) Kochelev, K. K.; Bulavka, V. N.; Golovin, V. E.; Kocheleva, G. A.; Gekhman, A. E. *Proceedings IS&T's NIP 18: 2002 International Conference on Digital Printing Technologies* **2002**, 670.
(378) Kanemitsu, Y; Imamura, S. *Jpn. J. Appl. Phys.* **1989**, *28*, 240.

CR900173R